THE HYDRATION OF MAGNESIUM OXIDE WITH DIFFERENT REACTIVITIES BY WATER AND MAGNESIUM ACETATE

by

MATHIBELA ELIAS APHANE

submitted in fulfilment of the requirements for
the degree of

MASTER OF SCIENCE

in the subject

CHEMISTRY

at the

UNIVERSITY OF SOUTH AFRICA

SUPERVISOR: DR E M VAN DER MERWE

JOINT SUPERVISOR: PROF C A STRYDOM

MARCH 2007

DECLARATION BY CANDIDATE

I hereby declare that THE HYDRATION OF MAGNESIUM OXIDE WITH DIFFERENT REACTIVITIES BY WATER AND MAGNESIUM ACETATE is my own original work and has not previously been submitted to any other institution of higher learning. I further declare that all the sources that I have used or quoted have been indicated and acknowledged by means of a comprehensive list of references.

.....

M. E. APHANE

ACKNOWLEDGEMENTS

I would like to express my deepest gratitude towards the following people, institutions and companies that contributed in making this study a success:

- My supervisor, Dr Liezel van der Merwe for her patience, guidance and comments during the study, advice, support and encouragement. I would also like to thank her for inviting me to join her in this research and for having trust in me.
- My co-supervisor, Prof. C. A. Strydom for her appreciation in my work and for her helpful comments.
- University of South Africa and NRF for financial support in my study.
- Magnesium Compounds Consortium for providing the MgO sample.
- Department of Chemistry for their facilities.
- Ms Maggie Loubser of University of Pretoria for doing the XRF and XRD analysis and interpretation of the results.
- I am grateful to Ms E. Ten Krooden and Mrs Tryphina Moeketsi for their assistance in finding the library books and journals.
- University of Pretoria for using their facilities.
- I am grateful to all Chemistry staff at UNISA.
- Thanks to the chairperson of chemistry department, Prof. M. J. Mphahlele for all the support in the postgraduate assistantship program.

DEDICATION

This study was dedicated to the following people:

- My late grandfather: Mathibela Elias Aphane the senior
- My grandmother: Monere Stephina Aphane
- My wonderful mother: Majalla Elizabeth Aphane
- My only sister: Rakgadi Aphane
- My late aunt: Leah Masadi Aphane, may your soul rest in peace
- My son: Tumelo
- My fiancée: Minkie

ABSTRACT

The use of magnesium hydroxide ($Mg(OH)_2$) as a flame retardant and smoke-suppressor in polymeric materials has been of great interest recently. Because it contains no halogens or heavy metals, it is more environmentally friendly than the flame retardants based on antimony metals or halogenated compounds. $Mg(OH)_2$ can be produced by the hydration of magnesium oxide (MgO), which is usually produced industrially from the calcination of the mineral magnesite ($MgCO_3$). The thermal treatment of the calcination process dramatically affects the reactivity of the MgO formed. Reactivity of MgO refers to the extent and the rate of hydration thereof to $Mg(OH)_2$. The aim of this study was to investigate the effect of calcination time and temperature on the reactivity of MgO, by studying the extent of its hydration to $Mg(OH)_2$, using water and magnesium acetate as hydrating agents.

A thermogravimetric analysis (TGA) method was used to determine the degree of hydration of MgO to $Mg(OH)_2$. The reactivity of MgO was determined by BET (Brunauer, Emmett and Teller) surface area analysis and a citric acid reactivity method. Other techniques used included XRD, XRF and particle size analysis by milling and sieving.

The product obtained from the hydration of MgO in magnesium acetate solutions contains mainly $Mg(OH)_2$, but also some unreacted magnesium acetate. Magnesium acetate decomposition reaction takes place in the same temperature range as magnesium hydroxide, which complicates the quantitative TG analysis of the hydrated samples. As a result, a thermogravimetric method was developed to quantitatively determine the amounts of $Mg(OH)_2$ and $Mg(CH_3COO)_2$ in a mixture thereof.

The extent to which different experimental parameters (concentration of magnesium acetate, solid to liquid ratio and hydration time) influence the degree of hydration of MgO were evaluated using magnesium acetate as a hydrating agent. Magnesium acetate was found to enhance the degree of MgO hydration when compared to water. By increasing the hydration time, an increase in the percentage of $Mg(OH)_2$ formed was observed.

In order to study the effect of calcining time and temperature on the hydration of the MgO, the MgO samples were then calcined at different time periods and at different temperatures. The results have shown that the calcination temperature is the main variable affecting the surface area and reactivity of MgO.

Lastly, an attempt was made to investigate the time for maximum hydration of MgO calcined at 650, 1000 and 1200^{o}C. From the amounts of $Mg(OH)_2$ obtained in magnesium acetate, it seems that the same maximum degree of hydration is obtained after different hydration times. A levelling effect that was independent of the calcination temperature of MgO was obtained for the hydrations performed in magnesium acetate. Although there was an increase in the percentage of $Mg(OH)_2$ obtained from hydration of MgO in water, the levelling effect observed in magnesium acetate was not observed in water as a hydrating agent, and it seemed that the extent of MgO hydration in water was still increasing.

The results obtained in this study demonstrate that the calcination temperature can affect the reactivity of MgO considerably, and that by increasing the hydration time, the degree of hydration of MgO to $Mg(OH)_2$ is enhanced dramatically.

CONTENTS

CHAPTER 6

The effect of MgO reactivity on its hydration to $Mg(OH)_2$

CHAPTER 7

Determination of maximum hydration time on the hydration of MgO using water and magnesium acetate as hydrating agents

ABBREVIATIONS USED

BET	:	Brunauer, Emmett and Teller
calc.	:	Calcination
CRTG	:	Controlled rate thermogravimetry
DMA	:	Dynamic mechanical analysis
DSC	:	Differential scanning calorimetry
DTA	:	Differential thermal analysis
DTG	:	Derivative thermogravimetry
EDXRF	:	Energy dispersive X-ray Fluorescence
EGA	:	Evolved Gas Analysis
et al.	:	And others
FTIR	:	Fourier Transform Infra Red
HDPE	:	High-density polyethylene
LOI	:	Loss on ignition
MgAc	:	Magnesium acetate
NRF	:	National Research foundation
PA-6	:	Polyamide-6
PA-6,6	:	Polyamide-6,6
PDF	:	Powder Diffraction File
PSDS	:	Position sensitive detectors
PVC	:	Polyvinyl chloride
SA	:	South Africa
TA	:	Thermal Analysis
TG	:	Thermogravimetry
TGA	:	Thermogravimetric Analysis
TMA	:	Thermomechanical analysis
URL	:	Uniform Resource Locator
WDXRF	:	Wavelength Dispersive X-ray Fluorescence
XRD	:	X-ray Diffraction
XRF	:	X-ray Fluorescence
ZBH	:	Zero Background Holder
ZPC	:	Zero Point Charge

NOMENCLATURE

Symbol	:	Explanation
Å	:	Angstrom
$Å^2\ mol^{-1}$	:	Angstrom squared per mole
atm	:	Atmosphere
α	:	Alpha
β	:	Beta
^oC	:	Degree Celsius
$^oC\ min^{-1}$	:	Degree Celsius per minute
$g\ ml^{-3}$	:	Grams per millilitre cube
$g\ mol^{-1}$	:	Grams per mole
g	:	Gram
h	:	Hour
h^{-1}	:	Per hour
hr	:	Hour
hrs	:	Hours
in^2	:	Inch squared
J	:	Joule
J s	:	Joule second
K	:	Kelvin
keV	:	Kilo electron volt
kV	:	Kilo volt
$kJ\ mol^{-1}$	:	Kilojoules per mole
kPa	:	Kilo Pascal
$m^2\ g^{-1}$	:	Metre squared per gram
M	:	Moles per litre
$mol\ g^{-1}$	:	Mole per gram
mg	:	Milligram
$ml\ min^{-1}$	:	Millilitres per minute
min^{-1}	:	Per minute
min	:	Minute

ml	:	Millilitre
m	:	Metre
$m\ s^{-1}$	:	Metres per second
mA	:	Milliamperes
mm Hg	:	Millimetres of mercury
N	:	Normality
nm^2	:	Nanometre squared
θ	:	Theta
pH	:	Negative logarithm of concentration of hydrogen ions
Pa	:	Pascal
%	:	Percentage
$\%\ {}^{o}C^{-1}$	:	Percentage per degree Celsius
rpm	:	Revolutions per minute
s	:	Second
t	:	Time
T	:	Temperature
temp.	:	Temperature
T_f	:	Furnace temperature
T_s	:	Sample temperature
T_r	:	Reference temperature
ΔT	:	Change in temperature
µm	:	Micrometer
µg	:	Microgram
w	:	Weight
wt %	:	Weight percentage

LIST OF MINERALS

Artinite	:	$MgCO_3 \cdot Mg(OH)_2 \cdot 3H_2O$
Barringtonite	:	$MgCO_3 \cdot 2H_2O$
Boehmite	:	$AlO(OH)$
Brucite	:	$Mg(OH)_2$
Calcite	:	$CaCO_3$
Dolime	:	$CaO \cdot MgO$
Dolomite	:	$CaMg(CO_3)_2$
Dypingite	:	$4MgCO_3 \cdot Mg(OH)_2 \cdot 5H_2O$
Fluorite	:	CaF_2
Hydromagnesite	:	$4MgCO_3 \cdot Mg(OH)_2 \cdot 4H_2O$
Hydrotalcite	:	$Mg_6Al_2 \cdot (CO_3)(OH)_{16} \cdot 4H_2O$
Lansfordite	:	$MgCO_3 \cdot 5H_2O$
Magnesite	:	$MgCO_3$
Nesquehonite	:	$MgCO_3 \cdot 3H_2O$
Periclase	:	MgO
Quartz	:	SiO_2
Serpentine	:	$MgSiO_{10}(OH)_8$

CHAPTER 1

INTRODUCTION

1.1 Aims of the study on the hydration of MgO with different reactivities by water and magnesium acetate

A fairly extensive work on the hydration of magnesium oxide (magnesia, MgO) to form magnesium hydroxide ($Mg(OH)_2$) has been carried out by earlier workers; ranging from the utilization of magnesium hydroxide produced from MgO hydration as fire retardant (Rocha and Ciminelli, 2001); the mechanism of magnesia hydration in magnesium acetate solutions (Filippou et al., 1999); the effect of surface area and pore structure of the calcined magnesite and subsequent hydration of MgO produced (Girgis and Girgis, 1969); hydration of calcined magnesite (Barnejee et al., 1967; Birchal et al., 2000; Ranjitham and Khangaonkar, 1989; Sharma and Roy, 1977); to the effect of magnesium acetate concentrations, hydration time, amount of MgO and hydration temperature (van der Merwe et al., 2004). Anderson et al. (1965) and Kuroda et al. (1988) have also studied the interaction of water with magnesium oxide surfaces. Recently, van der Merwe and Strydom (2006) investigated the effect of different hydrating agents on magnesia hydration to $Mg(OH)_2$.

The use of magnesium hydroxide as a flame retardant and smoke-suppressor in polymeric materials has been of great interest recently. Magnesium hydroxide has been reported to be superior to flame retardants based on antimony metals or halogenated (chlorinated and brominated) compounds. Because it contains no halogens or heavy metals, it is more environmentally friendly than these compounds. The decomposition products of the halogenated compounds are thought to cause environmental concerns, as there is a risk of release of corrosive vapors (Gibert et al., 2000). Aluminium hydroxide ($Al(OH)_3$) has also been applied as a flame retardant in many polymeric materials, but as a result of its low decomposition temperature

(approximately 180°C), its application has been limited since most polymers are processed at higher temperatures. Due to magnesium hydroxide's high decomposition temperature (350°C), it is the mineral flame retardant most often used (Rocha and Ciminelli, 2001). Calcium hydroxide, $Ca(OH)_2$, can also be used since when heated, a highly endothermic dehydration reaction is observed. However, it may act as an efficient combustion promoter when combined with organic materials, and because of its high decomposition temperature (approximately 580°C), it is not suitable as a flame retardant additive (Focke et al., 1997).

Magnesium hydroxide produced by the hydration of magnesium oxide can be successfully employed as a fire retardant for polymers; however, producing this hydroxide for fire retardant filler applications via hydration of commercial MgO can be costly. For this application, there is a need for purification steps, which subsequently increase the cost of the product (Rocha and Ciminelli, 2001). By directly hydrating MgO obtained from calcination of magnesium carbonate, which occurs in nature as the mineral magnesite, can be an interesting option.

Raw magnesium carbonate (magnesite) is mined at Chamotte Holdings S.A, and heated in rotary kilns to produce magnesium oxide, which is subsequently upgraded and then processed to produced hydrotalcite, magnesium hydroxide and magnesium carbonate light. These products are used as flame retardant additives in plastics and they are intended to replace toxic heavy metals salts currently used as heat stabilizers in plastics manufacturing. Flame retardants are essential additives to numerous plastics, including polyolefin found in products such as pipe, containers, bags and bottles. They are also essential in PVC (polyvinyl chloride) processing such as extrusion and injection molding to remove the hydrochloric acid that forms on heating and cause degradation of the plastic.

In this study, firstly, the aim was to develop suitable methods that can be used to quantitatively determine the amounts of $Mg(OH)_2$ and magnesium acetate in a mixture thereof by using a thermogravimetric analysis (TGA) method. Magnesium hydroxide obtained as a product from MgO hydration in magnesium acetate solutions may contain some magnesium acetate which is left after hydration. The influence of different experimental variables was also investigated.

In order to study the effect of the reactivity of MgO on hydration, the effect of calcination temperature, calcination time and particle size were studied. The time for maximum hydration of MgO under different conditions was also determined. A comparative study was performed to compare the degree of hydration of MgO by using both water and magnesium acetate as hydrating agents.

The degree or the extent of hydration was determined by using thermogravimetric analysis (TGA) method, while the different reactivities of the calcined MgO were determined by applying both the citric acid reactivity test and the BET surface area analysis methods. Other techniques used included XRD, XRF spectroscopic techniques and particle size analysis by milling and sieving.

1.2 Physical properties of $Mg(OH)_2$, MgO and $MgCO_3$

1.2.1 Physical properties of magnesium hydroxide

Magnesium hydroxide ($Mg(OH)_2$), also known as the mineral brucite, is a white solid with a formula mass of 58.30 g mol^{-1} and a density of 2.40 g ml^{-1}. The compound decomposes at 623 K (350^oC) with a theoretical mass loss of 30.9 %. Magnesium hydroxide is slightly soluble in water with a solubility of 0.0012 g in 100 g of water at room temperature (URL-1).

1.2.2 Physical properties of magnesium oxide

Magnesium oxide (MgO), also known as magnesia, is an alkaline earth metal oxide. It is a white powdery solid material with a formula mass of 40.31 g mol^{-1}, and a density of 3.58 g ml^{-1}. Magnesium oxide has a cubic system crystal structure and melts at a high temperature of 2827 ± 30^oC. It has a solubility value of 0.00062 g in 100 g of water at room temperature (Mellor, 1924 and URL-2).

1.2.3 Physical properties and occurrence of magnesium carbonate

Magnesium carbonate ($MgCO_3$), also known as the mineral magnesite, is a white solid that occurs abundantly in nature. Several hydrated and basic forms of magnesium carbonate also exist as minerals, and these include the di, tri and pentahydrates known as barringtonite ($MgCO_3 \cdot 2H_2O$), nesquehonite ($MgCO_3 \cdot 3H_2O$),

and lansfordite ($MgCO_3 \cdot 5H_2O$), respectively. Some basic forms such as artinite ($MgCO_3 \cdot Mg(OH)_2 \cdot 3H_2O$), hydromagnesite ($4MgCO_3 \cdot Mg(OH)_2 \cdot 4H_2O$), and dypingite ($4MgCO_3 \cdot Mg(OH)_2 \cdot 5H_2O$) also occur as minerals. These minerals form commonly from the alteration of magnesium-rich rocks during low grade metamorphism while they are in contact with carbonate-rich solutions (Mellor, 1924 and URL-3).

Magnesium carbonate is ordinarily obtained by mining of these mineral forms of magnesite. It can also be prepared by mixing solutions of magnesium and carbonate ions under a carbon dioxide atmosphere. It can also be produced by exposing magnesium hydroxide slurry to CO_2 under pressure (3.5 to 5 atm) below 50^oC, to give soluble magnesium bicarbonate (URL-3):

$$Mg(OH)_2\,(s) + 2CO_2\,(g) \rightarrow Mg(HCO_3)_2\,(aq)$$

Following the filtration of the solution, the filtrate is evaporated under vacuum to give magnesium carbonate as a hydrated salt:

$$Mg^{2+}\,(aq) + 2HCO_3^-\,(aq) \rightarrow MgCO_3\,(s) + CO_2\,(g) + H_2O$$

Magnesium carbonate has a molar mass of 84.32 g mol^{-1}, with a density value of 2.96 g ml^{-1}. It decomposes at a temperature of approximately 662^oC and it has a solubility of 0.0106 g in 100 g of water at room temperature. It has a trigonal crystal structure.

1.3 Production of magnesium oxide

Magnesium oxide was discovered by A Scacchi as a mineral contaminated with ferrous oxide, and called it periclase, which is the high temperature form of magnesium oxide. Being the product of oxidation of the metal, this oxide has been reported to be produced in the amorphous or crystalline form by calcination of the salts of magnesium, which among other examples include the carbonates, nitrates, sulphate, etc. (Aramendia et al., 2003 and Mellor, 1924).

Magnesium oxide has also been reported to be a cream pinkish white mineral which cannot be readily found in nature because it does not form salt deposits or rocks since it is converted by water vapor from the atmosphere to give magnesium hydroxide (Aral et al., 2004). It can be formed from the dehydration of magnesium hydroxide (L'vov et al., 1998 and Yoshida et al., 1995) or by thermal decomposition of magnesium chloride (Jost et al., 1997). Magnesium hydroxide recovered from sea water, brines or bitterns can be calcined to produce magnesium oxide (Briggs and Lythe, 1971).

The majority of MgO produced currently involves thermal treatment of naturally occurring magnesia-rich minerals, of which magnesium carbonate ($MgCO_3$), is the most common mineral used. Other sources of MgO production include minerals such as dolomite ($CaMg(CO_3)_2$), hydromagnesite ($Mg(CO_3)\cdot 4H_2O$), brucite ($Mg(OH)_2$), and serpentine ($MgSiO_{10}(OH)_8$). Sea water, underground salt deposits of brines and salt beds where magnesium hydroxide is processed are also sources for the production of magnesia (Aral et al., 2004; Briggs and Lythe., 1971; Canteford, 1985; Girgis and Girgis, 1969; Mellor, 1924; Rizwan et al., 1999; Sharma and Roy, 1977).

Magnesium carbonate ($MgCO_3$) decomposes into MgO and CO_2 when calcined from 650 to 700^{o}C. In this process, an active phase of magnesia sensitive to moisture hydration is produced, and it is reported to be highly active for removal of silica from industrial water (Liu et al., 1997 and Sharma and Roy, 1977).

$$MgCO_3\ (s) + \text{heat} \rightarrow MgO\ (s) + CO_2\ (g)$$

On further heating of the carbonate, the MgO formed may be of different forms. The extent of calcination temperature or time may result in the formation of different types or grades of MgO being produced. These various types of MgO include: light burnt (or caustic calcined) magnesia, hard burnt magnesia, dead burnt magnesia and fused magnesia, and are discussed in more detail in the following sections.

1.4 Grades of magnesium oxide

The thermal decomposition of natural magnesite into magnesia and carbon dioxide gas in the temperature range from 600^{o}C up to 3000^{o}C results in different forms or types of magnesium oxide being produced, and as a result, the MgO produced may have different chemical properties. These properties are dependent on the mode of origin of the original magnesite, the mineralogical composition of the natural magnesite and the calcination temperature chosen. Table 1.1 gives the chemical properties of different grades of magnesium oxide.

Light burnt (or caustic calcined) magnesia, also known as medium reactive magnesia, is produced by calcining magnesium carbonate in the temperature range between 600^{o}C and 1000^{o}C. Hard burnt magnesia is produced in the temperature range between 1100 to 1650^{o}C, while dead burnt magnesia is produced by calcining between 1450 and 2200^{o}C. Dead burning of magnesite results in the formation of periclase, a crystalline variety of MgO that is inert to hydration. Fused magnesia is prepared either from light burnt magnesia to dead burnt magnesia or raw magnesite by melting in an electric arc furnace between 2800 and 3000^{o}C (Aral et al., 2004 and Canteford, 1985).

Table 1.1 Chemical properties of different grades of magnesium oxide (Aral et al., 2004 and Canteford, 1985)

Property	Caustic calcined MgO	Hard burnt MgO	Dead burnt MgO	Fused MgO
Surface area	1-200 $m^2 g^{-1}$	0.1 to 1.0 $m^2 g^{-1}$	< 0.1 $m^2 g^{-1}$	Extremely small surface area
Crystal size	1-20 μm	Characterized by moderate crystallite size	Characterized by large crystal size (30 to 120 μm)	Extremely large crystal size, single crystal weighs 200 g or more
Acid solubility	Readily soluble in dilute acids	Readily soluble only in concentrated acids	Reacts very slowly with strong acids	Reacts very slowly with strong acids
Hydration behaviour	Readily absorbs water vapor and carbon dioxide from the atmosphere to form a basic magnesium carbonate Hydrates rapidly in cold water Converts to $Mg(OH)_2$ upon exposure to moisture or water	Hydrates very slowly to form magnesium hydroxide	Does not readily hydrate or react with CO_2	Does not readily hydrate or react with CO_2
Chemical reactivity	Moderate to high chemical reactivity	Characterized by low chemical reactivity	Characterized by very low chemical reactivity	Characterized by very low chemical reactivity

1.5 The reactivity of magnesium oxide

In the literature the reactivity of a substance is reported as the characteristics of the chemical activity of substances which amongst all take into account the variety of chemical reactions in which a given substance takes part, and the rate of the chemical reactions taking place with the participation of this substance. The composition and the structure of molecules are amongst the main factors determining reactivity in classical chemistry. The rate constant of the reaction is normally used as a measure of reactivity. The physical and chemical properties of substances are determined by the relative arrangements of atoms, ions or molecules due to the disturbance occurring during formation of the crystals and other various kinds of treatment, and as a result, this has a big influence on the reactivity of the substance. The relationship between the reactivity of solid materials and their history; i.e. the method of preparation and subsequent treatment can thus be known and be used to relate the two (Boldyrev, 1993).

The most important physical properties of calcined magnesia are the crystal size and the surface area, which determine the reactivity of magnesium oxide (Kimyongur and Scott, 1986). For the purpose of this study, the reactivity of magnesium oxide refers to the extent and the rate of hydration of MgO to give $Mg(OH)_2$ when exposed to water or magnesium acetate solutions.

Girgis and Girgis (1969), who investigated the surface and pore structure of talc-magnesite, mentioned that the calcination temperature and the duration of thermal treatment are among the important factors determining the surface properties of calcined MgO and hence the reactivity of MgO since less surface area and pores are available for reaction with other compounds.

During the hydration of magnesium oxide, the reactivity of magnesium oxide gives an indication of the extent or the degree of hydration to $Mg(OH)_2$ when magnesium oxide is exposed to water, moisture or any other hydrating agent. The thermal treatment of the calcination process has an effect on the surface area and the pore size and hence the reactivity of magnesia formed from $MgCO_3$. The source of magnesia also determines the level and nature of impurities present in the calcined material. The most common impurities in magnesium oxide are CaO, Al_2O_3, Fe_2O_3, SiO_2 and B_2O_3.

There are several methods that may be used in order to measure the reactivity of magnesium oxide produced from magnesite on calcination (Canteford, 1985). These methods include:

(i) Acid reactivity, where the time taken for a given mass of magnesia to react with a given amount (in volume) of acid, such as citric acid or acetic acid. The time reported gives an indication of the type of MgO formed.
(ii) Iodine number, which is determined by the amount of iodine absorbed by the solid sample.
(iii) BET method, which determines the specific surface area of magnesium oxide by the adsorption method.

In this study, the magnesium oxide reactivity was determined by using the citric acid reactivity test and by determining the specific surface area of the MgO samples. Both the techniques are discussed further in Chapter two.

1.6 Applications and uses of magnesium oxide

1.6.1 Agricultural uses

Hard burnt magnesia is used in agriculture as a fertilizer or animal feed due to its lower chemical reactivity. Crops such as corn, potatoes, carrots, cotton, tobacco, oil palm etc., are very sensitive to magnesium deficiency, and without sufficient magnesia in the soil or applied as fertilizer, plants and grazing animals can die. MgO is also a source of nutrients for chickens, cattle and other animals. Cattle and sheep require magnesium to guard them against the disease called hypomagnesia (Aral et al., 2004 and Canteford, 1985).

1.6.2 Environmental uses

The environmental uses of magnesium oxide include waste water and sewage treatment (e.g. silica and heavy metals precipitation from industrial waste water), scrubbing of sulphur dioxide and sulphur trioxide from industrial flue gas and as a neutralization agent for some industrial waste water (e.g. rayon manufacture and industrial acid neutralization).

1.6.3 Refractory applications

Dead burnt magnesia can be used in the form of refractory bricks in cement kilns, furnaces, ladles, glass-tank checkers, and secondary refining vessels in the metal refining industry. Refractory grade MgO has a very high resistance to thermal shock and is therefore used in steel production to serve as both protective and replaceable linings for equipment used to handle molten steel (Aral et al., 2004).

Fused magnesia is used in a variety of refractory applications. Due to its excellent strength, abrasion resistance, and chemical stability, it is superior to refractory performance and erosion resistance. Other applications include thermal insulation and electrical insulation (electric ovens and appliances).

1.6.4 Other applications

Caustic calcined magnesia can be used in the extraction of magnesium, production of fused magnesia, in cement, insulation and paper production. It is used as a fertilizer and in animal feeds. It is also used as a stabilizer during vulcanization of rubber and for the production of uranium. Other applications include manufacture of plastic and rubber in industries (Birchal et al., 2001).

Due to light burnt magnesia's wide reactivity range, industrial applications are quite varied and include plastics, rubber, and pulp processing, steel boiler additives, adhesives and acid neutralization.

1.7 Production of magnesium hydroxide

Magnesium hydroxide is a mineral found naturally in the crystalline limestone or as a product of magnesium silicates by decomposition. It can also be recovered from sea water and from the magnesium containing brines and bitterns by precipitation, or it can be produced by the reaction of magnesium containing minerals (such as magnesite or dolomite) with an acid followed by precipitation (Aral et al., 2004). In the laboratory, magnesium hydroxide is prepared by the reaction of MgO obtained from $MgCO_3$ with a range of hydrating agents, where water is the mostly preferred hydrating agent. This hydration process is discussed in Section 1.9.

1.7.1 Magnesium hydroxide from MgO

The laboratory production of magnesium hydroxide from magnesium oxide involves the reaction of a specific amount of MgO with a hydrating agent by the hydration process. In chemical terms, hydration refers to the formation of a hydrated compound from the reaction of water with a solid chemical compound. In this process, a certain quantity of MgO is allowed to react with a certain amount of a hydrating solution for a specific period of time and at a particular reaction temperature, and the precipitate formed in the process is filtered off and dried. The reaction is either stirred or left unstirred for a specified period of time. During the hydration of MgO, some important physical or chemical properties can be investigated, and examples of these include

kinetics of hydration, surface properties of MgO and of the products obtained, mechanism of hydration, mass of products prepared, etc.

1.7.2 Magnesium hydroxide from brines or sea water

Brigss and Lythe (1971) have studied the precipitation of magnesium hydroxide from brines or sea water with an alkali. Their procedure of precipitating the magnesium hydroxide from the brines or sea water took place according to the following two stages:

(i) Mixing brine or sea water in an alkaline medium with an amount of alkali in excess of the stochiometric amount necessary to precipitate all of the magnesium ions in the brine or sea water as $Mg(OH)_2$, and thereafter

(ii) mixing fresh brine or sea water in a single stage, two, or more sub-stages, where separate amounts of fresh brine or sea water being added at each sub-stage with the alkaline suspension prepared in step (i) containing the precipitated $Mg(OH)_2$ to precipitate further amounts of magnesium hydroxide.

They used either calcium or sodium hydroxide as their alkali for precipitating the magnesium hydroxide in their process. The precipitated $Mg(OH)_2$ was subsequently washed with an aqueous solution of NaOH or $Ca(OH)_2$. After washing, the magnesium hydroxide was then recovered by filtration where the filtrate aliquots were retuned for further use in the washing steps.

According to Aral et al. (2004), the reactions for production of magnesium hydroxide can be written as follows:

(i) Calcination of dolomite:

$$CaMg(CO_3)_2 \rightarrow CaO{\cdot}MgO + 2CO_2\ (g)$$

(ii) Slaking of dolime:

$$CaO{\cdot}MgO + 2H_2O\ (\ell) \rightarrow Ca(OH)_2 + Mg(OH)_2$$

(iii) Precipitation of $Mg(OH)_2$:

$$Ca(OH)_2 + Mg(OH)_2 + MgCl_2\ (aq) \rightarrow 2Mg(OH)_2 + CaC1_2\ (aq)$$

1.8 Applications and uses of magnesium hydroxide

Magnesium hydroxide has many applications and some of them include the neutralization of acid effluents, removal of heavy metals from industrial effluents, and for flue-gas scrubbing. Magnesium hydroxide can be used as a smoke and flame retardant filler in polymers, as well as the precursor for the production of other magnesium chemicals (Aral et al., 2004).

Magnesium hydroxide can be used to replace lime and gypsum in flue-gas desulphurization plants, especially in power generation and in incineration plants. Scrubbing with lime produces gypsum, which needs to be landfilled in most cases, while scrubbing with sodium hydroxide is very expensive (Aral et al., 2004).

As a medication, magnesium hydroxide (usually called 'milk of magnesia') is used as an antacid for short-term relief of stomach upset and as a laxative for short-term treatment of constipation (URL-2).

1.8.1 Application of $Mg(OH)_2$ in industrial water treatment

Magnesium hydroxide can be applied in the treatment of industrial waste water as 58-62 wt % solids slurry to raise the pH of acidic solutions in an environmentally accepted manner. It is a safer acid neutralizing compound alternative when compared to other acid neutralizing compounds such as caustic soda (sodium hydroxide) or lime, which are commonly used in the neutralization of acidic metal bearing industrial waste (Aral et al., 2004).

Magnesium hydroxide is safe and non-hazardous and will not cause chemical burns as compared to caustic soda or lime. Magnesium hydroxide has the added advantage of having a smaller chance of drastic pH changes when compared to caustic soda and lime. Excessive additions of caustic soda and hydrated lime will result in the pH being raised to 12 and higher, well above the environmentally accepted alkalinity levels for discharge, while wastewater treated $Mg(OH)_2$ will not exceed a pH of 9-10 even if the magnesium hydroxide is added in excess.

1.8.2 $Mg(OH)_2$ as a flame-retardant filler

Magnesium hydroxide has found several industrial applications as was explained earlier. Recently, there has been a growing interest in the use of magnesium hydroxide as a flame-retardant additive and smoke-suppression additive in polymer production (Innes and Cox, 1997; Hornsby and Watson, 1990; Johnson et al., 1999; Molesky, 1991; Rothon and Hornsby, 1996; Zhang et al., 2004).

Magnesium hydroxide has been reported to be the world's mostly widely used flame retardant (Focke at al., 1997). Because it contains no halogens or heavy metals, it is more environmentally friendly than the flame retardants based on antimony metal or halogenated (chlorinated and brominated) compounds. Although the halogenated flame retardants are very effective due to their influence in flame chemistry, their decomposition products are thought to cause environmental concerns, as there is a risk of release of corrosive vapors (Gibert at al., 2000). At approximately 300^{o}C the water molecules in $Mg(OH)_2$ are released in an endothermic reaction. This decomposition temperature is a good match for many polymer systems, and is at a high enough temperature to allow the material to be successfully compounded into most polymers. The released water molecules then quench the surface of the surrounding materials, thus providing flame retardance and smoke suppression. The water molecules should be released at a temperature close to that at which the polymer degrades (Rothon and Hornsby, 1996).

Magnesium hydroxide has been reported to have all the characteristics needed to be a successful flame retardant filler, offering high levels of flame retardency without the smoke and corrosive fumes associated with some other types of flame retardants (Rothon and Hornsby, 1996). Magnesium hydroxide functions as a flame retardant by releasing water vapour in the case of fire and diverts heat away from the flame, thereby reducing the formation of combustible gases. It retards combustion by absorbing heat and by cooling the substrate as it decomposes to MgO and water vapour. In this reaction, heat is taken away from the flame, and the possibility of combustible materials is minimized or stopped. Magnesia with a high surface area forms as the product remaining after the water is released from $Mg(OH)_2$ during fire. This magnesia product can also absorb some smoke. $Mg(OH)_2$ fillers are free of toxic

or corrosive decomposition products, and is therefore safer for the environment and living creatures exposed to fire.

Rocha and Ciminelli (2001) investigated the use of magnesium hydroxide prepared from MgO hydration as a fire retardant in polymers. According to these authors, the halogenated (bromine and chlorine) or phosphorous containing flame retardants generate toxic and highly corrosive fumes during the course of a fire. They also reported that the application of $Al(OH)_3$ as a flame retardant has been limited due to its low decomposition temperature (approximately 180^oC). Magnesium hydroxide decomposes at 350^oC, and as a result of this high decomposition temperature, it is the most generally used flame retardant. In their study, they used magnesium hydroxide from MgO hydration as a fire retardant for nylon 6-6,6, and compared the performance of this filler with that of a commercial produced by the precipitation from brines. Their results demonstrated the potential application of magnesium hydroxide obtained from MgO hydration as fire retardant for a copolymer of nylon 6-6, 6.

Hornsby et al. (1996) have studied the thermal analysis of polyamides modified with magnesium hydroxide fire retardant filler using combined TGA, DSC, EGA and on-line FTIR techniques. They investigated the thermal decomposition of polyamide-6 (PA-6) and polyamide-6, 6 (PA-6, 6) with and without $Mg(OH)_2$ and found that there is a greater overlap between thermal decomposition of PA-6 and the $Mg(OH)_2$ fire retardant filler. According to these authors, $Mg(OH)_2$ functions by endothermic decomposition and concomitant release of water vapour at a temperature in excess of 300^oC, giving an oxide residue which limits thermal feedback to the underlying substrate. It also inhibits polyamide dripping during burning and reduces the level of combustible materials.

The work on the effect of magnesium hydroxide, polyphosphate and diammonium hydrogen phosphate as flame retardants, was performed by Grexa et al. (1999). They prepared flame retardant treated and untreated plywood samples in order to investigate the effect of these samples on plywood. Their results showed that the smoke production during the process decreased with an increase in uptake of flame retardants, but found that the combustible gas (CO) yield, did not increase for samples containing $Mg(OH)_2$, but increased for samples containing the phosphorous type flame retardants.

Wu et al. (1999) have also studied thermal analysis on high density polyethylene-maple wood flour composites using $Mg(OH)_2$ as a flame retardant agent. They prepared various composites of high-density polyethylene (HDPE) with the addition of the compatibilizer, maleic anhydride, and the flame-retardant agent, $Mg(OH)_2$, and it was found that magnesium hydroxide increases the flame-retardancy of the composites.

Camino et al. (2001) compared the flame retardant effect of inorganic hydroxides (aluminium hydroxide and $Mg(OH)_2$) in ethylene vinyl acetate copolymer with that of other inorganic fillers (boehmite and hydrotalcite) using DSC, TG and XRD techniques. They observed the significant flame retardant effects using mass loss calorimetry, which indicated that the poly(ethylene-co-vinyl acetate) polymer filled with 50 wt % of hydrotalcite had the lowest amount of heat released and the lowest evolved gas temperature.

Hornsby and Mphupha (1994) studied the rheological characterization of polypropylene filled with $Mg(OH)_2$. In their results, they illustrated the effects of filler particle size, morphology and surface coating on the rheology of the composites, where the presence of $Mg(OH)_2$ in the composites caused a significant increase in the shear viscosity of polypropylene relative to unfilled polymer.

1.9 Previous studies related to this study

1.9.1 Hydration of MgO to $Mg(OH)_2$ in water

Hydration in chemical terms refers to the formation of a hydrated compound (such as magnesium hydroxide, calcium hydroxide, etc.) from the reaction of water with a solid compound. The study of the hydration of magnesia (MgO) using water as a hydrating agent has been done in the past for various purposes. Most authors focused their studies on the kinetics of the hydration of MgO obtained from calcined magnesite.

Rocha et al. (2004) have studied the kinetics and mechanism of caustic magnesia hydration. In their study, the hydration of magnesia with a high purity was studied in a batch reactor. They studied the effects of temperature (308-363 K), reaction time (0.5 to 5 h), initial slurry density (1-25 % wt) and particle size in the range -212 ± 75 μm and 45 ± 38 μm. In their findings, they found that magnesia hydration rates increased with an increase in hydration temperature. They also observed that the hydration of MgO increases significantly up to about 4-5 % wt with initial slurry density, stabilizing afterwards. Their reaction was almost unaffected when magnesia with different particle sizes was hydrated because of the similar specific surface areas involved.

The work that was performed by Birchal et al. (2000) was based on the effect of magnesite calcination conditions (i.e. calcination temperature and residence time). They studied the relationship between the reactivity tests of calcined MgO and the response of these tests to MgO hydration. According to these authors, temperature was the main variable affecting surface area and reactivity of MgO, where both increased as temperature increased up to 900^{o}C, and then decreased as the temperature increased beyond 900^{o}C.

Raschman and Fedorockova (2004) studied the effect of acid concentration on the dissolution rate of MgO during the hydration of dead-burnt magnesite. After studying the effects of parameters like temperature, activity of H^{+} ions, particle size and the composition of the solid, they discovered that the dissolution of MgO was strongly

affected by temperature (from 45 to 75^{o}C) and particle size (from 63 to 355 μm), while the effect of the composition of the solid was weak. According to Raschman and Fedorockova, the dissolution is controlled by the chemical reaction of MgO with H^{+} ions at the liquid-solid interface.

Smithson and Bakhshi (1969) studied the kinetics and mechanism of the hydration of MgO in a batch reactor. They investigated the kinetics of the reaction between water and MgO powders at 9, 18, 28 and 38^{o}C in a stirred batch reactor. They studied six commercial samples of MgO prepared from $Mg(OH)_2$ plus two of unknown origin with specific surface areas of 12 to 80 $m^2\ g^{-1}$, and after correcting for particle size distribution, they found that the rate of reaction was found to be directly proportional to the surface area .

In the study performed by Maryska and Blaha (1997), the effect of temperature and time of calcination of magnesium hydroxide carbonate on the hydration rate of the oxide formed were investigated. Their results showed that the hydration rate of MgO depends on the hydration temperature, calcining temperature and time of calcination. The degree of crystallization and sintering of MgO measured by its specific surface area were also factors that influenced the hydration rate.

Blaha (1995) investigated the rate at which magnesium oxide reacts with water by studying the kinetics of hydration of MgO in an aqueous suspension via a solution mechanism. According to the author, there is an increase in the degree of conversion of magnesium oxide to the hydroxide with both time of hydration and temperature of hydration.

In the study performed by Ekmekyapar et al. (1993), the calcination of magnesite and hydration kinetics of magnesium oxide in aqueous CO_2 gas was investigated. They investigated the calcination of magnesite at different temperatures and for different particle sizes and studied the hydration kinetics of the calcined magnesite using water with CO_2 gas bubbled through as a hydrating agent. The effects of hydration temperature, particle size, stirring speed, CO_2 flow rate, solid/fluid ratio and calcination temperature on the hydration were determined. In their results, they showed that the rate of dissolution of magnesia in aqueous CO_2 increases with

hydration temperature between 10 and 40°C, and with a decrease in its particle size. They also showed that the rate of dissolution was not affected by the flow rate of CO_2 between 26.85 and 78.73 h^{-1}. The dissolution was also slightly affected by stirring speed. According to these authors, the solid to liquid ratio is an important factor on the dissolution, and the dissolution is increased with a decrease in this ratio. The hydration reaction was confirmed to be a homogenous first order reaction, with activation energy and pre-exponential factor of 32.7 and 2.51 kJ mol^{-1}, respectively.

Khangaonkar et al. (1990) performed studies on the particle breakage during the hydration of calcined magnesite in water at different time intervals and different temperatures between 30 and 80°C. The particle size of magnesia decreases continuously during hydration in spite of the increase in mass due to hydration and a reduction in density, both involving an appreciable increase in volume. An apparent breakage is due to chemical reaction, with the product layer of hydroxide causing stresses leading to breakage, instead of continued growth of the layer. This breakage causes a fresh magnesia surface to be made available, leading to further rapid reaction and breakage. The repetitive cycle leads to an exponential rise in the number of particles and particle surface area, during the later stages of the reaction.

Ranjitham and Khangaonkar (1989) have investigated the hydration of calcined magnesite at elevated temperatures under turbulence conditions. They studied the kinetics of the reaction between water and calcined magnesite and the effect of temperature, particle size, and calcination temperature on the rate of hydration. They have shown that the rate of hydration increases with a rise in reaction temperature, and that the rate of hydration is controlled by the rate of the chemical reactions taking place at the MgO particle surface.

The results reported by Sharma and Roy (1977), on the thermal studies of the hydration of burnt magnesite indicate that the hydration of magnesium oxide is greatly minimized if magnesite is dead burnt. Periclase, a crystalline variety of MgO, is formed on dead burning of magnesite. Their results have shown that the hydration tendency of magnesite calcined at any temperature between 550 and 750°C is of the same order, but calcination at higher temperatures result in a decrease in the hydration tendency, probably due to the formation of the more stable periclase. These results

agree with the results found by Birchal et al. (2000), who found that the specific surface areas of the calcined MgO are nearly constant at 850 to 900^{o}C and then decreases with further increase in calcination temperature of magnesia. According to them, as the temperature increases, crystal size increases and thus surface area decreases, which then decreases the hydration tendency of MgO. Razaouk and Mikhail (1959) have also reported that by raising the calcination temperature of magnesium oxide, sintering is increased until a temperature is reached when the oxide becomes dead burnt.

In general, these authors showed that the most important parameters that can influence the performance of MgO towards hydration to $Mg(OH)_2$ are the calcination temperature and time, hydration temperature, hydration time, surface area and crystal size of MgO, initial slurry density, particle size, solid to liquid ratio and also the stirring speed.

1.9.2 Hydration of MgO to $Mg(OH)_2$ in magnesium acetate

Hydration of magnesium oxide in solutions of magnesium acetate has been studied by several authors, and will be discussed briefly in this section.

Filippou et al. (1999) have studied the kinetics of magnesia hydration in magnesium acetate solutions. In their work, industrially heavily burnt magnesia powders were hydrated in 0.01 to 0.1 M magnesium acetate solutions at temperatures ranging between 333 to 363^{o}C. They found by analysis of their kinetic data that the hydration of heavily burnt magnesia in magnesium acetate solutions proceeds via dissolution precipitate process and it is controlled by the dissolution of the magnesia particles. They observed that the acetate ions play a very important role in enhancing the rate of MgO hydration, due to its complexation power. Their proposed mechanism is discussed further in Section 1.9.3.

Van der Merwe et al. (2004) performed a thermogravimetric study on the hydration of medium reactive industrial MgO using magnesium acetate as a hydrating agent. They found that the degree of hydration measured as the percentage $Mg(OH)_2$ formed, increases from about 56 % using 0.5 M magnesium acetate at 25^{o}C to 64 % at 50^{o}C, and up to more than 70 % at 70^{o}C. They also reported that the increase in temperature increases the solubilities of magnesium oxide and magnesium acetate. This increase in solution temperature resulted in a higher concentration of magnesium ions in solution, which precipitated out as magnesium hydroxide, being less soluble than magnesium acetate.

1.9.3 Mechanism of MgO hydration

The study of the hydration of magnesium oxide has resulted in an interest in the investigation of the mechanism of MgO hydration by several authors. The rate of dissolution of magnesium oxide particles during hydration is one of the important factors involved in the mechanism of MgO hydration (Vermilyea, 1969).

In the study of the kinetics and mechanism of the hydration of MgO performed by Smithson and Bakhshi (1969), it was reported that the hydration mechanism can be considered to comprise of the following consecutive steps:

(i) The water vapor is firstly adsorbed chemically on MgO and then physically adsorbed on the MgO surface to form a liquid layer.

(ii) The formed liquid layer then reacts with MgO to form a $Mg(OH)_2$ layer.

(iii) The $Mg(OH)_2$ subsequently dissolves in this water layer.

(iv) The layer becomes saturated with $Mg(OH)_2$ and precipitation occurs. In this process, the nuclei are formed at the interface between the chemically and physically adsorbed water at points where active sites occur on the MgO surface.

According to the mechanism proposed above, the rate of hydration may be limited by the rate at which $Mg(OH)_2$ is removed from the MgO surface when an excess of nuclei are available. Also, the mechanism will apply for the hydration of any aqueous MgO slurry, as the difference will only be in the thickness of the water layer in contact with the solid. A dissolution-reprecipitation process was proposed, not a solid state reaction, since the particles of MgO undergoing hydration was observed to decrease in size with time.

The kinetics of the hydration reaction must be carefully controlled in order to obtain a $Mg(OH)_2$ with desirable properties. Very rapid hydration of magnesia may result in the formation of relatively large hydroxide aggregates having submicroscopic crystallites with a very high surface–particle morphology which may be unacceptable for certain applications (Fillippou et al., 1999).

According to Smithson and Bakhshi (1969), there are two surface chemical reactions taking place when MgO reacts with water and goes into solution as $Mg(OH)_2$. These are the formation of $Mg(OH)_2$ and the removal of $Mg(OH)_2$ from the MgO surface. Since MgO reacts very quickly with water and because of the high concentration of these two reactants in contact with one another, it seems that the formation of $Mg(OH)_2$ will be more rapid than its removal on the surface, and as a result, the removal of product $Mg(OH)_2$ from the surface of MgO seems to be the rate controlling step.

The hydration of MgO hydration in water occurs according to the following reaction equation (Kato et al., 1996):

$$MgO\ (s) + H_2O\ (\ell) \rightarrow Mg(OH)_2\ (s)$$

The above reaction equation involves steps of magnesia dissolution followed by magnesium hydroxide precipitation (Birchal et al., 2001 and Rocha et al., 2004). The water molecules adsorb chemically on the surfaces of the metallic oxide as follows:

$$MgO\ (s) + H_2O\ (\ell) \rightarrow Mg(OH)_2\ (s)$$
$$\rightarrow Mg(OH)^+\ (surface) + OH^-\ (aq)$$

The above equation indicates that the surface of magnesium oxide, if hydroxylated in the presence of water, contains OH^- in equilibrium with $Mg(OH)^+$ sites at the surface of the solid.

According to Rocha et al. (2004), magnesium oxide has a zero point charge (ZPC) value of 12.5 ± 0.5, and $MgOH^+$ sites seem to predominate on the MgO surface at pH values below 12.5 ± 0.5. However, the $MgOH^+$ ions do not predominate in solution below pH 11.5, and so the Mg^{2+} ions are mostly in solution, and they proposed that the following reaction may occur in the system:

$$Mg(OH)^+ (surface) \rightarrow Mg^{2+} (aq) + OH^- (aq)$$

Rocha et al. (2004) then proposed that the reaction is controlled by the MgO dissolution for particles of constant size, and the mechanism consists of the following steps:

(i) Water adsorbs at the surface and diffuses inside porous MgO particles simultaneously;
(ii) Oxide dissolution occurs within particles, changing porosity with time;
(iii) Creation of supersaturation, nucleation and growth of $Mg(OH)_2$ at the surface of MgO.

Razaouk and Mikhail (1958) have reported that the initial stage during the hydration of magnesia with water vapor is the uptake of water vapor by the oxide which is essentially a rapid van der Waals physical adsorption, together with slower chemisorption, which is followed by a diffusion process to the inside of the solid. The last stage in the hydration process is the recrystallization of the magnesium oxide-water complex ($MgO\text{-}H_2O$) to give a stable magnesium hydroxide lattice. This complex is formed by the interaction of water molecules with magnesium oxide crystallites.

A possible mechanism for MgO hydration in magnesium acetate solutions has been proposed by Fillippou et al. (1999). According to these authors, the acetate ions play a crucial role in increasing the rate of magnesia hydration due to its complexation

power. It is reported that the magnesia particles first dissolve to give magnesium-acetate complex ions, where they migrate away from their mother particles to give a precipitate of magnesium hydroxide. They proposed the following mechanism of MgO hydration in the presence of acetate ions:

Magnesium acetate dissociation

(i) $(CH_3COO)_2Mg\ (aq) \rightleftharpoons 2CH_3COO^-\ (aq) + Mg^{2+}\ (aq)$

Magnesia dissolution by complexation:

(ii) $MgO\ (s) + CH_3COO^-\ (aq) + H_2O \rightarrow CH_3COOMg^+\ (aq) + 2OH^-\ (aq)$

Or even by direct attack by acetic acid which is formed in the bulk of the solution:

(iii) $CH_3COO^-\ (aq) + H_2O \rightarrow CH_3COOH\ (aq) + OH^-\ (aq)$

(iv) $MgO\ (s) + CH_3COOH\ (aq) \rightarrow CH_3COOMg^+\ (aq) + OH^-\ (aq)$

Dissociation of the magnesia complex and magnesium hydroxide precipitation in the bulk of the solution due to supersaturation:

(v) $CH_3COOMg^+\ (aq) \rightarrow CH_3COO^-\ (aq) + Mg^{2+}\ (aq)$

(vi) $Mg^{2+}\ (aq) + 2OH^-\ (aq) \rightarrow Mg(OH)_2\ (s)$

Fillippou et al. (1999) went on to verify their proposed mechanism by performing the hydration tests using NaOH. Their results showed that the rate of magnesium oxide hydration in NaOH without any acetate ions is higher than that in pure water but still lower than that in magnesium acetate. And they also reported that the rate of magnesium hydration is lower in magnesium chloride solutions than in magnesium acetate solutions.

In summary, the mechanism of MgO hydration proposed above in either water or acetate ions is largely controlled by the formation of $Mg(OH)_2$ on the surface of MgO solid and the subsequent precipitation and removal of $Mg(OH)_2$ from the MgO surface. As a result, the MgO hydration is a dissolution precipitation process.

CHAPTER 2

Experimental techniques and methods applied in this study

2.1 Thermal Analysis (TA)

2.1.1 Introduction

Generally, the most important and ubiquitous parameter influencing the efficiency and performance of many materials is temperature. Thermal analysis is an ideal technique for the study of materials and composite structures because the thermal behaviour of a material usually determines the range of operational temperatures of most materials. The physical properties measured during a thermal analysis experiment, are also often directly related to the performance specifications of that material. The study of the effect of heat on a material is thus very important.

Thermal analysis is a generalized term applied to a group of thermal techniques having a common operating principle: a sample is heated or cooled according to a predetermined temperature programme. It is a branch of material science where the properties of samples of matter are studied as they change with temperature. These techniques involve the measurements of certain physical and chemical properties of a substance as a function of temperature, whilst the substance is subjected to a controlled temperature programme (Brown, 1998; Daniels, 1973; Hatakeyama and Liu, 1998).

The properties involved are mainly enthalpy, heat capacity, mass, coefficient of thermal expansion, and will be briefly explained in Section 2.1.2. According to Daniels (1973), the primary requirements that the thermal technique must have are:

(i) A measuring unit
(ii) A temperature control unit
(iii) A recording unit

The main use of thermal analysis measurements is to study the property measurement as a function of temperature by making use of a thermal analysis curve, which defines a measured physical property of a sample recorded as a function of temperature. By interpretation of the thermal analysis curve, both physical and chemical changes occurring in the sample on heating can thus be studied.

Thermal analysis techniques may be classified into three groups, depending on the type of the parameter recorded on the thermal analysis curve (Daniels, 1973):

(i) The absolute value of the measured property itself, e.g. the sample weight,
(ii) The difference between some property of the sample and that of a standard material, e.g. their temperature difference (differential measurements),
(iii) The rate at which the property is changing with temperature or time, e.g. the rate of weight-loss (derivative measurements).

2.1.2 The main thermal analysis techniques

Application of only one thermal analysis technique might not be enough to investigate the thermal behaviour of materials. There are several commonly used thermal analysis techniques, of which the main techniques are: Thermogravimetric analysis (TGA), Differential thermal analysis (DTA), Differential scanning calorimetry (DSC), Dynamic mechanical analysis (DMA) and Thermomechanical analysis (TMA). These are briefly discussed below, and are summarized in Table 2.1.

Table 2.1 The main thermal analysis techniques (Brown, 1988 and Daniels, 1973)

Property	Measured property	Technique	Abbreviation
Weight	Sample weight	Thermogravimetric analysis	TGA
Temperature	Temperature difference between sample and reference	Differential thermal analysis	DTA
Enthalpy	Energy difference between sample and reference	Differential scanning calorimetry	DSC
Mechanical	Sample modulus and damping	Dynamic mechanical analysis	DMA
Mechanical	Compressibility, and extensibility of a sample	Thermomechanical analysis	TMA

Thermogravimetric analysis (TGA) is a technique which measures the weight changes of a substance as a function of temperature or time, whilst the substance is subjected to a controlled temperature programme. A plot of mass or mass percent as a function of temperature or time is called a *thermogram* or *thermal decomposition curve* (Skoog et al., 1998).

Differential thermal analysis (DTA) is a technique in which the temperature difference between a substance and a reference inert material is measured whilst both the substance and the reference are subjected to a controlled temperature programme. This technique is therefore capable of measuring the heat content or heat capacity of the material. Usually, the temperature programme involves heating the sample and the inert reference material in such a way that the temperature of the sample (T_s) increases linearly with time. The difference in temperature (ΔT) between the sample temperature and the reference temperature T_r ($\Delta T = T_r - T_s$) is then monitored and plotted against the sample temperature to give a differential thermogram (Hatakeyama and Liu, 1998; Skoog et al., 1998; West, 1999).

Differential scanning calorimetry (DSC) is a technique in which the difference in energy inputs into the sample and the inert reference material is measured whilst both the sample and the reference are subjected to a controlled temperature programme (Hatakeyama and Liu, 1998). This technique provides valuable information such as curing kinetics, glass transition, melting points, specific heat, crystallinity, oxidative degradation etc. The basic difference between DTA and DSC is that the latter is a calorimetric method in which differences in energy are measured, while DTA records the differences in temperature.

Dynamic mechanical analysis (DMA) is a technique in which the dynamic modulus and damping of a substance under oscillatory load is measured as a function of temperature, whilst the substance is subjected to a controlled temperature programme. Thermomechanical analysis (TMA) measures the change in the linear or volumetric dimensions of a sample as a function of temperature or time (Hatakeyama and Liu, 1998). TMA provides data on the coefficient of thermal expansion, glass transition temperature, gel time and temperature, delaminating temperature, resign flow, materials compatibility and the stability of films and fibres (Daniels, 1973 and Hatakeyama and Liu, 1998).

The abovementioned thermal techniques are by far the most common techniques applicable to material analysis, however, only TGA will be applied in this study since we are interested in the amounts (in mass) of the products produced during the study. This technique will be discussed further in detail in Section 2.2.

2.1.3 Thermal events

By definition, thermal events are those properties in the sample (chemical reactions or physical transitions) resulting from the change in sample temperature. When a single pure solid substance is heated in an inert atmosphere, the resultant increase in molecular, atomic or ionic motion, may lead to changes in crystal structure, sintering, melting or sublimation (Brown, 1988). The main thermal events normally taking place when a solid sample A is heated are summarized in Table 2.2.

Table 2.2 Thermal events taking place on a heated sample (Brown, 1988)

$A (s_1) \rightarrow A (s_2)$, phase transition
$A (s) \rightarrow A (\ell)$, melting
$A (s) \rightarrow A (g)$, sublimation
$A (s) \rightarrow B (s) + \text{gases}$, decomposition
$A (s) \rightarrow \text{gases}$, decomposition
$A (\text{glass}) \rightarrow A (\text{rubber})$, glass transition
$A (s) + B (g) \rightarrow C (s)$, oxidation or tarnishing
$A (s) + B (g) \rightarrow \text{gases}$, combustion or volatilization
$A (s) + (\text{gases})_1 \rightarrow A (s) + (\text{gases})_2$, heterogeneous catalysis
$A (s) + B (s) \rightarrow AB (s)$, addition
$AB (s) + CD (s) \rightarrow AD (s) + CB (s)$, double decomposition

The interpretation of a thermal analysis curve therefore consists in relating the features of the property-temperature curve (peaks, discontinues, changes of slope etc.) to possible thermal events in the sample, i.e. chemical reactions or physical transitions resulting from the change in the sample temperature.

2.1.4 Thermal analysis equipment

Generally, the conformations of thermal analysis (TA) apparatus have a number of features in common. A thermal analysis instrument normally allows a sample to be heated at a uniform rate whilst its physical properties are measured and recorded. A TA instrument consists of a measuring device, a physical property sensor, a controlled atmosphere furnace, the temperature control unit and a recording unit. A schematic presentation of a TA instrument is shown in Figure 2.1.

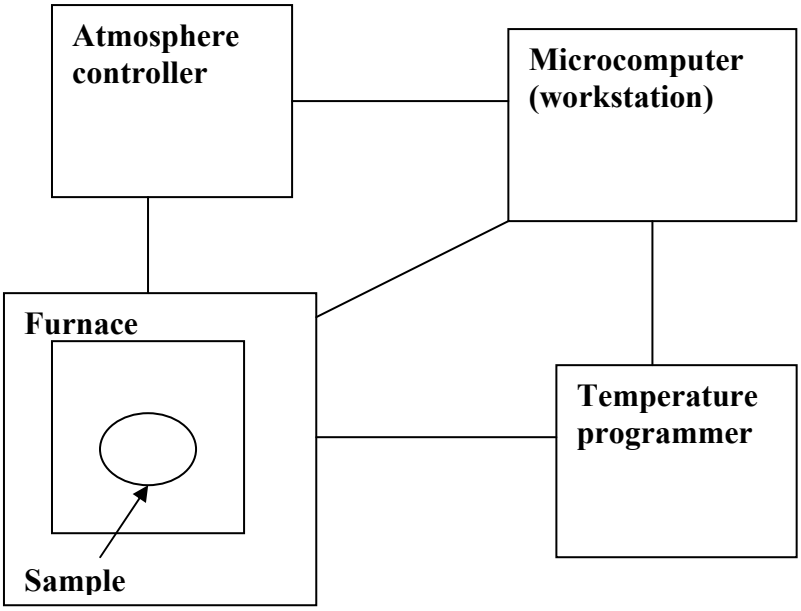

Figure 2.1 A schematic presentation of a TA instrument (Hatakeyama and Liu, 1998)

The measuring device comprises a holder which fixes the position of the sample in the furnace, a system for controlling the atmosphere around the sample, a thermocouple for sensing the sample temperature, and the property sensor itself. The temperature control unit consists of a furnace and a programmer. The function of this unit is to alter the sample temperature in a manner predetermined by the operator, but in many instruments it is the furnace temperature rather than the sample temperature which follows the set programme. The microcomputer unit receives the signals from the property sensor and the sample thermocouple, amplifies them and displays them as a thermal analysis curve.

2.2 Thermogravimetric analysis (TGA)

TGA measures weight changes as a function of temperature. Thermal events are brought about by the thermal changes in the sample. Mass change in the sample can be due to decomposition, sublimation, reduction, desorption, absorption, or vaporization, and these can be measured in TG. These changes are reported directly as milligrams of weight change, or as a percentage of the sample's original weight.

2.2.1 Thermogravimetric instrument

The changes of sample weight in TGA are recorded using a thermobalance. The principal elements of a thermobalance are a combination of a suitable electronic microbalance, a furnace, a temperature programmer, an atmospheric controller, and a computer which records the output from these devices simultaneously. A schematic diagram of a thermobalance is shown in Figure 2.2.

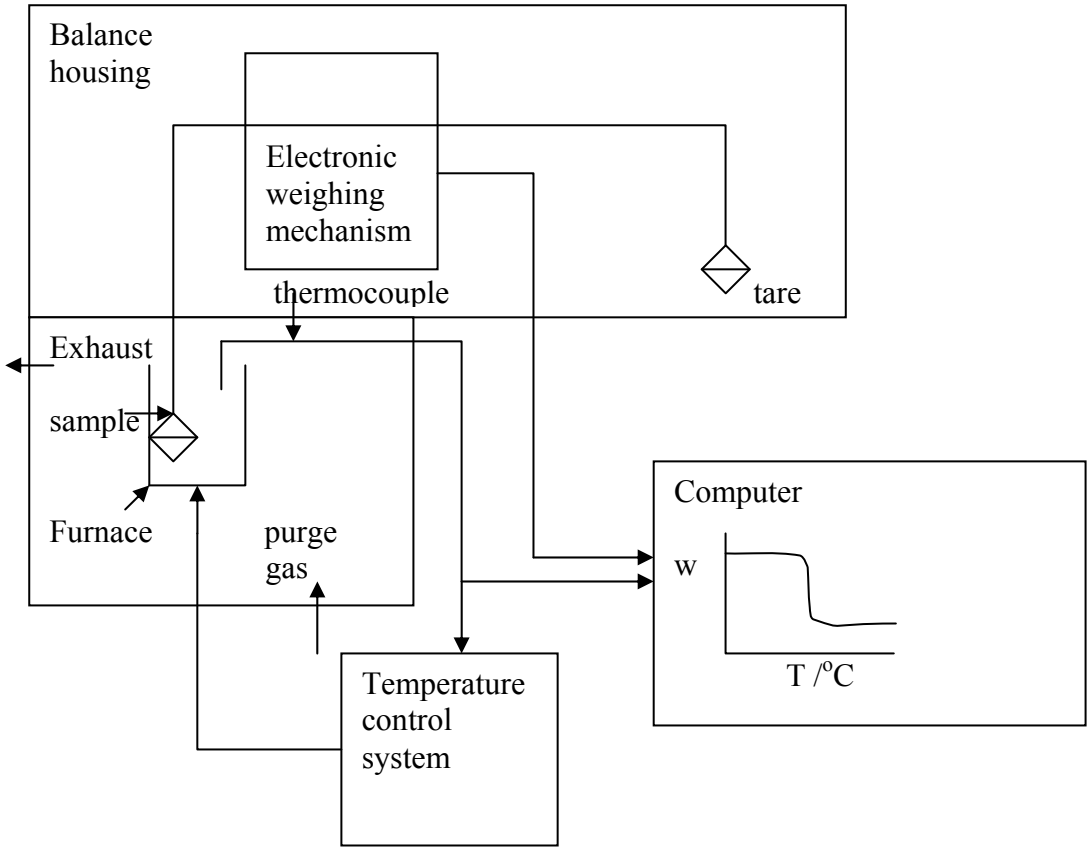

Figure 2.2 A schematic diagram of a thermobalance (Brown, 1988)

In this study, the instrument used was a TGA Q500 from TA instruments depicted in Figure 2.3. The TGA Q500 offers the highest sensitivity (0.1 mg) with a very low baseline drift over the temperature range from ambient to 1000^{o}C. Sample pan loading and furnace movement are automated. The TGA Q500 autosampler is a programmable multi-position sample tray, and allows the routine unattended analysis of up to 16 samples. Purge gas flow rates are settable from 0 to 240 ml min^{-1} in increments of 1 ml min^{-1}.

Figure 2.3 A picture of the TGA Q500 (TA instruments, 2004)

A simplified explanation of a TGA sample evaluation may be described as follows: A sample is placed into a tared TGA sample pan which is attached to a sensitive microbalance assembly. The sample holder portion of the TGA balance assembly is subsequently placed into a high temperature furnace. The balance assembly measures the initial sample weight at room temperature and then continuously monitors changes

in sample weight (losses or gains) as heat is applied to the sample. TGA tests may be run in a heating mode at some controlled heating rate, or isothermally. Typical weight loss profiles are analyzed for the amount or percent of weight loss at any given temperature, the amount or percent of noncombusted residue at some final temperature, and the temperatures of various sample degradation processes.

2.2.2 The electronic microbalance

The balance mechanism (which gives the samples weight signal), forms part of the most important measuring device in TGA. It consists of a mechanical system supporting the sample in a holder so that any change in the sample weight disturbs the mechanical equilibrium and produces a proportional response in the system to counteract the disturbance and restore equilibrium. This counteraction should occur automatically in any balance used for thermogravimetry since continuous automatic recording of weight changes is essential in TG (Daniels, 1973).

Various designs of microbalances can be used. These include beam, spring, cantilever and torsion balances. These balances can operate on measurements of deflection, while others operate in a null mode mechanism. The null mode mechanism is favoured in TG because it ensures that the sample remains in the same zone of the furnace irrespective of changes in mass (Brown, 1988 and Daniels, 1973).

The sensitivity and the maximum load which the thermobalance can accept (without damaging its mechanism), are the two most important characteristics of a thermobalance, and these are interdependent. The maximum load of a balance decreases as its sensitivity increases, but since small samples are preferred in TG, this presents no real difficulty. Typical values are maximum loads of 1 g and sensitivities of the order of 1 μg.

2.2.3 Heating the sample

The sample is heated inside the furnace, which is normally electrically powered through resistive heating. The furnace can be housed within the walls, be part of the housing or can be outside the housing walls. Certain conditions should be met for the furnace when heating the sample (Brown, 1988). The furnace should:

(i) Be non-inductively wound.
(ii) Be capable of reaching 100 to 200^{o}C above the maximum desired working temperature.
(iii) Have a uniform hot-zone of reasonable length.
(iv) Reach the required starting temperature as quick as possible (i.e. have a low heat capacity).
(v) Not affect the balance mechanism through radiation or convection.

Transfer of heat to the balance mechanism can be minimized by the inclusion of radiation shields and convection baffles. To reduce heat transfer by conduction, the furnace tube should extend well beyond the furnace itself and may also have a coolant jacket. The shields or baffles should not cause turbulence or gas streams of sufficient force to disturb the weight measurements when used with a flowing atmosphere (Brown, 1988 and Daniels, 1973).

2.2.4 The atmosphere

The control of the atmosphere around the sample is an important factor since different atmospheres can result in different results during TG analysis. TG is usually measured under various atmospheric conditions, with the choice of a reactive or inert gas in static, flowing or dynamic conditions. For controlled atmospheres, an enclosed balance housing capable of withstanding a vacuum is needed. Thermobalances are normally housed in glass or metal systems to allow for operation at pressures ranging from high vacuum (< 10^{-4} Pa) to high pressure (> 3000 kPa), of inert, oxidizing, reducing or corrosive gases.

The main disadvantage of using a static atmosphere is the possibility of reaction products condensing on the cooler parts of the instrument. In static conditions, the gas composition in the vicinity of the sample varies when a gas generating reaction occurs. These may corrode the balance mechanism or cause a weighing error if deposited on the pan support. The use of a flowing atmosphere or reduced pressure will usually prevent such condensation. Gases normally employed in TG are air, Ar, Cl_2, CO_2, H_2, HCN, H_2O, N_2, O_2, and SO_2 (Brown, 1988; Daniels, 1973; Hatakeyama and Liu, 1998).

Another problem often encountered at low pressures (10^{-2} to 270 Pa), is the thermomolecular flow, which results when there is a temperature gradient along the sample holder and support (Brown, 1988 and Daniels, 1973). This gradient causes streaming of molecules in the direction from hot to cold, giving up spurious weight changes. This problem of thermomolecular can be minimized by:

(i) Working outside the pressure range by adding an inert gas;
(ii) Careful furnace design and sample placement;
(iii) Determination of corrections required using an inert sample.

In a flowing atmosphere, the following advantages during operation of TG can be achieved:

(i) Condensation of reaction products on cooler parts of the weighing mechanism is reduced.
(ii) Corrosive products are flushed out.
(iii) Secondary reactions are reduced.
(iv) The flowing atmosphere acts as a coolant for the balance mechanism.

To allow for the removal of evolved gases during heating of the sample, the sample should be spread thinly around the sample pan (crucible), and the sample crucible should be of low weight and made of an inert material.

A heating rate chosen between 5 and 10^{o}C min^{-1} can be satisfactory, but it will depend on the type of sample and apparatus. A fast heating rate might increase the temperature at which a reaction appears to start, and at which the rate of mass-loss reaches a maximum. It can also extend the range over which a mass-loss is observed. A very slow rate can also extend the temperature range by accentuating the initial slower portion of the reaction.

2.2.5 The sample and crucibles (sample pans)

The sample's physical form can greatly influence the rate of mass-loss by affecting the diffusion of volatiles or transfer of heat through the sample. The rate of diffusion of volatile products to the sample surface must be greater than the rate at which they are generated by the reaction if the measured mass-loss is to reflect the rate of the reaction and not the rate of diffusion. Samples for TG analysis may be in the form of a powdered solid (either compressed to pellets, or spread thinly over the pan surface), thin films or a liquid (Brown, 1988 and Daniels, 1973).

The sample is normally placed in a low mass crucible which is made of an inert material such as platinum or a high temperature ceramic. The sample should be spread out across the crucible so as to facilitate the removal of any gases that are evolved. This also ensures that the sample geometry is uniform between the experiments. Crucibles are chosen according to the purpose of each experiment.

The size of the sample should be small. This is because heat transfer is non-uniform in larger samples and that self heating or cooling may occur within the sample when a reaction occurs. The exchange of volatile products with the atmosphere is also inhibited with larger samples. This all leads to irreproducibility. Small samples also lessen the risk of explosion. Small sample sizes of about 10 mg are usually preferred in TGA since large samples tend to give poorly resolved curves. Also, the choice of sample size is limited by the sensitivity of the balance (minimum size) and the design of the sample holder (maximum size) (Brown, 1988 and Daniels, 1973).

2.2.6 Measurements of temperature and calibration

The temperature programme is most often a linear increase in temperature, but isothermal measurements can also be carried out, when the changes in sample weight with time are followed. The temperature of the sample (T_s) normally lags slightly behind the furnace temperature (T_f), because the heat is transferred from the furnace to the sample. The lag, ($T_f - T_s$), may be as much as 30^{o}C depending on the operating conditions, and increases with an increase in the rate of heating and can thus be more significant in systems under vacuum or when high heating rates are employed (Brown, 1988 and Daniels, 1973).

Measurement of the sample temperature at any point other than in the sample itself will result in an error. A direct sample temperature measurement is also not possible as it affects the weighing process, because if a thermocouple is placed directly in the sample during mass-loss measurements, mechanical interference by the thermocouple leads will cause a weighing error. Therefore, it is advisable to have separate thermocouples for measuring T_s and T_f in order to avoid this mechanical interference.

Following the discussion above, it is therefore necessary to calibrate the TG instrument for temperature using standard materials with known melting points. This can be achieved by performing Curie point measurements on ferromagnetic materials. On heating a ferromagnetic material, its ferromagnetism is lost at a characteristic temperature known as the Curie point. The Curie point of a ferromagnetic material is defined as the temperature at which the ferromagnetic material becomes paramagnetic and the measured magnetic force is reduced to zero (Brown, 1988; Daniels, 1973; Hatakeyama and Liu, 1998).

When performing a temperature calibration, a ferromagnetic sample is placed on the sample pan, and a magnet is positioned just below the sample pan and the furnace. The total downward force on the sample pan is the sum of the sample mass and the magnetic force. Upon heating of the sample, it loses its ferromagnetism at a characteristic temperature, the Curie point of the sample. At the Curie point, the magnetic force is reduced to zero, and an apparent mass-loss is observed. Using several ferromagnetic materials, a multi-point temperature calibration may be achieved under normal operating conditions of the balance (Brown, 1988 and Daniels,

1973). A multiple-point calibration is more accurate than a single-point calibration. Ferromagnetic materials commonly used include Gadolinium (16^{o}C), Alumel (163^{o}C), Permanorm 3 (266.4^{o}C), Nickel (354.4^{o}C), Mumetal (385.9^{o}C), Permanorm 5 (459.3^{o}C), Perkalloy (596^{o}C), Trafoperm (754.3^{o}C), Iron (770^{o}C), Hisat 50 (1000^{o}C) and Cobalt (1131^{o}C) (Brown, 1988 and URL-4).

2.2.7 Precautions when performing TG

During the operation of a TG instrument, there are some precautions and procedures to be followed in order to obtain good TGA results. Some of the most important precautions are discussed below:

(i) Do not exceed the operating temperature of the furnace, as this can damage the instrument.

(ii) Make sure that the thermocouple is in close proximity to the sample, failure to do so may result in spurious results.

(iii) Make sure that the pan/sample does not touch the side of the furnace.

(iv) Make sure that the exhaust remains clean and open, because the exhaust is at lower temperature than the sample, material that sublimes, may easily precipitate here.

(v) Always operate the instrument using flow rates recommended by the manufacturer. Too high flow rates may blow the sample out of the pan leading to spurious mass changes. Too low flow rates may lead to spurious changes where sample condenses in the cooler part of the furnace.

(vi) Avoid large samples. Large samples will take longer to lose mass. Explosive gas build up may occur within the sample causing sample to jump out of the pan.

(vii) Beware of sample geometry effects; this can often be overcome by crushing powder samples in a mortar and pestle prior to analysis.

(viii) Calibrate for temperature.

(ix) Beware of leaks into the gas system.

2.2.8 Typical TG curves

During TG analysis, a sample decomposes upon heating and then loses volatile materials which escape from the sample causing a decrease in weight. As the temperature increases, successive decomposition reactions will occur, and a TG curve is obtained. A TG curve shows a series of weight-losses separated by plateaus of constant mass. Figure 2.4 shows a schematic weight-loss measurement.

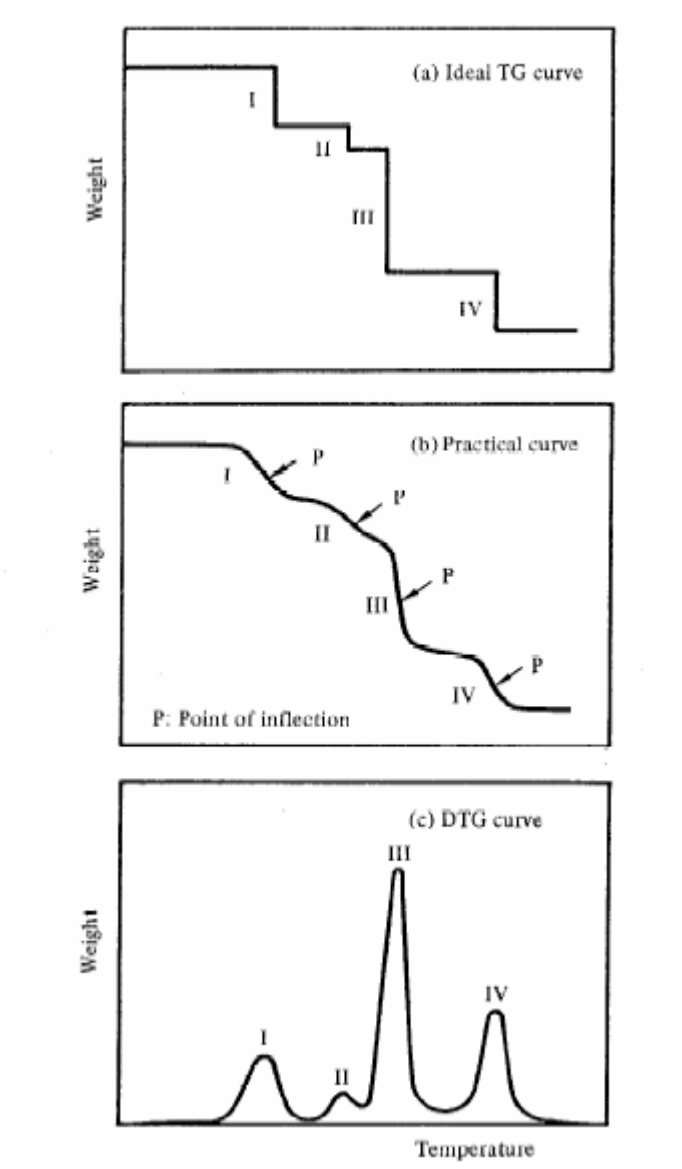

Figure 2.4 A schematic weight-loss measurement of a typical TG curve (Daniels, 1973)

Ideally, one can expect a TG curve like the one in Figure 2.4 (a), however, since chemical reactions are temperature dependent rate processes, weight losses do not occur at one temperature, but over a range, and as a result, some reactions may overlap so that a constant mass plateau does not necessarily occur between them, and the overall step like appearance of the ideal TG curve (Figure 2.4 (a)) is smoothed out in practice by the TG curve obtained in Figure 2.4 (b). The number of these decomposition stages and the temperature range and fractional mass-loss of each stage can thus be evaluated directly from the TG curve if stages are clearly resolved. Resolution of stages of more complex TG curves can be improved by recording DTG (derivative thermogravimetry) curves shown in Figure 2.4 (c). Figure 2.5 shows some of the typical curves normally obtained in thermogravimetric experiments.

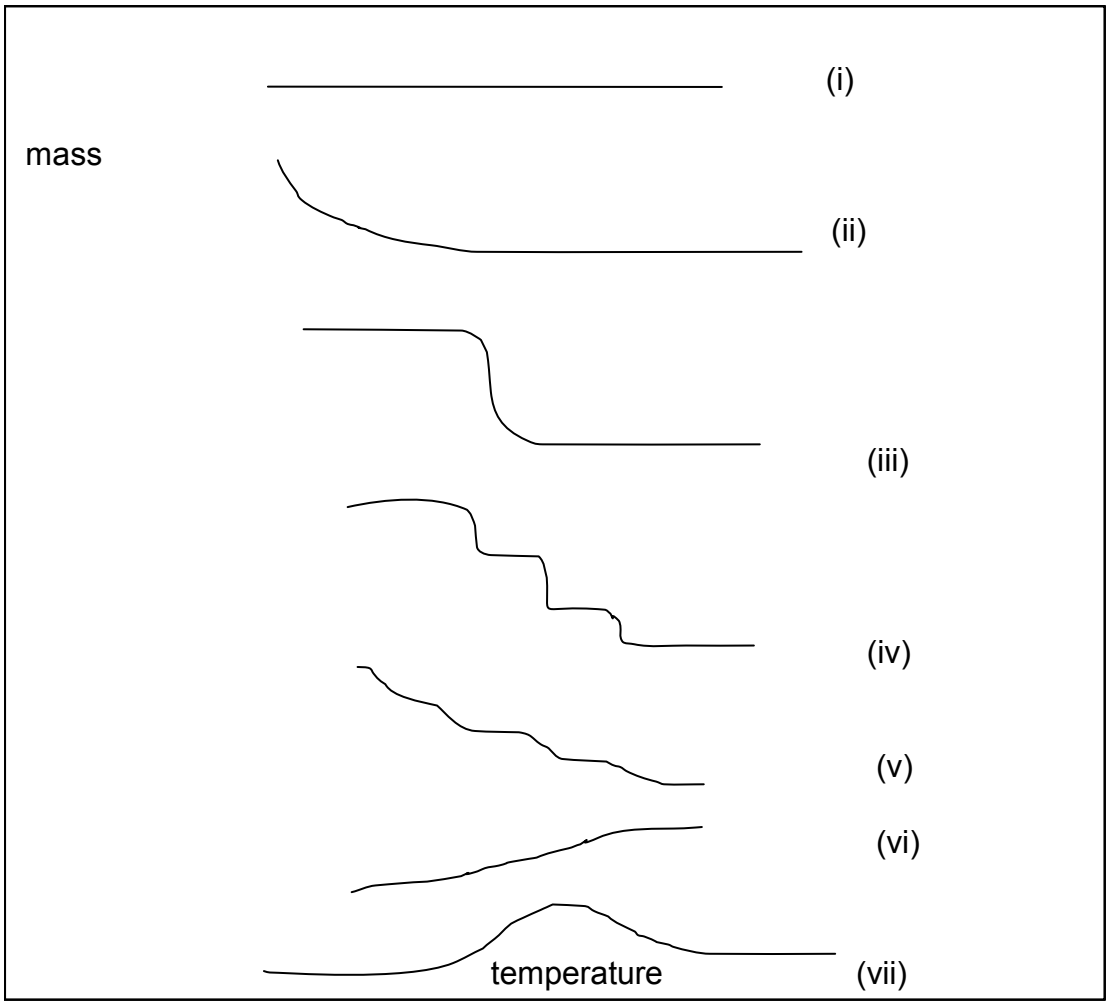

Figure 2.5 Typical TGA curves (Brown, 1988)

(i) The sample undergoes no decomposition, with no loss of volatile products over the temperature range shown. The sample is stable over the temperature range.

(ii) This is a rapid desorption which is characteristic of drying experiments. Such curves often indicate wet samples or samples containing high amounts of solvent.

(iii) This shows a single stage decomposition, which can be used to define the limits of stability of the reactant, to determine stoichiometry of a reaction, or to investigate the kinetics of the reaction.

(iv) Decomposition occurs in multi-stages, with relatively stable intermediates which can also be used to define the limits of stability of the reactant.

(v) Decomposition in multi-stages typical of unstable intermediates.

(vi) Mass increase as a result of interaction of the sample with the surrounding atmosphere, e.g. oxidation of metal sample.

(vii) Here the product of an oxidation reaction in (vi) decomposes at still higher temperature (e.g. $2Ag + 0.5O_2 \rightarrow Ag_2O \rightarrow 2Ag + 0.5O_2$).

To increase the resolution of TG curves, it is necessary to change the heating rate in coordination with the decrease in mass. This technique is called controlled rate thermogravimetry (CRTG). Dynamic rate control, step-wise isothermal control, and constant decomposition rate control are those types of techniques usually employed for controlling the temperature and improving the TG curves (Hatakeyama and Liu, 1998).

2.2.9 Applications of TG

Thermogravimetry has a wide range of applications, of which some important ones are given below (Daniels, 1973):

Physical studies

(i) Reaction kinetics

(ii) Information for the construction of phase diagrams

(iii) Sorption measurements (and surface area determination based upon gaseous adsorption techniques)

(iv) Volatility or sublimation measurements

Chemical studies

(i) Desolvation (particularly dehydration)

(ii) Purity determination

(iii) The evaluation of catalysts and additives in materials

(iv) Thermal and thermo-oxidative degradation

(v) Evaluation of precipitates

(vi) Assessment of the effect of different atmosphere (i.e. corrosion and chemical resistance tests)

(vii) Identification of materials

2.3 BET Surface Area Analysis

2.3.1 Introduction

Surface area and porosity are the two most important physical properties that determine the quality and utility of many materials. Differences in the surface area and porosity of particles within a material can greatly influence its performance characteristics. The surface area of particles serves as a measure of how fast the reaction at the exposed surface area will take place. Specific surface area is defined as the ratio area/mass (unit: $m^2 g^{-1}$) between the absolute surface area of a solid and its mass (sample weight). The surface area includes all parts of accessible inner surfaces (mainly pore wall surfaces). For a given mass of a solid, the specific surface area increases dramatically as the particle size decreases, i.e., subdivision of a solid sample usually leads to an increase in the surface area.

2.3.2 Adsorption

Physical adsorption of gases is a very popular method for the characterization of mesoporous solids, materials often encountered as adsorbents, molecular sieves, catalysts and fillers (Muller and Mehnert, 1997). The attachment of particles on the surface of a solid is termed *adsorption*, and the substance that adsorbs is called the *adsorbate.* Adsorption is brought about by the forces acting between the solid and the molecules of the gas. These forces are of two kinds: physical and chemical, and they give rise to physical adsorption and chemisorption respectively (Gregg and Sing, 1967). A number of methods exist to characterize a solid surface area, depending on the degree of information needed.

Solid surfaces to be analyzed by physical adsorption methods must be free of previously adsorbed (physisorbed) materials. One example of these materials is water which is normally strongly adsorbs on most samples of matter. To free samples from these adsorbed materials, samples are treated at elevated temperatures to enhance the cleaning process. This is normally achieved by allowing either vacuum or an inert gas (e.g. N_2) to flow over the sample for some period of time (Gregg and Sing, 1967).

Two methods are usually used to determine the adsorption isotherm which is normally constructed by measuring the uptake of gas (adsorptive) at increasing partial pressures over the sample (adsorbent). The adsorption isotherm is the plot of the amount gas adsorbed (in mol g^{-1}) as a function of the relative pressure. These methods are the volumetric and gravimetric experiments. In volumetric methods, the amount of gas adsorbed at each consecutive step in the process is derived from the residual gas pressure over the sample after the pressure-equilibrium is achieved. In gravimetric methods, the amount of gas adsorbed is directly determined by weighing the mass increase of the sample with a microbalance (Muller and Mehnert, 1997).

2.3.3 Determination of surface area: BET theory

The most widely used technique for the determination of surface area by gas adsorption is the physical adsorption of nitrogen gas at low temperature (the boiling point of liquid nitrogen) by the BET method. The theory behind BET (Brunauer, Emmett and Teller) surface area analysis is that the surface area of a sample can be described by the amount of a gas of known surface area that sorbs on the surface of the sample. To do this, samples are degassed at an elevated temperature for several hours to pull off any atoms or molecules (such as water) attached to the surface of the sample. A pure gas (such as N_2) is then allowed to flow over the sample at a fixed temperature. Any gas that remains (the difference between the amount flowing in and that flowing out) is attached to the surface of the sample.

The BET method involves the determination of the amount of the adsorbate or adsorptive gas required to cover the external and the accessible internal pore surfaces of a solid with a complete monolayer of adsorbate. This monolayer capacity can be calculated from the adsorption isotherm by means of the BET equation which describes the adsorption of a gas upon a solid surface.

The monolayer capacity is defined as the quantity of the adsorbate which can be accommodated in a completely filled, single layer of molecules (a monolayer) on the surface of the solid. The specific surface area S, (in $m^2 g^{-1}$), is directly proportional to the monolayer capacity, and they are related by the following equation (Gregg and Sing, 1967):

$$S = \left(\frac{X_m \cdot N}{M \times 10^4} \right) \cdot A_m \times 10^{-16}$$

$$= \left(\frac{X_m}{M} \right) \cdot N \cdot A_m \times 10^{-20}$$

where:

N = Avogadro constant (= 6.023 x 10^{23} molecules mol^{-1})

X_m = the monolayer capacity in grams of adsorbate per gram of solid.

M = the molar mass of the adsorbate.

A_m = the surface area in square Ångstrom units occupied per molecule of adsorbate in the completed monolayer.

The gases used as adsorptives have to be only physically adsorbed by weak bonds at the surface of the solid due to van der Waals forces, and can be desorbed by a decrease in the pressure at the same temperature. The most common gas is Nitrogen at its boiling temperature (-195.9°C). In the case of a very small surface area (< 1 m^2 g^{-1}), the sensitivity of the instruments using nitrogen is insufficient and Krypton, boiling at -195.9°C should be used.

In order to determine the adsorption isotherm volumetrically, known amounts of adsorptive are admitted stepwise into the sample cell containing the sample previously dried and outgassed by heating under vacuum. The amount of gas adsorbed is the difference of gas admitted and the amount of gas filling the dead volume (free space in the sample cell including connections). The adsorption isotherm is the plot of the amount gas adsorbed (in mol g^{-1}) as a function of the relative pressure, p/p_o (p = equilibrium pressure, and p_o = vapour pressure).

The BET theory uses the BET equation to calculate the monolayer capacity from the amounts adsorbed at different relative pressures (Muller and Mehnert, 1997):

$$\frac{p}{n(p^o - p)} = \left(\frac{1}{n_m C} \right) + \frac{C - 1}{C n_m (p/p^o)}$$

where:

n = the amount of gas adsorbed at relative pressure p/p^o

n_m = the monolayer capacity

C = BET constant, which is related to the heat of adsorption (enthalpy) at the first adsorbed layer. It describes how strongly the adsorbate molecules are attracted to the adsorbent surface. Its value is normally in the range 20-200 for reliable surface area results.

The BET equation implies that there is a linear relationship (y = a + bx) between, y = p/ n(p^o-p) and x = p/p^o, and both the intercept (a = 1/ n_mC), and the slope (b = (C-1)/ Cn_m), can be determined by means of linear regression. This straight line is called the BET plot, and occurs within a range 0.05 to 0.30 p/p^o. By solving the BET equation, the monolayer capacity (n_m), can be calculated (Gregg and Sing, 1967).

Assuming a close-packed monolayer, a cross-sectional area for the nitrogen adsorbate molecule (a_m) of 0.162 nm^2 is generally accepted. For Krypton, the value of a_m = 0.202 nm^2 is used. The specific surface area is then calculated using:

$$A_{BET} = n_m \cdot L \cdot a_m$$

where:

L = Avogadro constant = 6.023 x 10^{23} molecules mol^{-1}

A_{BET} = Surface area

a_m = a cross-sectional area of the adsorbate

n_m = the monolayer capacity

The standard BET method requires three or more points in the relative pressure range from 0.05 to 0.30 p/p^o to be taken. If routine measurements are to be performed, a single point on the isotherm usually in the range 0.25 to 0.30 p/p^o is recorded, provided that C >> 100. The monolayer capacity is then calculated by the reduced formula:

$$n_m = \frac{n}{1 - (p/p^o)}$$

When reporting the BET surface area results, it is very important to state the outgassing conditions (temperature, time), the linearity range for the BET plot, as well as the values for p^o, n_m and C.

In this study, a NOVA 1000^e Surface Area and Pore size analyzer from Quantochrome instruments, using nitrogen gas as an adsorbent, was used to determine the surface area of the samples. The surface area of the samples was analyzed and measured by applying a Single Point B.E.T method to the N_2 adsorption data, where the molecular area of N_2 is 16.20 $Å^2\,mol^{-1}$.

2.4 Citric acid reactivity test

It was mentioned earlier in Section 1.5 that the degree of calcination of magnesite ($MgCO_3$) dramatically affects the reactivity of MgO formed by changing its surface area, density and its crystallinity. The end uses of MgO are therefore highly dependent on the calcination temperate achieved. The reactivity of MgO determines the rate and extent of hydration $Mg(OH)_2$ when exposed to water.

It is then imperative to develop test methods that can help in predicting the extent of hydration of a given MgO sample. The information provided by these methods can then be used to control the quality of the sample or to establish process conditions.

Reactivity is generally measured in terms of one or more of the following methods (Canteford, 1985):

(i) Acid reactivity, the time taken for a given weight of magnesia to react with a given volume of organic acid (usually citric or acetic). The time is very much dependent upon particle size.
(ii) Iodine number, the amount of iodine absorbed.
(iii) Specific surface area, determined by the BET method.

In this study, the methods of acid reactivity using citric acid, and the specific surface area were employed. In the citric acid reactivity test, the time needed for the MgO sample to neutralize the citric acid solution was measured.

In this study, a 0.38 M (0.40 N) citric acid solution was prepared, and 2 g ± 0.01 g of the dried powdered MgO sample was transferred into 100 ml of the 0.38 M citric acid solution at 30^{o}C and shaken with phenolphthalein as an indicator until the colour of the slurry changed from white to pink. The time taken for the slurry to change the colour was then reported as the citric acid reactivity. This value gives an indication of the type of MgO formed, whether the MgO formed is highly reactive or less reactive towards hydration. The longer the time it takes for the MgO slurry to change the colour, the lesser reactive is the MgO towards hydration, and vice versa.

Industry uses values of less than 60 s to define a highly reactive (soft burnt) MgO. Medium reactive MgO gives values between 180 and 300 s, while a low reactive MgO (hard burnt) gives a value of more than 600 s and a dead burnt MgO gives values of about more than 900 s.

2.5 X-ray Fluorescence analysis (XRF)

2.5.1 Introduction

X-rays are electromagnetic radiation with wavelengths from approximately 10^{-5} to 100 Å (Angstrom unit, where 1 Å = 10^{-10} m). They were discovered by the German physicist W.E. Roentgen in 1895. Unlike ordinary light, X-rays are invisible but can travel in straight lines, and they have the ability to penetrate different materials to different depths (Jenkins and Snyder, 1996 and Skoog et al., 1998).

X-ray Fluorescence Spectroscopy is a technique used for the total determination of major and trace elements by measuring secondary X-ray emission after a solid sample is bombarded with a primary X-ray beam. These elements have characteristic energy levels for secondary X-ray emission with the intensity of the emission characteristic of the concentration. In XRF spectroscopy, the analyst uses wavelengths between the U Kα at 0.1 Å (10^{-11} m) and F Kα at 20 Å (2 x 10^{-9} m). Another description of X-rays is as particles of energy called photons.

The energy of an X-ray photon is measured in kiloelectron volt (keV), a unit of energy acquired by an electron when it is accelerated by a potential of 1 volt (1 volt = 1.602 x 10^{-19} J). The energy of an X-ray photon is measured by using the Duane-Hunt law given by Nuffield (1966):

$$E = \frac{h \times c}{\lambda}$$

where:
h = Planck's constant (6.626 x 10^{-34} J s)
c = Speed of light (3.00 x 10^{8} m s^{-1})
λ = wavelength (m) (1 Å = 10^{-10} m)

Thus E (keV) = 12.4/ λ (Å). The above equation implies that the higher the energy, the smaller the wavelength.

2.5.2 Generation of X-rays

X-rays are produced when high energy charged particles (such as electrons) are accelerated through a very high potential difference and collide with matter. In this process, a beam of electrons accelerated at high potential (usually in the order 30-60 kV) are allowed to strike a piece of a metal target attached to the anode. The incident electrons must have enough energy in order to ionize some of the 1s (K shell) electrons, Figure 2.6 (Jenkins and Snyder, 1996; Nuffield, 1966; West, 1999).

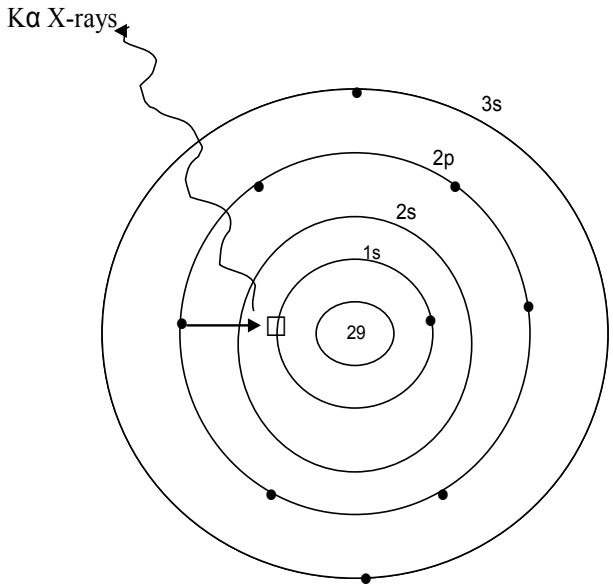

Figure 2.6 Generation of Kα X-rays (West, 1999)

In the above figure, an electron in an outer orbital (2p or 3p; L or M shell) immediately drops down to occupy the vacancy created in the 1s level (K shell), and the energy released in the process appears as X-radiation or X-ray photon. X-rays are produced inside the X-ray tube shown schematically in Figure 2.7.

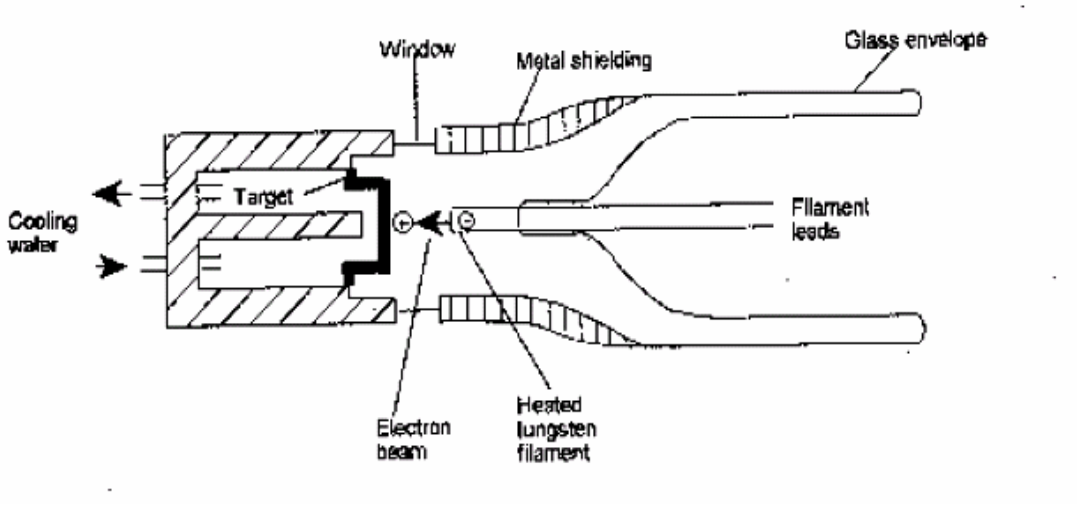

Figure 2.7 Schematic diagram of an X-ray tube (Whitson, 1987)

Inside the X-ray tube, one finds a tungsten filament (cathode, negatively charged), which is heated by an electric current (in mA), through the external filament terminals. This process then produces a cloud of electrons that are accelerated along the focusing tube by the potential difference (in kV), which is applied between the filament and the anode (positively charged). The electrons then hit the anode (the target material) and the X-rays are generated and pass through a beryllium (Be) window to the sample. The absorption of X-rays on passing through materials depends on the atomic weight of the elements present and as a result, light metal atoms such as beryllium (atomic number 4) or aluminium (atomic number 13) are the most suitable window materials (West, 1999).

The target material must be made of a high melting material which has a good thermal conductivity. In general, the higher the atomic number of the target material, the more intense the beam of radiation produced by the tube. Typical target materials include transitional metals such as molybdenum, tungsten, copper and chromium (Jenkins and Snyder, 1996 and West, 1999).

During operation, the X-ray tube is normally evacuated to avoid the oxidation of the tungsten (W) filament. Only a small fraction (< 1 %) of the energy of the incident electron beam is converted into X-rays. Most of the energy is converted into heat, and consequently, continuous cooling with water of the anode is necessary to prevent the target material from melting.

2.5.3 Characteristic radiation

Characteristic radiation is produced from the interaction between the atomic electrons of the target material and the incident particles (high voltage electrons), provided that the energy of the particle is greater than the binding energy of the electrons to the nucleus in the target material. In short, this characteristic radiation is produced when the bombarding electrons have enough energy to dislodge electrons from the inner shell (K shell) in the atoms of the target material. This process then leaves the atom with a vacancy, which is filled by transferring an outer orbital electron (M or L shell) to fill its place. Associated with this transfer and the subsequent lowering of the ionized energy of the atom, is the production of X-rays, a fluorescence X-ray photon of definite wavelength, Figure 2.8. The final resting place of the transferred electron determines the type of radiation emitted (L, M, etc) (Jenkins, 1999 and Nuffield, 1966).

The vacancy in the K shell filled by an L electron produces a $K\alpha_1$ or $K\alpha_2$ X-radiation, depending on the subshell of the electron involved in the transition. If the vacancy in the K shell is filled by an electron from the M shell, the X-ray photon is produced as $K\beta$ radiation. L radiation is produced in a similar way.

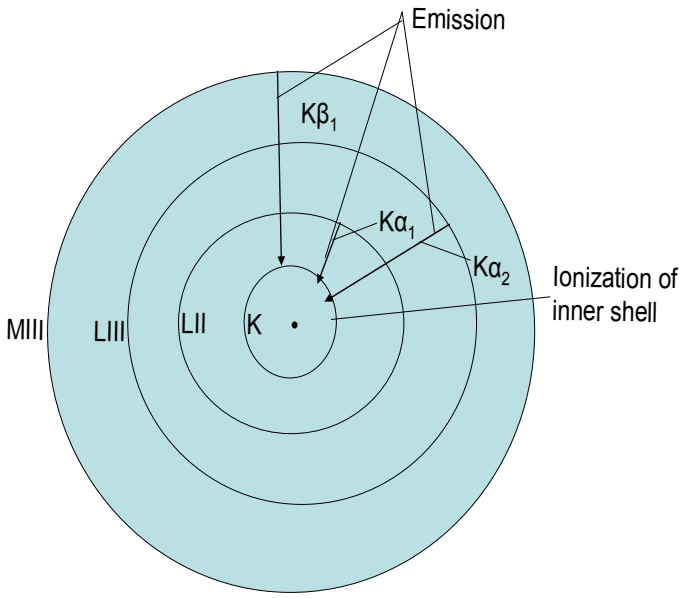

Figure 2.8 Generation of X-rays (Whitson, 1987)

The transition energies have fixed values, and as a result a spectrum of characteristic X-rays results, Figure 2.9. The X-ray spectra have two components, a broad spectrum of wavelengths called white radiation and a number of fixed or monochromatic wavelengths lines of the target material. The white radiation (or continuum) is produced when the electrons are slowed down or stopped by the collision and some of their lost energy is converted into electromagnetic radiation (Jenkins and Snyder, 1996).

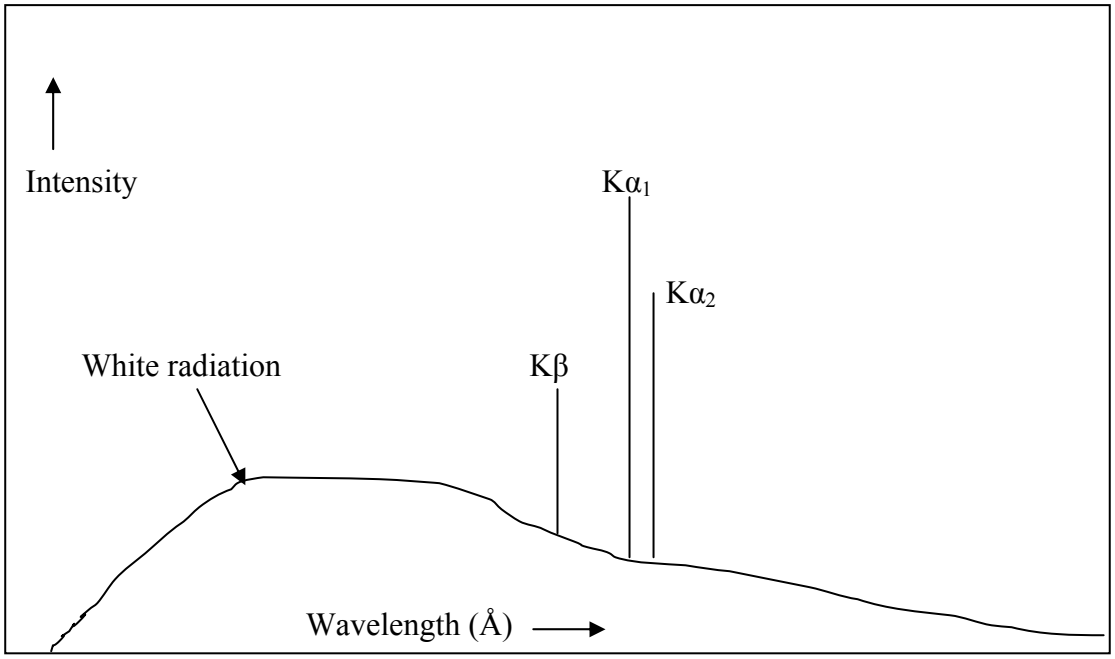

Figure 2.9 X-ray emission spectrum (Nuffield, 1966)

2.5.4 Instrumentation: The X-ray Spectrometer

X-ray Fluorescence (XRF) spectroscopy is a spectroscopic technique capable of providing a non-destructive analytical method capable of analyzing solids from a few parts per million to near 100 % for a wide range of elements. Ideally, this technique is thus suited for the analysis of rocks, soils, dust, contaminated land samples, mineral concentrated products, archaeological artefacts synthetic materials and metals (Brewer and Harvey, 2005). XRF analysis of elements with very low atomic numbers is not possible because the X-rays are actually absorbed before they can be measured.

Nearly all spectrometers comprise an excitation source which is a means of separating and isolating characteristic lines, plus a device for measuring characteristic line intensities. There are two main types of XRF spectrometers: The energy dispersive spectrometer (EDXRF) and the wavelength dispersive spectrometer (WDXRF).

In wavelength dispersive spectrometry, the X-rays or photons emitted are separated by diffraction on a single crystal before being detected. In energy dispersive spectrometry, the detector allows the determination of the energy of the photon when it is detected. The energy dispersive spectrometer is smaller (even portable), cheaper, the measurement is faster, but the resolution and detection limit is far worse than the WDXRF as can be seen from Figure 2.10 below. The overall resolution for WDXRF is much better due to the use of analytical crystals and collimators (Jenkins, 1999).

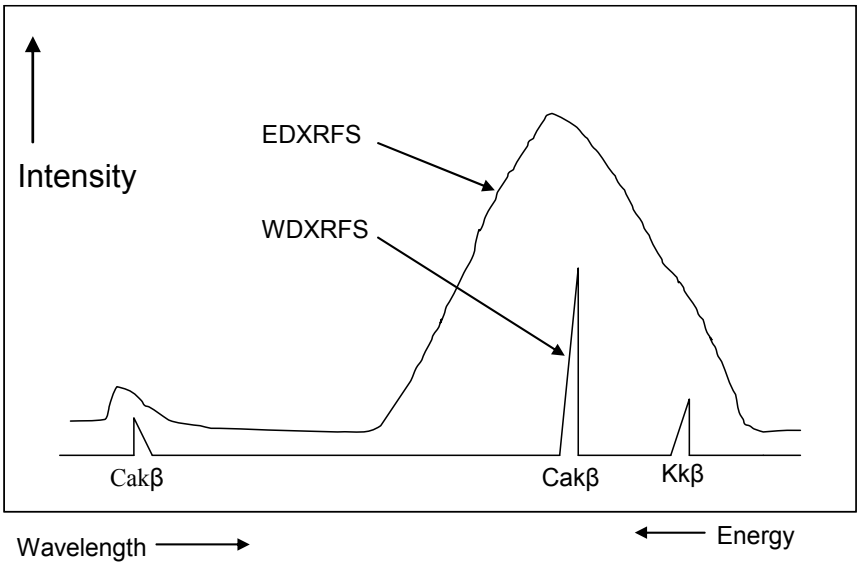

Figure 2.10 Resolution of EDXRF (dotted line) and WDXRF (solid line) (Jenkins, 1999)

EDXRF involves the use of ionizing radiation to excite the sample, followed by detection and measurement of the undispersed secondary X-ray beam comprising all excited lines of all the specimen elements leaving the sample, by the lithium drifted silicon detector. The amplified detector output is then subjected to the pulse height selection in which the pulse distributions are separated on the basis of their photon energies. In EDXRF, the resolution of peaks due to the Si(Li) detector is excellent compared to the scintillation and flow proportional detectors used in WDXRF (Jenkins, 1999).

In a WDXRF spectrometer, the analyzing crystal disperses (splits up) the secondary spectrum from the sample in such a way that each wavelength may be measured individually. Figure 2.11 shows a simplified layout of an XRF wavelength dispersive spectrometer. An X-ray Fluorescence spectrometer consists of three principal sections (Jenkins, 1999 and Jenkins and Snyder; 1996):

(i) The excitation source, where the characteristic X-rays in the sample are excited via the X-ray fluorescence process.

(ii) The sample presentation apparatus, which holds the sample in a precisely defined position during analysis, and provides for introduction and removal of the sample from the excitation position.

(iii) The X-ray spectrometer, which is responsible for separating and counting the X-rays of various wavelength or energies emitted by the sample.

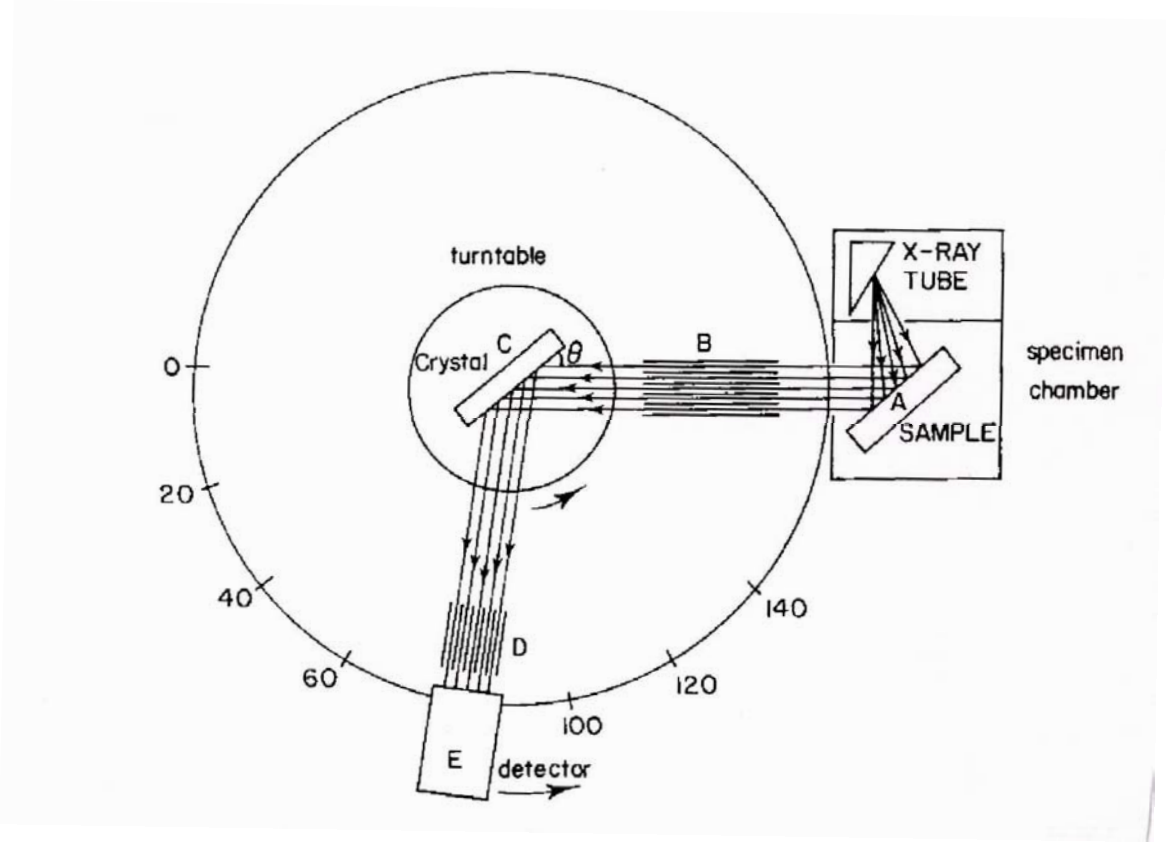

Figure 2.11 Layout of an XRF wavelength dispersive spectrometer (Whitson, 1987)

In practice, a beam of primary X-rays produced from the X-ray tube irradiates the sample (A) and causes it to fluoresce such that each element in the sample will produce its own characteristic X-radiation. Part of the radiation is then collimated by a system of slits (B) onto an analyzing crystal (C). A multi-position crystal changer is usually incorporated in order to cover the full wavelength range of the spectrometer, and it consists of a turntable arrangement holding up to six crystals. The crystal is mounted on a turntable which can be rotated by a motor.

The angle (θ) presented to the fluorescent rays changes as the crystal is rotated, and whenever the Bragg equation is fulfilled for a particular X-ray wavelength, this part of the beam is reflected by the crystal. The reflected beam then passes through a set of collimating slits (D) and enters the detector (E). The crystal table and the detector are connected in such a way that they always rotate together. They are also geared so that when the crystal rotates through an angle θ, the detector rotates through 2θ.

The detector is an electronic device called a counter. It converts the X-rays fluorescent by a sample into electrical pulses in the circuit to which they are connected, and can thus be measured electronically. The detector is always in the correct position to receive any rays reflected by the crystal.

Wavelength dispersive XRF spectrometry is based on the Bragg's law, which is derived with the help of a Figure 2.12 below. In the Bragg approach to diffraction, crystals are regarded as built up in layers or planes such that each acts as a semi-transparent mirror. Some of the X-rays are reflected off a plane with the angle of reflection equal to the angle of incidence, but the rest are transmitted to be subsequently reflected by succeeding planes.

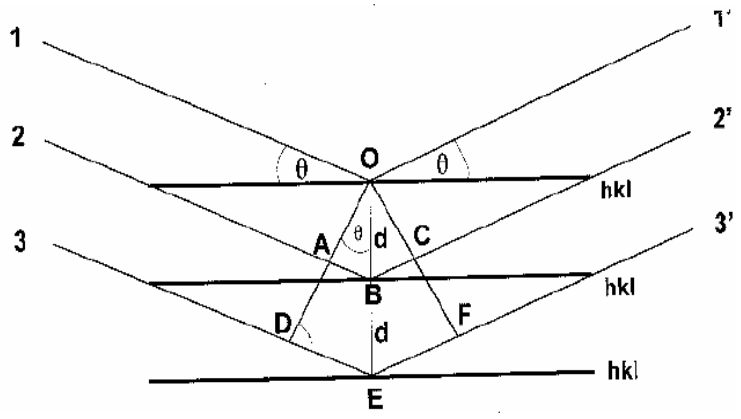

Figure 2.12 The Bragg angle of reflection (Jenkins and Snyder, 1996)

In Figure 2.12, three crystallographic planes with Miller indices (hkl) are shown. Three X-ray beams (1, 2, and 3) are reflected from these three adjacent planes within the crystal, and we wish to know that under what conditions the reflected beams (1', 2' and 3') are in phase. The wave reflecting from the second plane must travel a distance ABC further than the one from the top. The wave reflecting from the third plane must travel DEF further. So, all the waves reflecting from planes below the top plane will be phase retarded with respect to the first wave causing interference. Plane geometry shows that when the distance ABC is exactly equal to one wavelength (λ), the distance DEF will be equal to 2λ, etc, and the reflections from plane of any depth

will be in phase, producing constructive interference (= diffraction). At angles of incidence other than the Bragg angle, reflected beam are out of phase and destructive interference or cancellation occurs (Jenkins and Snyder, 1996 and West, 1999)

The perpendicular distance between pairs of adjacent planes, the d-spacing (d), and the angle of incidence (θ), are related to the distance AB by:

$AB = BC = d \sin \theta$
But, $ABC = n\lambda$, where n is an integer (1, 2, 3 etc)
Therefore $n\lambda = 2d \sin 2\theta$, called Bragg's law

where:
n = order of the diffracted beam and is numerically equal to the path difference, in wavelengths, for successive planes.
d = interplanar spacing of diffracting planes (Å)
θ = Bragg angle, the angle between the incident X-rays and the diffracting planes
λ = wavelength of the spectral line (Å)

A portion of X-rays arriving at each crystal plane is scattered in all directions and they are usually out of phase and undergo destructive interference. In certain directions, they may be in phase and reinforce one another (constructive interference). This is called diffraction and a group of such in one direction is called a diffracted X-ray beam.

An analyzing crystal is a material with a regular, three dimensional periodic arrangement of atoms. Crystal planes reflect X-ray photons like a mirror reflects light with the difference that in a crystal certain conditions for diffraction must be met. A good analyzing crystal must have a high diffraction intensity (reflectivity) and high resolution (good dispersion of peaks). There should be no interfering elements and a low thermal expansion coefficient is important, especially for older generation spectrometers without good temperature control. Commonly used crystals include: LiF, Ge, and graphite.

2.5.5 XRF qualitative analysis

Qualitative analysis in XRF spectroscopy determines which elements are present in an unknown sample of matter. In order to do this, a wavelength scan is done by rotating the analyzing crystal so that all angles between about 15^{o} and 145^{o} are presented to the X-ray beam and the intensity peaks are interpreted. Detected X-rays are then amplified and recorded as a series of peaks on a strip of chart paper or on a computer screen; consequently, both peak positions and intensities (peak heights) are readily obtained from the chart to make this a very useful and a rapid method for elemental analysis (West, 1999).

A scale of 2θ is recorded automatically and all the elements are identified from their tables in conjunction with an appropriate set of wavelength tables for each analyzing crystal. These tables are represented in two parts: the first part is ordered in elements of increasing atomic number, and is used for finding the 2θ position for a specific element. The second part is a list of all the 2θ lines in increasing order, with all the previous information included, and is used when interpreting wavelength scans. The interpretation of an XRF trace then involves reading off the 2θ values of the peaks and then referring to the 2θ line wavelength tables applicable to the analyzing crystal used.

2.5.6 XRF quantitative analysis

Quantitative analysis is the determination of the amount of a particular element that is present in a sample under investigation. To achieve quantitative analysis in XRF, the crystal is set to remain in a fixed position, the goniometer is set on a specific 2θ angle, and the recorded intensity of the peak (count per second) is proportional to the element concentration.

The peak intensity of the analyte is normally not directly proportional to the concentration because of matrix effects, otherwise if this was the case, it could have been achieved by simply comparing the counts obtained from the sample to counts obtained from a standard with a known concentration of the element to be determined. These matrix effects include absorption and enhancement, which are in turn a function of the composition of the sample and the primary spectrum from the X-ray tube because different materials interact differently with X-rays. Quantitative analysis

involves choosing a calibration strategy that can accommodate or attempt to eliminate these effects, and most methods attempt to achieve a simple linear relationship between measured spectral line intensity and concentration (Brewer and Harvey, 2005).

There is a very wide range of methods available to overcome matrix effects, and the three most common include the use of calibration curves, making standard additions and mathematical corrections. Calibration curves are suitable to do routine analyses of samples where standards are readily available. Standard additions are applicable to infrequent analyses where standards are not available. Mathematical corrections are suitable for the routine analysis of large numbers of samples.

2.5.7 Sample preparation for XRF analysis

Preparation of the sample for XRF analysis is a very crucial step since it can form one of the major sources of analytical errors because the final analysis can only be as good as the sample preparation was. Sampling errors can also arise from the taking of small representative subsamples from a large sample. These errors can be minimized by either reducing the particle size or by taking larger subsamples for analysis.

Two of the most used sample preparation methods for XRF analysis are: (i) Fused beads, in which the sample is mixed with a suitable flux and then fused into a glass by either cast or pressed into a disk, and (ii), Pressed powder pellets (briquettes), where the sample powder with or without a binding agent is compressed to produce a solid powder tablet (Brewer and Harvey, 2005).

(a) Fused beads method

Fusion method for XRF analysis involves the fusion of a test portion of a prepared sample with a suitable flux such as lithium metaborate ($LiBO_2$) or lithium tetraborate ($Li_2B_4O_7$) at a temperature between 1000^{o}C to 1200^{o}C, depending on the material type, in a platinum/ 5 % gold crucible. The flat disc can then be presented directly to the XRF for elemental analysis using a casting method. Sample to flux ratios commonly used range from 1:4, up to 1:10. To prevent the sample from sticking to the crucible, a few milligrams of a non-wetting agent is used, and typical agents include KI, LiBr, LiI, and NaI.

Advantages of using the fused beads are:

(i) Homogenous mixtures

(ii) No particle size effects

(iii) No mineralogical effects

(iv) Matrix effects diluted

(v) Mirror surface

(b) Pressed powder pellets / Briquettes

The pressed powder method is mostly suitable when analyzing trace elements in a sample. In this method, the sample powder is mixed with a suitable binder (such as somar mix, sugar, starch, ethyl cellulose, polyvinyl alcohol, urea, boric acid or graphite), and then pressed at ± 7 tons/in^2. The binder must be free of any interfering elements.

The sample prepared using the pressed powder method can also be suitable for XRF analysis, but there can be problems with its homogeneity (Brewer and Harvey, 2005).

2.6 X-ray Diffraction analysis (XRD)

2.6.1 Introduction

Diffraction of X-rays by matter is most powerful when applied to crystalline materials. However, it can also provide important information when applied to amorphous solids or liquids. In diffraction experiments, wavelengths used lie between approximately 0.5 and 2.5 Å. Because it considers the crystal structure of sample of matter, XRD spectroscopy can be used to identify minerals in the sample under investigation.

The diffraction of X-rays from a fine grained crystalline powder is based on the principle that a beam of X-rays that strikes a crystal will pass through it, but with scattering or diffraction of the photons in the beam. Since the particles in the crystal are in a regular or symmetrical arrangement, the X-rays will be scattered in a regular pattern.

X-ray crystallography is a technique in which the pattern produced by the diffraction of X-rays through the closely spaced lattice of atoms in a crystal is recorded and then analyzed to reveal the nature of that lattice (Nuffield, 1966). This generally leads to an understanding of the material and its molecular structure. The spacing in the crystal lattice can be determined by using Bragg's law; which was derived in Section 2.5.4.

In the case of XRD, the system is set up similarly to an XRF spectrometer. The main differences are that the sample gets irradiated by monochromatic radiation (one wavelength) and that it has no analyzing crystal. The sample itself acts as the analyzing crystal and limits XRD analysis to crystalline materials. Since it considers the crystal structure, XRD can identify minerals where XRF is limited to identifying the elements present.

2.6.2 Sources and Detectors for X-radiation

Typically, an X-ray source for powder diffraction measurements has three major components: the line-voltage supply, a high voltage generator and an X-ray tube (Jenkins and Snyder, 1996). The output from an X-ray tube is described in terms of the radiation flux, which is the density of electrons per unit area per second. Figure 2.13 provides a schematic cutaway view of a sealed x-ray tube. Inside the tube, the tungsten filament is heated by the filament current (mA) producing a cloud of electrons, which are accelerated along the focusing tube by the potential difference (kV) between the filament and the anode. The generated X-rays then pass through the Be window to the sample. The conversion of electrons to X-rays is a very inefficient process (< 1 %) since most of the energy is converted to heat. The tube must therefore be cooled with water (West, 1999). Copper anode tubes are the most commonly used in XRD, but other anodes are also used for specific applications and these include Cr, Fe, Co Rh and Mo.

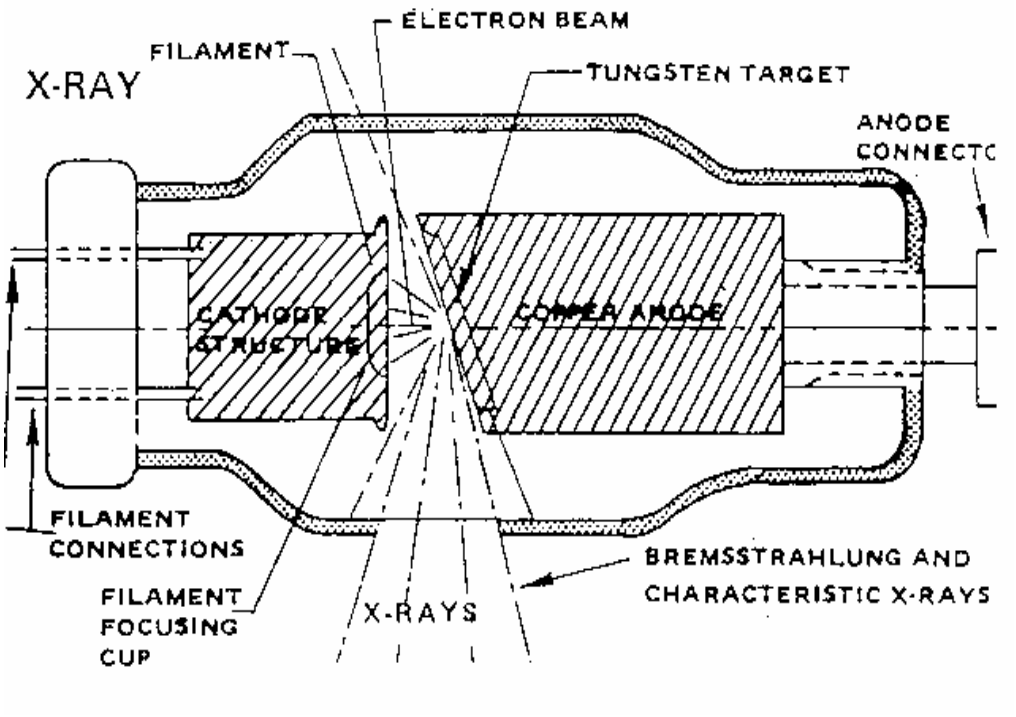

Figure 2.13 A schematic cutaway view of an X-ray tube (URL-5)

The photographic film is the oldest method of detecting X-rays, and is still being used today. Modern conventional X-ray powder diffractometers commonly employ one of the three types: scintillation detector, the gas proportional counter and the [Si(Li)] detector. Position sensitive detectors (PSDS) are finding increasing application in X-ray powder diffraction. The latest generation is capable of very fast data acquisition without loss of detail (Nuffield, 1966 and Jenkins and Snyder, 1996).

2.6.3 Principles of X-ray Diffraction

The physics of X-rays and the geometry of crystals can be fitted together to look into the phenomenon of X-ray diffraction (XRD), which is an interaction of the two. Bragg's law is one of the approaches normally used to treat diffraction by crystals. Measuring distances (d) between units in crystals by X-ray diffraction is achieved by the Bragg method. The units in each Bragg plane act as the X-ray scattering sources and the X-ray beam striking the crystal will act as if it had been reflected from these evenly spaced planes. This will give rise to reinforcement of the beam at certain angles and destruction at others, so that the spacing between the planes can be determined. The condition for reinforcement is that λ, the wavelength of the X-ray, and d, the distances between planes, are related to the angle (θ) of incident.

2.6.4 Instrumentation: The powder diffractometer

The X-ray diffraction experiment requires an X-ray source, the sample under investigation and a detector to pick up the diffracted X-rays. These three variables governing the different X-ray techniques are (West, 1999):

(i) Radiation, monochromatic or of variable wavelength
(ii) Sample, single crystal, powder or a solid piece
(iii) Detector, radiation counter or photographic film

The most important X-ray diffraction techniques are listed in Table 2.3, and only the powder diffractometer method will be discussed further.

Table 2.3 The different X-ray diffraction techniques (West, 1999)

Wavelength	Sample	Detector	Method
Fixed	Powder	Counter	Diffractometer
Fixed	Powder	Film	Debye-Scherrer
Fixed	Powder	Film	Guinier (Focusing)
Fixed	Single crystal	Film	Rotation (Oscillation)
Fixed	Single crystal	Film	Weissenberg Precession (Buerger)
Fixed	Single crystal	Counter	Automatic Diffractometer
Variable	Solid piece	Film	Laue

The principle of the powder diffractometry method implies that a monochromatic beam of X-rays strikes a finely powdered sample that ideally has crystals randomly arranged in every possible orientation. The various lattice planes in such a powder sample are also present in every possible orientation. For each set of planes, at least some crystals must be oriented at the Bragg angle (θ) to the incident beam and diffraction will occur for these crystal and planes. The diffracted beams are detected by using a movable detector such as a Geiger counter or scintillation counter connected to a chart recorder or computer (diffractometer) (Jenkins, 1999; Nuffield, 1966; West, 1999).

The powder diffractometry technique gives a series of peaks on a strip of chart paper or on a computer screen. Both peak positions and intensities (peak heights) are readily obtained from the chart to make this a useful and rapid method of phase analysis. This method is very useful for the qualitative identification of crystalline phases or compounds. The powder diffractometer has a proportional, scintillation or Geiger counter which scans a range of 2θ values at a constant angular speed. In the range from 10 to 80^{o}, 2θ is usually sufficient to cover the most useful part of the powder pattern. The scanning speed of the counter is usually 2^{o} 2θ min^{-1}.

Figure 2.14 shown below presents the layout of a typical powder diffractometer, and is set similar to the wavelength dispersive spectrometer explained earlier for XRF spectrometry. In order to record a diffraction pattern, the detector is set at or close to 0^o (or driven from clockwise from about 170^o) on the graduated 2θ scale and driven by a motor at constant speed of 2^o per minute. The X-rays reaching the detector are then recorded and displayed on a recorder as a series of peaks.

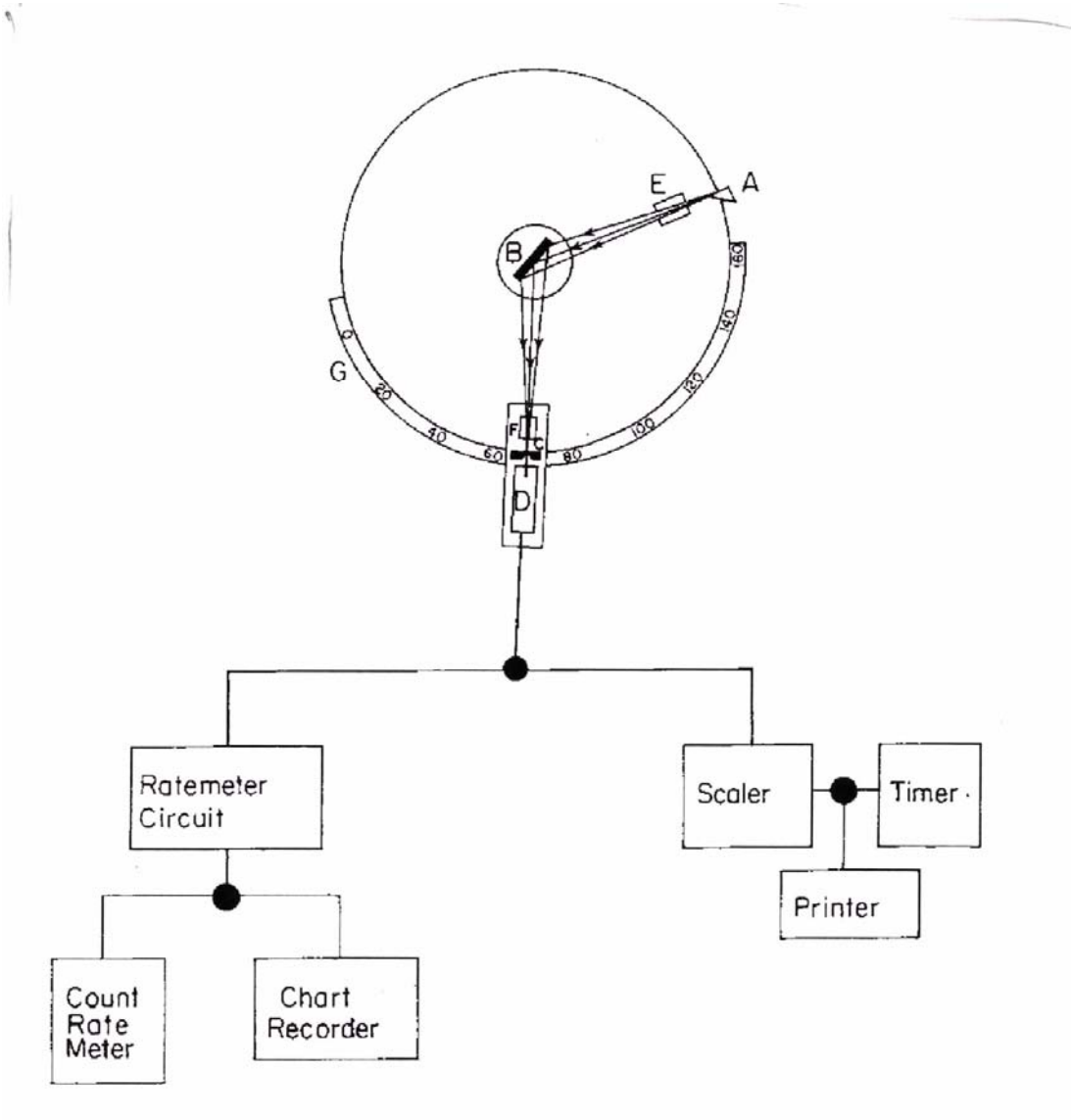

Figure 2.14 Layout of a powder diffractometer (Whitson, 1987)

As in WDXRF, the incident X-rays produced from the source (A) are collimated by a system of slits (E) and then part of the collimated X-rays are diffracted by the sample (B). The diffracted beam of X-rays are further collimated by a system of slits (F) and then converge to a focus at the slit (C) and finally enters the detector (D), which converts the diffracted X-rays into electrical pulses in the circuit to which they are connected. The number of pulses produced is directly proportional to the intensity of the beam entering the detector.

2.6.5 Qualitative XRD analysis

The powder method is used most importantly in the qualitative identification of crystalline compounds. Most methods of analysis give information about elements present in a sample; however, the powder diffractometer is different and gives the information about which crystalline compounds or phases are present but with no information about their chemical constitution.

In principle, each crystalline phase has a unique X-ray diffraction powder pattern, and therefore a study of diffraction patterns offers a powerful tool for qualitative determination of phases within a sample. Two main factors which determine the powder pattern are the size and shape of the unit cell and the line intensity which in turn depends on the atomic number and position of the atoms in a crystal (West, 1999).

Two variables in a powder pattern can be measured, and are the peak position (d-spacing), and the intensity, which can be measured either qualitatively or quantitatively to identify unknown crystalline materials in a sample. This is achieved in consultation with the database reference comprising of some known reference phases called the Powder Diffraction File. This Powder Diffraction Files (PDF) is a collection of a single-phase X-ray powder diffraction patterns in the form of tables of interplanar spacing (d) and relative intensities (Jenkins and Snyder, 1996; Nuffield, 1966; West, 1999).

2.6.6 Sample preparation for XRD analyses

As mentioned earlier, sample preparation is a very important step in any analysis. Errors can be introduced both in taking of the original sample by the person requesting the analysis and in attempting to take a small representative of sub-samples for analysis by the analyst.

A crystalline powder must meet certain requirements to obtain a satisfactory powder pattern, and the most crucial factors requiring attention in preparation of the sample for the diffractometric powder technique are discussed below:

(a) Preparation of powders

The most used methods for the preparation of powders are, (i) Front loading (standard method), in which the powdered sample is placed onto the sample holder and then pressed into the holder with a glass slide, (ii) Back loading, in which the sample cavity of the sample holder is filled from the back with an optimized amount of sample. A cylinder is then pressed onto the sample with pre-defined pressure, and the bottom plate is removed from the sample holder. (iii), Sprinkle loading, where an adhesive (sticky) substance such as Vaseline is applied to the sample holder and the sample powder sprinkled onto that (Jenkins and Snyder, 1996).

Samples should be ground to a crystallite size of < 15 μm, or even better < 5 μm. To obtain satisfactory results, the number of crystallites contributing to each reflection should be large enough to generate signals of reproducible intensity. The surface area of the sample irradiated also influences the counting statistics, so the sample can also be ground too fine making it amorphous for X-ray diffraction.

(b) Sample thickness

The required sample thickness, which is dependent on the diffraction angle (θ), is closely linked to the depth of X-ray penetration. Considering a flat specimen, the thickness of the sample must be large enough to give a maximum diffracted intensity (± 99 %). A criterion for this condition is:

$$\mu t \geq (3.45) \cdot (\rho/\rho') \cdot \sin \theta$$

$$t \geq (3.45)/\mu \cdot (\rho/\rho') \cdot \sin \theta$$

$$t \geq (3.45) \cdot (\mu'/\rho') \cdot \sin \theta$$

where:

t = the sample thickness in centimetres

μ = the linear absorption coefficient

ρ = the density of the material composing the powder

ρ' = the density of the powder including interstices

$\mu' = (\mu/\rho)$ = mass absorption coefficient

(c) Preferred orientation

Each grain in a polycrystalline aggregate normally has a crystallographic orientation different from that of its neighbours. The orientation of all the grains may be considered as randomly distributed in relation to some selected frame of reference, or they may tend to cluster about some particular orientation, and such condition is said to have a preferred orientation. Reduction of the crystallite size helps in greatly reducing preferred orientation. The method of mounting the sample is of great importance and several methods, such as back and side loading can be followed.

(d) Small samples

Sample support and position are important if very small amounts of samples are to be analyzed. Effective sample supports like single crystals (e.g. fluorite, calcite, MgO, Si, quartz), either cleaved or cut on or off Bragg planes can be used. The sample must then be placed in the centre of the X-ray beam; the technique called the ZBH (Zero Background Holder), and can thus be used on samples as small as 1.0 mg (Jenkins and Snyder, 1996).

(e) Special samples

Slightly reactive, hygroscopic materials, slurries and liquids can be sealed by placing them in a sample holder and covering them with a thin film (e.g. Mylar foil) or even cellophane tape. The diffraction pattern of the sealing material must be recorded and subtracted from the sample (Jenkins and Snyder, 1996).

CHAPTER 3

Thermogravimetric analysis of known mixtures of $Mg(OH)_2$ and $Mg(CH_3COO)_2$

3.1 Introduction

Thermogravimetric analysis (TGA) can be used to determine the degree of dehydration (decomposition) of magnesium hydroxide, $Mg(OH)_2$, to magnesium oxide (MgO) by comparing the experimental mass loss of the decomposition of magnesium hydroxide to its theoretical mass loss (30.9 %). Magnesium hydroxide decomposes according to the following reaction at temperatures exceeding 300^{o}C (Halikia et al., 1998):

$$Mg(OH)_2\ (s) \rightarrow MgO\ (s) + H_2O\ (g)$$

Filippou et al. (1999) have reported that the acetate ions from the magnesium acetate solution can play a very important role in enhancing the rate of magnesia (MgO) hydration due to its complexation power. Magnesium acetate decomposes at a temperature of approximately 323^{o}C, which is in the same decomposition range as magnesium hydroxide, and has the following decomposition scheme:

$$Mg(CH_3COO)_2\ (s) \rightarrow MgO\ (s) + CO_2\ (g) + CH_3COCH_3\ (g)$$

The magnesium hydroxide obtained as a product from MgO hydration, using magnesium acetate as a hydrating reagent, may contain some magnesium acetate which is left after hydration. The aim of the present study was to develop a suitable thermogravimetric method that can be used to quantitatively determine the amounts of magnesium hydroxide and magnesium acetate in a mixture thereof.

3.2 Experimental

3.2.1 Samples

The samples used in this study were pure magnesium hydroxide, $Mg(OH)_2$, and magnesium acetate, $Mg(CH_3COO)_2 \cdot 4H_2O$, obtained from Merck, South Africa.

3.2.2 Sample preparation and experimental procedure

The pure $Mg(OH)_2$ and $Mg(CH_3COO)_2 \cdot 4H_2O$ were dried in a laboratory oven at 200^oC for about 2 hours in order to remove moisture and water of crystallization. Mixtures of these substances were then ground together using a mortar and pestle in different mass percentage ratios as shown in Table 3.1 below. A thermogravimetric analysis was then performed on each of the mixtures.

Table 3.1 Composition of the mixtures of $Mg(OH)_2$ and $Mg(CH_3COO)_2$

Mixture	% $Mg(OH)_2$	% $Mg(CH_3COO)_2$
1	100	0
2	95	5
3	90	10
4	85	15
5	80	20
6	70	30
7	60	40
8	50	50
9	0	100

3.3 Instrumental analysis

3.3.1 TG analysis

To do a quantitative analysis on the mixtures of magnesium hydroxide and magnesium acetate, a Q500 TGA (TA instruments) was used to perform the thermogravimetric analyses. A heating rate of 10^oC min^{-1} was used in a nitrogen atmosphere using platinum pans, and sample masses were weighed to approximately 10 mg.

3.4 Results and Discussion

Figure 3.1 shows the TGA curves of some of the mixtures of $Mg(OH)_2$ and $Mg(CH_3COO)_2$. TG analysis of the sample containing only magnesium hydroxide (i.e. 100 % $Mg(OH)_2$) gave a mass loss of 26.8 % in the temperature range between 200 and 450^oC. This mass loss value differs from the theoretical value (30.9 %), and can be ascribed to the presence of MgO and some impurities, and the purity of sample seems to be 86.7 % $Mg(OH)_2$.

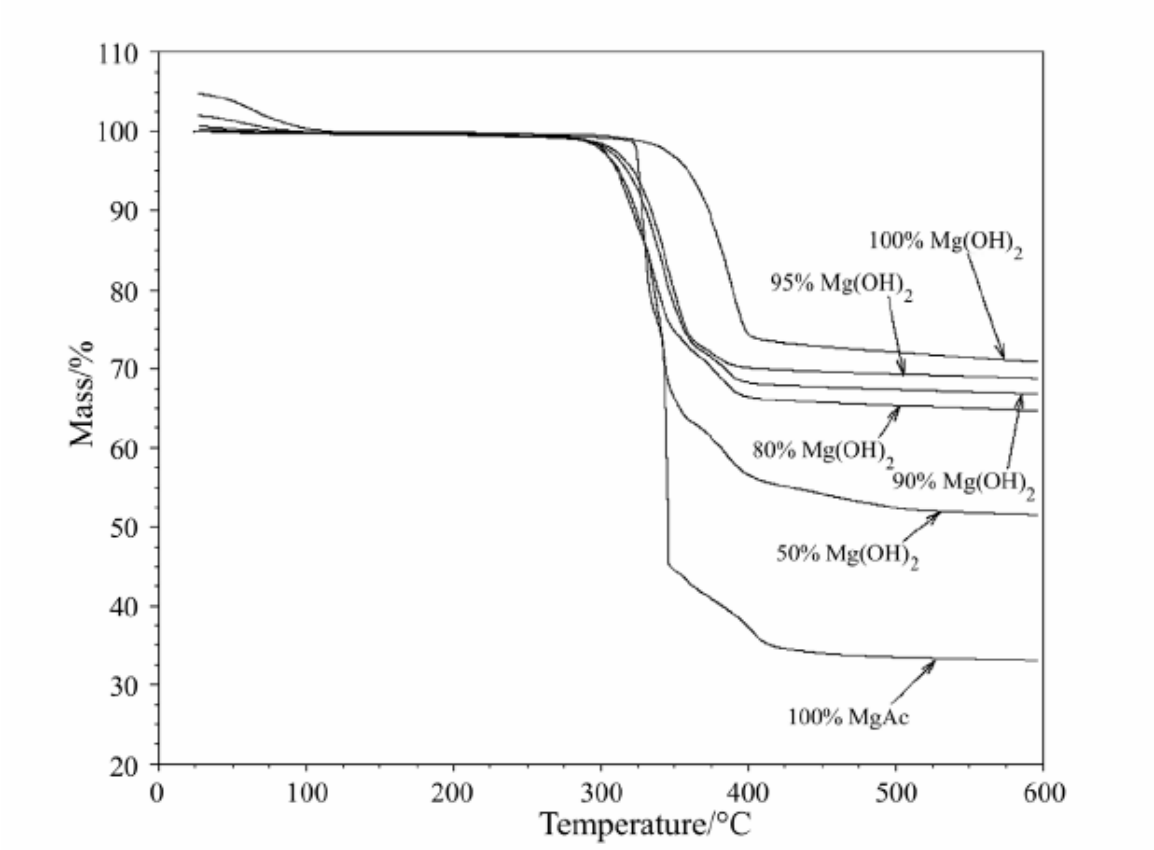

Figure 3.1 Thermogravimetric curves for different mass percentage mixtures of $Mg(OH)_2$ and $Mg(CH_3COO)_2$

In the figure above, a sudden mass loss between 30 and 150^oC was observed for some of the mixtures containing magnesium acetate. This mass loss could be due to the fact that magnesium acetate rehydrated back by absorbing moist, before the thermal analysis runs were performed on the mixtures. Therefore, in order to calculate the mass losses of the decomposition of the magnesium acetate in the mixtures, the mass

loss due to this uptake of moisture (water of crystallization) had to be subtracted first before calculating the mass percentages. This means that a new initial mass was obtained at 150^{o}C, from which the mass percentages were recalculated. Decomposition of the sample containing only magnesium acetate revealed a mass loss of 69.6 %, which compared well to the theoretical value (71.7 %). The purity of the sample seems to be 97.1 % magnesium acetate.

In the present study, the calculation of the mass losses of the decomposition of magnesium hydroxide and magnesium acetate in a mixture were evaluated using thermogravimetric method of analysis. For this purpose, experiments in TGA were carried out in non-isothermal conditions in temperatures up to 600^{o}C, which resulted in mass loss percentage as a function of temperature. In order to determine the experimental amounts of both $Mg(OH)_2$ and $Mg(CH_3COO)_2$ in the mixtures, three different methods were used. The first method involved the determination of the amounts of $Mg(OH)_2$ and $Mg(CH_3COO)_2$ by using the minimum in the derivative of the mass loss curve versus temperature to determine the decomposition mass losses for the mixtures over the same temperature range as for the pure compounds. The second method also used the minimum in the derivative mass loss curve versus temperature, but in this case, the mass losses were determined by using the two decomposition reactions in the TG curves. The first mass loss above 200^{o}C was taken as due to decomposition of $Mg(OH)_2$, while all other steps was considered to be that of $Mg(CH_3COO)_2$. The third method employed the total experimental mass loss for both decomposition reactions.

Method 1

The amounts of $Mg(OH)_2$ and $Mg(CH_3COO)_2$ in the mixtures were determined by obtaining curves of mass (%) and derivative mass (% $^{o}C^{-1}$) versus temperature (^{o}C). The percentage mass loss due to decomposition of $Mg(OH)_2$ (27.68 %; 200 to 370^{o}C) and $Mg(CH_3COO)_2$ (4.39 %; 370 to 450^{o}C) were then determined by using the minimum in the derivative mass loss curve versus temperature.

Figure 3.2 shows the curves for a mixture of 90 % $Mg(OH)_2$ and 10 % $Mg(CH_3COO)_2$ as an example. The two decomposition reactions overlap between 350 and 370°C. After recalculating the initial mass loss at 150°C, a mass loss of 26.3 % was obtained for the decomposition of $Mg(OH)_2$, and 6.0 % for $Mg(CH_3COO)_2$. By using the mass loss obtained for the sample containing 100 % $Mg(OH)_2$ (26.8 % mass loss), and the mass loss obtained for the sample having 100 % $Mg(CH_3COO)_2$ (69.6 % mass loss), the calculated mass percentages for these samples were 98.1 % and 8.6 %, respectively.

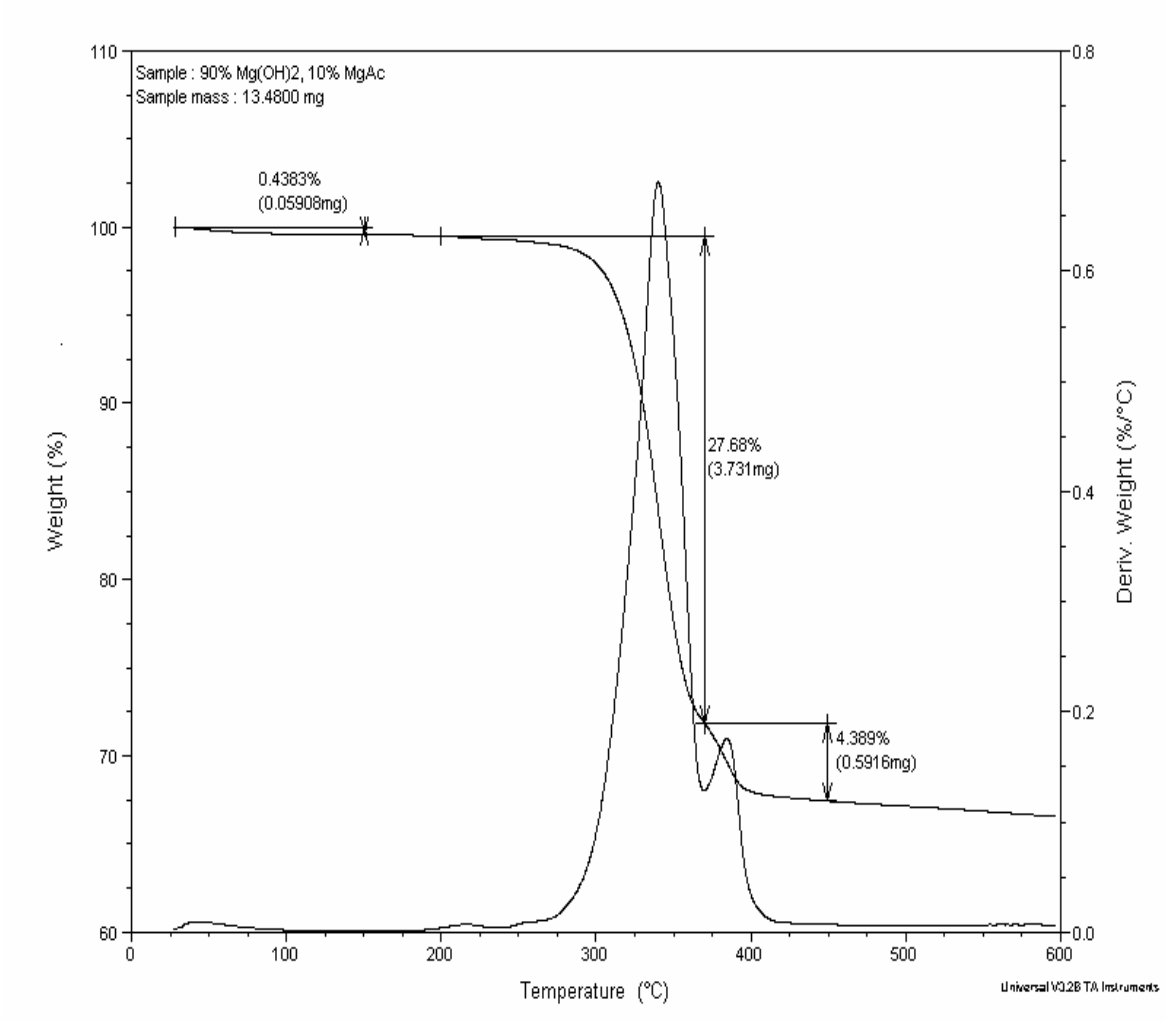

Figure 3.2 Thermogravimetric curves for the determination of the amount of $Mg(OH)_2$ and $Mg(CH_3COO)_2$ in a sample having 90 % $Mg(OH)_2$ and 10 % $Mg(CH_3COO)_2$ (first method)

When the same method was applied to the sample having 50 % $Mg(OH)_2$ and 50 % $Mg(CH_3COO)_2$ (Figure 3.3), mass losses of 41.3 % and 7.9 %, were obtained. The calculated mass percentages were 154.1 % for $Mg(OH)_2$ and 11.4 % for $Mg(CH_3COO)_2$, which were not comparable to the actual values. The results obtained for method 1 are summarized in Table 3.2. The results show that by increasing the amount of magnesium acetate in the mixtures, the inaccuracy of the results obtained also increases, and as a result this method was found not suitable for the quantitative analysis of these mixtures, and a more suitable method had to be developed.

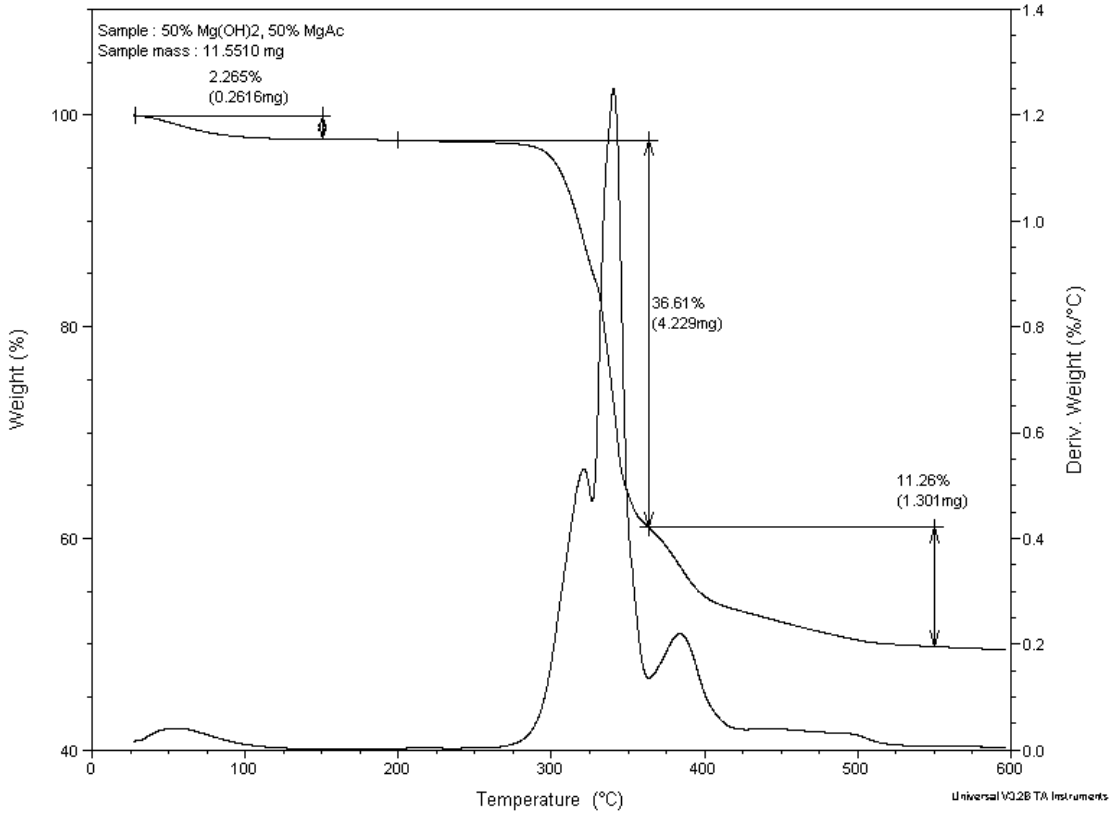

Figure 3.3 Thermogravimetric curves for the determination of the amount of $Mg(OH)_2$ and $Mg(CH_3COO)_2$ in a sample having 50 % $Mg(OH)_2$ and 50 % $Mg(CH_3COO)_2$ (first method)

Table 3.2 Results of the calculation of the mass percentage composition of different mixtures of $Mg(OH)_2$ and $Mg(CH_3COO)_2$ by the first method

Actual composition		**Experimentally determined composition**	
% $Mg(OH)_2$	**% $Mg(CH_3COO)_2$**	**% $Mg(OH)_2$**	**% $Mg(CH_3COO)_2$**
100	0	100	0
95	5	98.7	6.5
90	10	98.1	8.6
85	15	103.0	9.7
80	20	108.7	10.5
70	30	124.7	10.6
60	40	139.8	10.5
50	50	154.1	11.4
0	100	0	100

Method 2

By comparing the TG curves in Figure 3.1, it seems that by mixing these compounds, the decomposition temperature of $Mg(OH)_2$ is lowered with an increasing amount of $Mg(CH_3COO)_2$, while that of $Mg(CH_3COO)_2$ is increased. In other words, the decomposition temperature ranges for the two components in the mixtures, changes with a change in the sample composition.

The analyses of the TG curves of the sample having 50 % $Mg(OH)_2$ and 50 % $Mg(CH_3COO)_2$ were repeated in Figure 3.4 by using the second method. In this method, it was decided to take the mass loss due to the decomposition of $Mg(OH)_2$ as the minimum in the derivative mass loss versus temperature curve of the first mass loss above 200°C (between 200 and 327°C), and that for $Mg(CH_3COO)_2$ for all steps thereafter (between 327 and 543°C). This analysis gave the percentages of $Mg(OH)_2$ and $Mg(CH_3COO)_2$ as 52.9 % and 50.3 %, respectively, and compared well to the actual values. The method was repeated for all other mixtures, and gave good results. The results obtained for method 2 are summarized in Table 3.3. As can be seen, the method gave better results for samples containing more magnesium acetate, as compared to method 1.

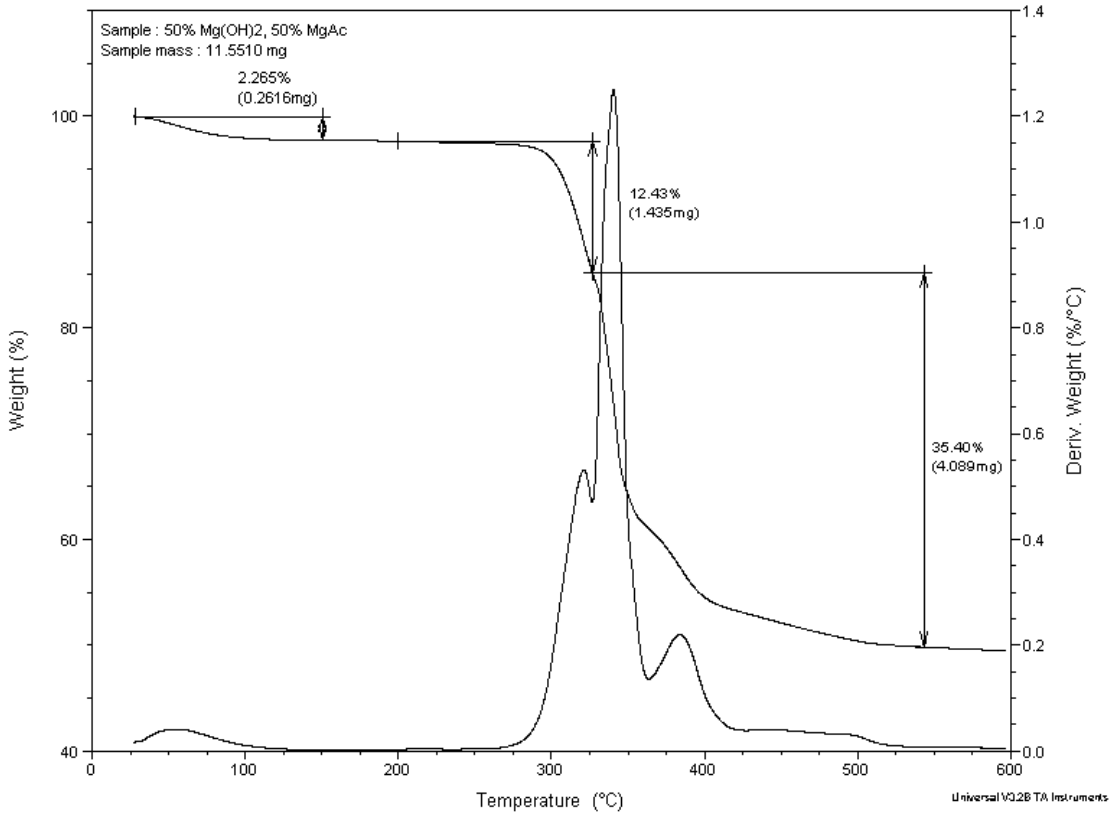

Figure 3.4 Thermogravimetric curves for the determination of the amount of $Mg(OH)_2$ and $Mg(CH_3COO)_2$ in a sample having 50 % $Mg(OH)_2$ and 50 % $Mg(CH_3COO)_2$ (second method)

Table 3.3 Results of the calculation of the mass percentage composition of different mixtures of $Mg(OH)_2$ and $Mg(CH_3COO)_2$ by the second method

Actual composition		**Experimentally determined composition**	
% $Mg(OH)_2$	**% $Mg(CH_3COO)_2$**	**% $Mg(OH)_2$**	**% $Mg(CH_3COO)_2$**
100	0	100	0
95	5	98.7	6.5
90	10	97.3	9.0
85	15	92.4	13.6
80	20	82.0	20.8
70	30	72.3	30.8
60	40	63.2	40.0
50	50	52.9	50.3
0	100	0	100

Method 3

The third method involved the total experimental mass loss for both decomposition reactions between 200 and 450^{o}C. Table 3.4 gives the experimentally determined total mass loss of both components against the mass percentages of magnesium acetate.

Table 3.4 Total mass loss (experimental) against actual mass percentage of magnesium acetate

Total experimental mass loss/ %	**Mass percentage, $Mg(CH_3COO)_2$ /%**
30.14	5
32.23	10
34.32	15
36.40	20
40.58	30
44.75	40
48.92	50

A plot of the total experimental mass percentages versus actual mass percentages magnesium acetate was then obtained (Figure 3.5). From the regression analysis, the following linear fit was obtained:

$$\mathbf{y = 0.4173x + 28.059;\ R^2 = 0.9982}$$

where:

y = experimental mass loss between 200-450^{o}C

x = actual mass percentage of magnesium acetate

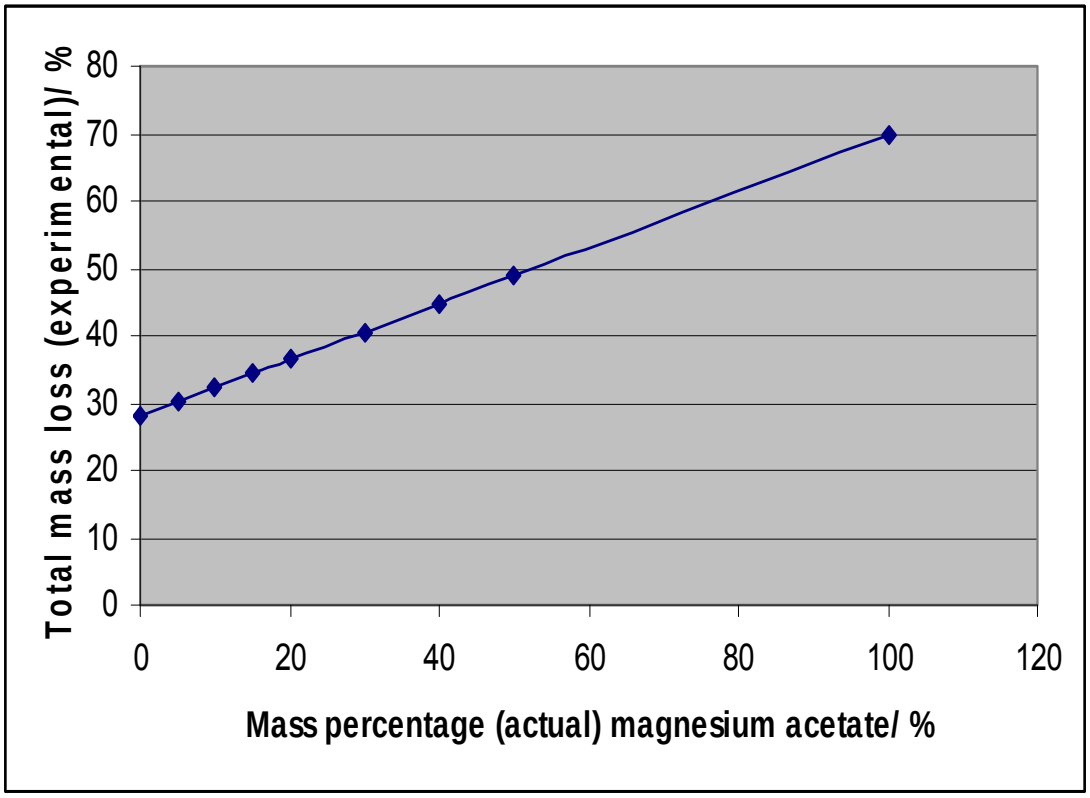

Figure 3.5 Total mass loss (experimental) against actual mass percentage of magnesium acetate

The above equation was used to determine the experimental mass percentages of magnesium acetate in a mixture of magnesium acetate and magnesium hydroxide. The mass percentages of $Mg(OH)_2$, were then calculated by subtracting the mass loss due to the decomposition of magnesium acetate from the total mass loss. The results obtained for method 3 are summarized in Table 3.5. There was also some improvement for the mixtures containing between 5 and 15 % magnesium acetate.

Table 3.5 Results of the calculation of the mass percentage composition of different mixtures of $Mg(OH)_2$ and $Mg(CH_3COO)_2$ by the third method

Actual composition		**Experimentally determined composition**	
% $Mg(OH)_2$	**% $Mg(CH_3COO)_2$**	**% $Mg(OH)_2$**	**% $Mg(CH_3COO)_2$**
95	5	97.4	7.0
90	10	94.1	10.2
85	15	89.0	15.1
80	20	83.8	20.2
70	30	73.0	30.6
60	40	63.1	40.1
50	50	52.4	50.4

3.5 Conclusion

Three methods for the quantitative determination of the amounts of magnesium hydroxide and magnesium acetate by TG were developed. The first method gave inaccurate results due to the fact that the decomposition temperatures of both $Mg(OH)_2$ and $Mg(CH_3COO)_2$ changed as the composition in the mixture changed. The results obtained by using method 2, where the minimum in the derivative mass loss (% $^oC^{-1}$) versus temperature (^oC) curve was used, compared well with the actual values. However, some improvement was needed especially for those mixtures containing less than 10 % magnesium acetate.

Method 3 employed TG analysis over the whole temperature range where both the magnesium hydroxide and magnesium acetate decomposition reactions took place. As a result, the total mass loss was used to calculate the percentages of both components in the mixture and good results were obtained. The results obtained using this method compared well to the actual values. This method of using the total mass losses can however only be employed where magnesium hydroxide and magnesium acetate are the only compounds in the samples that decompose between 200 and 600^{o}C.

CHAPTER 4

The effect of different experimental parameters on the hydration of MgO

4.1 Introduction

It has already been mentioned that magnesium acetate can be used to enhance the rate of MgO hydration (Filippou et al., 1999). Different variables such as concentration of magnesium acetate, solution temperature, solid to liquid ratio of MgO to magnesium acetate, and also the reaction time are among the factors that can greatly influence the hydration rate of a MgO sample. Ekmekyapar et al. (1993) have reported that the solid to liquid ratio is an important factor on the dissolution of MgO, and that the dissolution increases with a decrease in this ratio, and also that the dissolution is slightly affected by the stirring speed.

Maryska and Blaha (1997), who investigated the effect of hydration temperature in the temperature range between 6 to 80^{o}C, reported that the hydration rate of MgO depends on the temperature of hydration. An increase in the hydration temperature accelerates the course of hydration.

In this study, the effects of different experimental variables were investigated on the hydration of soft burned magnesium oxide to magnesium hydroxide. The effects of the following parameters were evaluated experimentally, i.e., hydration time (1-60 minutes), concentration of magnesium acetate (0 M to 0.2 M $Mg(CH_3COO)_2 \cdot 4H_2O$), and the amount of solid (MgO) to magnesium acetate solution (10 g/ 100 ml and 15 g/ 100 ml).

4.2 Experimental

4.2.1 Samples

Pure samples of magnesium acetate ($Mg(CH_3COO)_2 \cdot 4H_2O$) and citric acid, were obtained from Merck, South Africa. The medium reactive MgO was obtained from Chamotte Holdings, South Africa, and was obtained by calcination of the natural magnesite ($MgCO_3$).

4.2.2 Sample preparation

The medium reactive MgO obtained from Chamotte Holdings, South Africa, was dried for 2 hours at 650^{o}C before it was used in the hydration studies. XRD analysis was performed on the MgO before and after drying at 650^{o}C for 2 hours to determine the phases present, while XRF was also performed on the MgO before and after drying to perform a quantitative analysis. TG analyses were also performed on the raw magnesite, and on the MgO obtained after drying at 650^{o}C for 2 hours.

To study the influence of magnesium acetate concentration on MgO hydration, a concentration range between 0 M and 0.2 M was prepared using distilled water.

4.2.3 Experimental parameters and procedure

The experimental parameters used to study the influence of magnesium acetate concentration on MgO hydration are summarized in Table 4.1.

Table 4.1 Different experimental parameters for the hydration of MgO

Hydration temperature	25^{o}C
Concentration of magnesium acetate	0, 0.005, 0.01, 0.05, 0.1, 0.15, and 0.2 M
Solid to liquid ratio	10 g and 15 g MgO in 100 ml solution
Hydration time	1, 5, 10, 20, 30, and 60 minutes

A specified amount of MgO sample was stirred in a 250 ml glass beaker at a constant rate of 250 rpm in a 100 ml solution in a water bath at a constant temperature of 25^{o}C. After stirring for a specific time in minutes, the slurry was filtered and then dried in a laboratory oven at 200^{o}C for 2 hours. The percentage $Mg(OH)_2$ was determined by TG analysis. TG analysis was performed on all products, while the BET surface area analyses were only done on selected products.

4.2.4 Citric acid test

To determine the reactivity of MgO samples dried for 2 hours at 650^{o}C, the citric acid method of the determination of powder reactivity was used. This method was discussed in Chapter 2. The time taken by the MgO slurry to change from white to a pink colour was reported as the citric acid reactivity.

4.3 Instrumental analysis

4.3.1 TG analysis

A Q500 TGA (TA Instruments) was used to perform the thermogravimetric analysis on all the products. A heating rate of 10^{o}C min^{-1} was used in a nitrogen atmosphere. Platinum pans were used, and the masses of the sample were weighed to approximately 10 mg.

Method 2 which was developed in Chapter 3, was used to determine the amounts of $Mg(OH)_2$ in the products. Although method 3 was more accurate, it could not be used in this study, since it can only be applied to mixtures consisting of only magnesium hydroxide and magnesium acetate.

The products obtained in the hydration reaction contained mainly $Mg(OH)_2$ and the amounts thereof were calculated from the curves of mass (%) and derivative mass loss versus temperature up to a temperature of 600^{o}C. The first mass loss just above 200^{o}C was taken as due to decomposition of $Mg(OH)_2$. The percentage mass loss due to this $Mg(OH)_2$ decomposition was determined by using the minimum in the derivative mass loss versus temperature curve.

4.3.2 XRD analysis

X-ray powder diffraction analyses were performed on an automated Siemens D501 XRD spectrometer with a 40-position sample changer and monochromater CuK_{α} radiation. The results were analyzed with the use of the International Center of Diffraction PDF database sets.

4.3.3 XRF analysis

For the X-ray Fluorescence analysis, the MgO sample was ground to < 75 μm in a Tungsten Carbide milling vessel and roasted at 1000°C to determine the Loss on ignition (LOI) value. The milled MgO sample (1 g) was then mixed with 9 g of $Li_2B_4O_7$ and fused into a glass bead. Major elements analysis was executed on the fused bead using an ARL9400XP+ spectrometer. Another aliquot of the sample was pressed in a powder briquette for trace element analyses.

4.3.4 BET surface area analysis

A NOVA 1000^e Surface Area and Pore Size Analyzer from Quantachrome Instruments, using nitrogen gas as an adsorbent, was used to determine the surface areas of the products. Prior to the measurement of the adsorption isotherm, every sample (in the weight range 0.2 to 0.4 g) was evacuated (degassed) at 81 ± 0.2^oC for 30 minutes in a vacuum of 70 mm Hg to remove molecules (such as water) attached to the surface of the sample. The surface areas of the samples were finally analyzed and measured by applying a Single Point B.E.T method to the N_2 adsorption data, where the molecular area of N_2 is 16.200 $Å^2$ mol^{-1}. The amount of gas adsorbed is measured by the difference of gas admitted and the amount of gas occupying or filling the dead or empty volume (free space in the in the sample cell). The adsorption isotherm is the plot of the amount of gas adsorbed in (mol g^{-1}) as a function of the relative pressure, p/p^o.

4.4 Results and Discussion

4.4.1 XRD, XRF and surface area analyses of the raw and dried magnesite

The magnesium oxide powder used in the hydration experiments was characterized with respect to its chemical composition by X-ray Fluorescence analysis, phase analysis by X-ray Diffraction, loss on ignition (LOI), surface area analysis by N_2 adsorption and by TG analysis.

The XRD analysis results showed that the phases present in the sample before drying at 650^{o}C consisted mainly of periclase (cubic MgO), with some $MgCO_3$, SiO_2, $Mg(OH)_2$ and CaO or $CaCO_3$. After drying the MgO sample at 650^{o}C for 2 hours, the XRD analysis confirmed that the $MgCO_3$ and $Mg(OH)_2$ were converted to MgO. Figure 4.1 shows the XRD spectrum of the raw magnesite as obtained from Chamotte Holdings. The spectra exhibit a strong sharp peak at around the 50^{o} 2θ-position, which can be ascribed to periclase (MgO). The other peaks can be ascribed to impurities such as quartz (SiO_2), and small traces of magnesium carbonate.

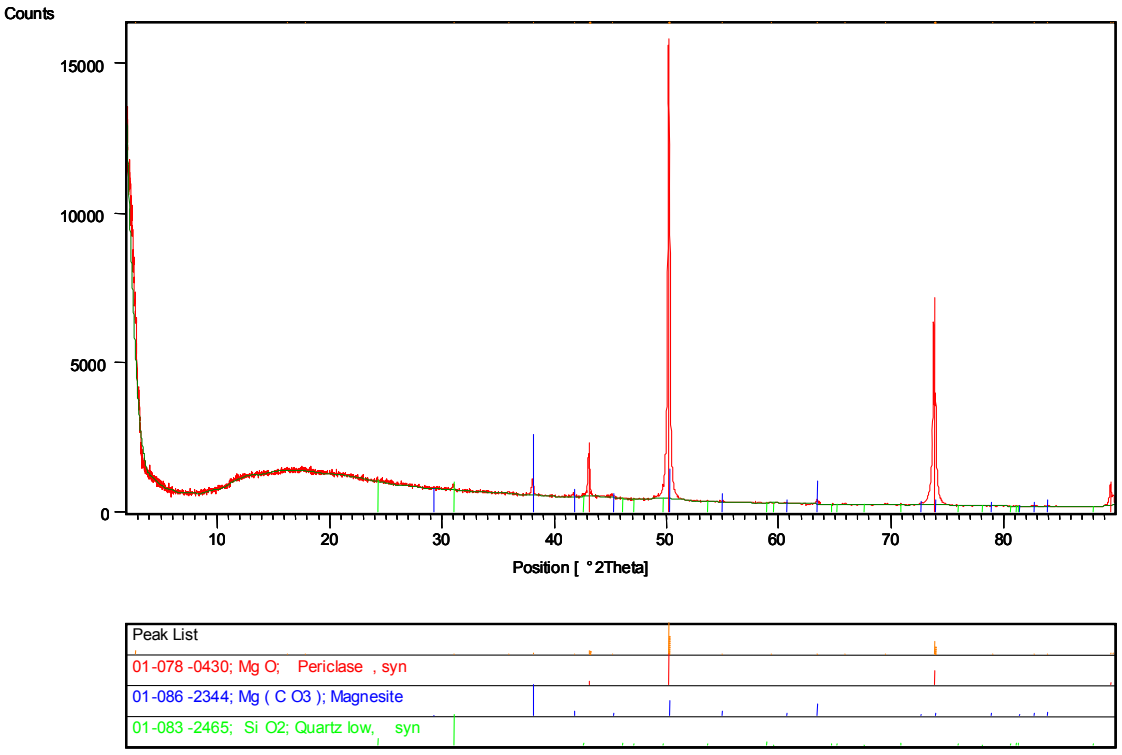

Figure 4.1 XRD spectrum of the raw magnesite

Table 4.2 gives the chemical composition of the raw magnesite obtained from Chamotte Holdings, as determined by XRF analysis before and after drying the sample at 650^{o}C for 2 hours. The XRF analysis indicated a MgO content of 85.00 % and a loss on ignition (LOI) value of 11.00 %. This LOI value shows that the MgO sample was hydrated to some extent prior to hydration studies. As a result, it was necessary to dry the MgO sample in order to remove the moisture.

Table 4.2 XRF analysis of magnesite obtained from Chamotte Holdings, before drying at 650^{o}C and after drying

Composition	**% wt, raw magnesite**	**% wt, dried magnesite**
MgO	85.00	96.00
SiO_2	1.74	1.74
Al_2O_3	0.44	0.44
CaO	0.87	0.87
Fe_2O_3	0.07	0.07
Other oxides	0.83	0.83
LOI	11.00	< 0.01
Total	**99.95**	**99.95**

The surface area of the raw magnesite (10.9 $m^2 g^{-1}$) increased to a value of 21.2 $m^2 g^{-1}$ after drying at 650^{o}C for 2 hours. XRF results have confirmed that drying at 650^{o}C for 2 hours was effective, since the loss on ignition value was reduced to zero.

4.4.2 TG analysis of raw magnesite and dried magnesite

Figure 4.2 shows the TGA curves obtained for the raw magnesite (before drying) and the dried magnesite sample. The dried sample shows stability over the temperature range shown, indicating that the sample consists mainly of MgO, and that no $Mg(OH)_2$ or $MgCO_3$ was present. Therefore, after drying the sample at 650^{o}C, the TG analysis confirmed that the $Mg(OH)_2$ and $MgCO_3$ were converted to MgO. The TGA curve of the raw material (uncalcined magnesite) exhibits a number of weight loss steps up to a temperature of 600^{o}C. These steps can be ascribed to moisture loss

(between 50 and 200°C), $Mg(OH)_2$ decomposition (after 200°C to 450°C) and $MgCO_3$ decomposition (just after 450 to 600°C). The TGA curve of the raw material stabilizes after 600°C, thus confirming that MgO is formed.

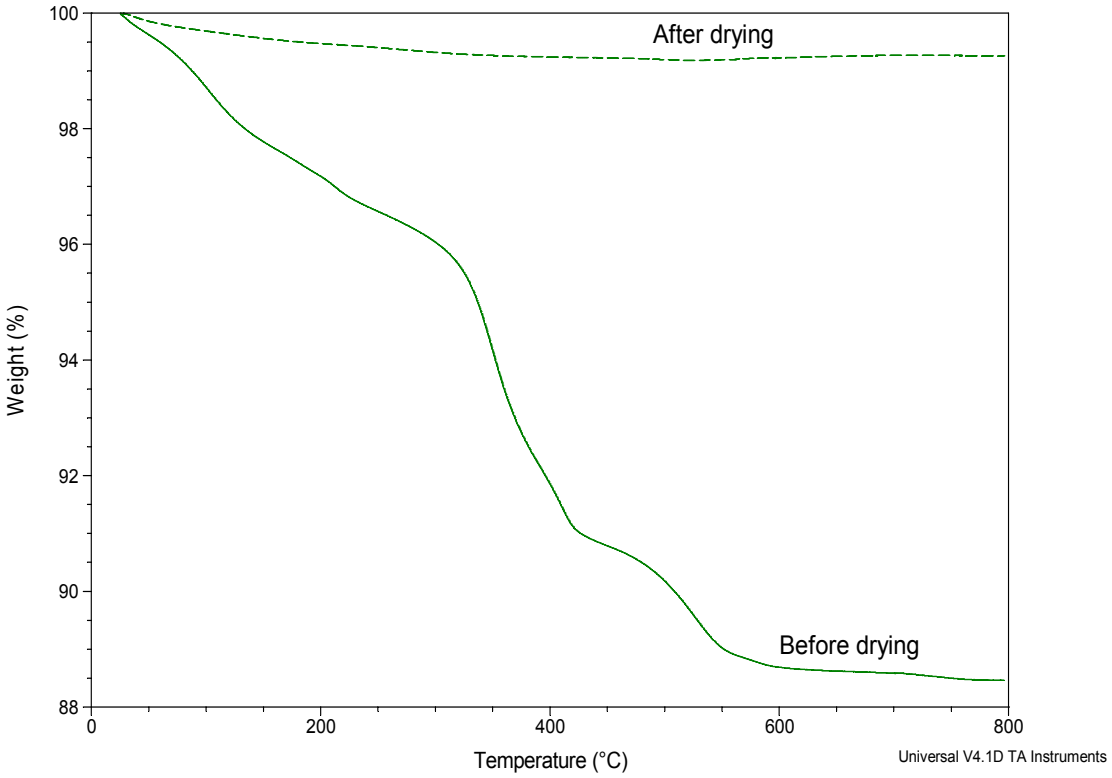

Figure 4.2 TG analysis of raw magnesite (solid line) and dried magnesite (dotted line) at 650°C

4.4.3 Citric acid reactivity test performed on MgO samples

A citric acid reactivity value of 215 s was obtained for the MgO sample after drying at 650°C for 2 hours. This value indicates that the MgO sample is a medium reactive.

4.4.4 Effect of varying the $Mg(CH_3COO)_2$ concentration between 0 and 0.2 M

Table 4.3 shows the results of percentage mass loss and percentage $Mg(OH)_2$ formed from the MgO hydrated in magnesium acetate solutions ranging from 0 and 0.2 M, using 15 g of MgO in 100 ml of solution. The percentage magnesium hydroxide in the samples was determined by TG analysis and was calculated by using the experimental mass loss obtained for the sample and the theoretical mass loss of magnesium

hydroxide (30.9 %). Figure 4.3 shows the effect of increasing the magnesium acetate concentration on the percentage of magnesium hydroxide formed.

Table 4.3 **Influence of magnesium acetate concentration (0-0.2 M) on the hydration of MgO (20 minutes hydration)**

[MgAc]/ (M)	% Mass loss	% $Mg(OH)_2$
Untreated	0.50	1.6
0	8.67	28.1
0.005	9.60	31.1
0.01	10.03	32.4
0.05	10.40	33.7
0.1	12.69	41.1
0.15	13.39	43.3
0.20	14.73	47.7

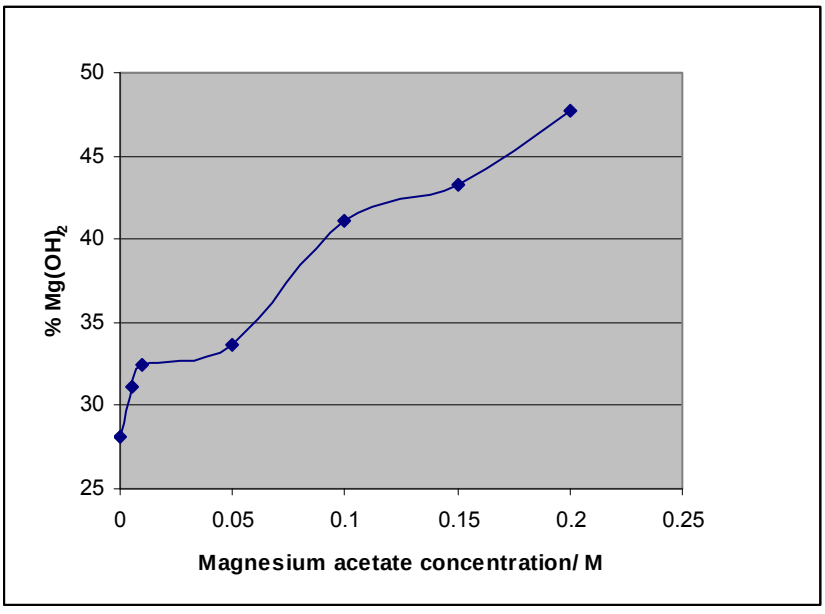

Figure 4.3 **Effect of increasing the magnesium acetate concentration on the percentage of magnesium hydroxide formed.**

The results clearly show that the degree of hydration increases with an increase in magnesium acetate concentration. The results also indicate that there was not a significant difference in the percentage $Mg(OH)_2$ obtained in magnesium acetate concentrations between 0 and 0.05 M. A higher percentage is seen after 0.1 M magnesium acetate, where 41 % $Mg(OH)_2$ was formed. As a result, the optimum concentration was found to be 0.2 M. This led us to investigate the effect of hydration time (1, 5, 10, 20, 30, and 60 minutes) and solid to liquid ratio (10 and 15 g solid) on the hydration of MgO in 0.2 M magnesium acetate.

Filippou et al. (1999) have reported that the magnesium acetate concentration has a positive effect on the rate of MgO hydration. The degree of hydration increases as the concentration of magnesium acetate solution is increased. They reported that the MgO hydration in magnesium acetate solutions is a dissolution-precipitation process which is controlled by the dissolution of magnesium oxide particles.

Van der Merwe et al. (2004) also reported that the degree of hydration of magnesium oxide in magnesium acetate solutions is increased with an increase in the magnesium acetate concentration, up to a concentration of 0.5 M. They also studied the effect of hydration temperature and reported that an increase in temperature increases the solubilities of magnesium oxide and magnesium acetate resulting in a higher concentration of magnesium ions in solution, which precipitates out as magnesium hydroxide, being less soluble than magnesium acetate. They also reported that the major part of hydration of the medium reactive MgO sample occurs within the first few minutes of the reaction for the temperature studied between 25^{o}C and 70^{o}C.

Tables 4.4 and 4.5 shows the percentage mass loss and percentage $Mg(OH)_2$ formed from the hydration of MgO in a 0.2 M magnesium acetate. It is clear that by increasing the hydration time, the percentage magnesium hydroxide obtained as the product increases for both solid to liquid ratios. In both cases, a fast rate of hydration within the first minute is observed, where $Mg(OH)_2$ percentages of 40 and 45 % were obtained, respectively. There is only a ± 10 % increase thereafter, and the hydration rate increases very slowly from 5 minutes of hydration up to 60 minutes.

Table 4.4 Effect of increasing the reaction time on MgO hydration using 10 g MgO/ 100 ml solution, Temperature = 25°C, [MgAc] = 0.2 M

Time (min)	% Mass loss	% $Mg(OH)_2$
1	12.30	39.81
5	13.42	43.43
10	13.54	43.82
20	15.05	48.71
30	15.21	49.22
60	15.84	51.26

Table 4.5 Effect of increasing the reaction time on MgO hydration using 15 g MgO/ 100 ml solution, Temperature = 25°C, [MgAc] = 0.2 M

Time (min)	% Mass loss	% $Mg(OH)_2$
1	14.04	45.44
5	14.67	47.48
10	14.84	48.03
20	15.34	49.64
30	15.58	50.42
60	16.57	53.62

Figure 4.4 summarizes the effect of reaction time for the different solid to liquid ratios studied. It was clear that there was not a significant difference between the results obtained for the two solid to liquid ratios studied, with the percentage $Mg(OH)_2$ formed in 15 g/ 100 ml slightly higher than that formed in the 10 g/ 100 ml slurry. As a result, the preferred solid to liquid ratio was found to be 10 g/ 100 ml. Ekmekyapar et al. (1993) have reported that the dissolution rate of magnesium oxide during hydration decreases as the solid to liquid ratio is increased, probably due to the increase of the amount of solid per unit liquid volume.

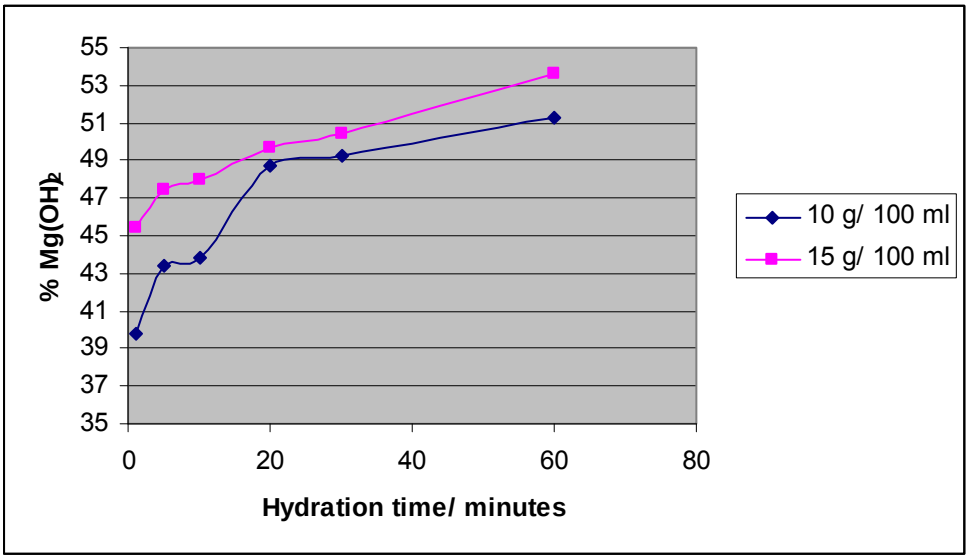

Figure 4.4 Effect of hydration time and solid to liquid ratio on the percentage of magnesium hydroxide produced

Rocha et al. (2004) have also studied, among all, the effect of solid to liquid ratio on the percentage $Mg(OH)_2$ produced from MgO hydration. Their results have shown that the rate of hydration of MgO increases significantly at lower solids content ratios (up to 4-5 %), and stabilizing after 10 % initial slurry density.

4.4.5 Surface area analyses

Table 4.6 shows the surface areas of some hydrated MgO samples after 20 minutes hydration time. The results show that the surface areas of the magnesium hydroxide products formed from hydrating MgO in 0.2 M magnesium acetate at 25^{o}C are higher than those using water (no added acetate) as a hydrating agent. This agrees with the results obtained for the percentage mass loss and percentage $Mg(OH)_2$ reported in Table 4.3, where a high percentage $Mg(OH)_2$ was obtained in 0.2 M magnesium acetate as compared to a low percentage $Mg(OH)_2$ from the hydration in water. The results also confirm the fact that the solid to liquid ratio of the slurry was not an important parameter to consider in these hydration reactions.

Table 4.6 BET surface areas of hydrated MgO samples

Hydrating agent	**MgO per 100 ml solution**	**Surface area / $m^2 g^{-1}$**
water	10	11
water	15	11
Magnesium acetate	10	21
Magnesium acetate	15	20

Following the discussion above, it seems essential to keep the solid to liquid ratio at 10 g per 100 ml of solution during hydration of MgO. An increase in the amount of MgO will result in a decrease in the dissolution rate of MgO. Also, a high solid to liquid ratio of more than 10g/100 ml, will result in about the same amount of magnesium hydroxide being formed.

4.5 Conclusion

XRD analyses have shown that the phases present in the raw magnesite consisted mainly of periclase (MgO) with some $MgCO_3$ and $Mg(OH)_2$. TG analyses have shown that drying the sample at 650^oC for 2 hours, converts the $MgCO_3$ and $Mg(OH)_2$ to pure MgO. XRF analysis has also shown that after drying the raw magnesite, the MgO content increased from 85.00 % to 96.00 %, and the LOI value decreased from 11.00 % to < 0.01 %.

Magnesium acetate increases the rate of hydration of MgO to $Mg(OH)_2$. The hydration in magnesium acetate solutions resulted in approximately double the amount of $Mg(OH)_2$ being produced in comparison to hydration in pure water. The chemical process, through which the magnesium acetate increases hydration, seems to be due to the difference in solubility of the various magnesium compounds in their slurries (Botha and Strydom, 2005). Magnesium acetate is the most soluble of the magnesium compounds in the slurry, giving magnesium and acetate ions. Acetate ions form acetic acid in water, which attack the magnesium oxide and dissolving some of the magnesium oxide that form magnesium ions and then reacts with water to form $Mg(OH)_2$. Magnesium acetate is therefore a better hydrating agent than water under these conditions.

By increasing the hydration time, an increase in the percentage of magnesium hydroxide being formed was observed, and therefore it is of great interest to investigate the time for maximum hydration of MgO to $Mg(OH)_2$. It was shown that there was no significant difference between the results obtained for the two solid to liquid ratios, and as result, a solid to liquid ratio of 10 g/ 100 ml is suggested.

CHAPTER 5

The effect of calcination time on the hydration of MgO

5.1 Introduction

The production of MgO from $MgCO_3$-containing ores in industry usually proceeds through the burning of these ores. The ores are normally calcined at temperatures ranging between 600 and 1400^oC, which result in MgO having varying reactivities. In this case, the reactivity of MgO defines the degree and the rate of MgO hydration to $Mg(OH)_2$ when exposed to water.

It is a well known fact that the temperature and the duration of thermal treatment are among the most important factors determining the surface properties of the MgO product, which subsequently determine the reactivity of the resulting MgO (Girgis and Girgis, 1969 and Canterford, 1985).

In this study, an attempt was made to investigate the effect of different calcination times on the hydration of MgO calcined samples at 1200^oC by varying the calcination time between 1 to 6 hours. The hydration parameters chosen in this study were: hydration temperature at 80^oC, a 0.1 M concentration of magnesium acetate and a solid to liquid ratio of 10 g/ 100 ml solution.

Filippou et al. (1999) and Rocha et al. (2004) have shown that the hydration temperature has a positive effect on the rate of MgO hydration. They studied the MgO hydration in magnesium acetate and water solutions, respectively, and found that the hydration of MgO at 90^oC results in higher amounts of $Mg(OH)_2$ obtained. The increase in hydration temperature seems to increase the solubilities of both magnesium oxide and magnesium acetate, resulting in a higher concentration of Mg^{2+} ions in solution which precipitates out as $Mg(OH)_2$, being less soluble than magnesium acetate. For this reason, a hydration temperature of 80^oC was chosen for this study.

Hydrating MgO at a hydration temperature of 80^{o}C in a concentration of magnesium acetate from 0.1 M and higher seems to give the same degree of hydration, irrespective of an increase in magnesium acetate concentration. This could be due to the fact that the hydration temperature of 80^{o}C is probably the rate determining factor during hydration of MgO. As a result, a 0.1 M concentration of magnesium acetate at a hydration temperature of 80^{o}C was suggested.

Calcination of magnesite between 650 and 1000^{o}C, only removes the moisture and converts $Mg(OH)_2$ and $MgCO_3$ to MgO. Sharma and Roy (1977) performed the thermal studies on hydration characteristics of burnt magnesite from 550 to 950^{o}C, and reported that the type of MgO obtained on calcining magnesite result in the same order of hydration rate. In order to reduce the reactivity of the MgO used in this study, it was necessary to apply a higher calcination temperature. A high calcination temperature (> 1200^{o}C) could not be chosen for economic reasons; the higher the temperature of calcination, the more expensive the magnesia, due to energy input demand.

5.2 Experimental

5.2.1 Samples

Pure samples of magnesium acetate ($Mg(CH_3COO)_2 \cdot 4H_2O$) and citric acid, were obtained from Merck, South Africa. The medium reactive MgO was obtained from Chamotte Holdings, South Africa.

5.2.2 Sample preparation

The MgO sample from Chamotte Holdings was obtained from calcining the natural magnesite. In order to study the effect of calcination time on the hydration of MgO, the MgO sample was calcined in a laboratory oven at 1200^{o}C for 1, 2, 4, and 6 hours. The MgO samples were milled by hand in a mortar and pestle and sieved to < 75 μm before they were used in the hydration studies. The reactivities of the resulting MgO samples were then tested by the citric acid reactivity test method and by BET surface area analysis.

5.2.3 Experimental parameters and procedure

The experimental parameters for the hydration of MgO samples calcined at 1200^{o}C for different times are summarized in Table 5.1.

Table 5.1 Experimental parameters for the hydration of MgO samples calcined and sieved to a particle size of < 75 μm.

Hydration temperature	80^{o}C
Concentration of magnesium acetate	0.1 M
Solid to liquid ratio	10 g in 100 ml solution
Hydration time	30 minutes

The reaction took place in a 250 ml glass beaker immersed in a thermostated water bath at 80^{o}C. A 10 g portion of the calcined and sieved MgO sample was poured into a 250 ml glass beaker having 100 ml of 0.1 M magnesium acetate solution at 80^{o}C, and the slurry was then continuously stirred at a constant rate of 250 rpm for 30 minutes. The reaction temperature was held constant at 80^{o}C. The products were then filtered under vacuum, dried in an oven at 200^{o}C for 2 hours and stored in a desiccator. The percentage $Mg(OH)_2$ was determined by TG analysis. BET surface area analysis was performed on the products.

5.2.4 Citric acid test

To determine the reactivity of all MgO samples calcined at 1200^{o}C, the citric acid method of the determination of powder reactivity was used. This method was discussed in Chapter 2. The time taken by the MgO slurry to change from white to a pink colour was reported as the citric acid reactivity.

5.3 Instrumental analysis

5.3.1 TG analysis

A Q500 TGA (TA Instruments) was used to perform the thermogravimetric analysis on all the products. A heating rate of 10^{o}C min^{-1} was used in a nitrogen atmosphere. Platinum pans were used, and the masses of the sample were weighed to approximately 10 mg. As in Chapter 4, the percentage $Mg(OH)_2$ in the products which were determined by TG analysis, were obtained from the curves of mass loss (%) and derivative mass (% $^{o}C^{-1}$) versus temperature up to a temperature of 600^{o}C.

5.3.2 BET surface area analysis

A NOVA 1000^{e} Surface Area and Pore Size Analyzer from Quantachrome Instruments, using nitrogen gas as an adsorbent, was used to determine the surface areas of the products. The procedure as discussed in Chapter 4 was also applied in this study.

5.4 Results and Discussion

Table 5.2 is a summary of the results obtained for the citric acid reactivity test for MgO samples calcined at 1200^{o}C for different time periods, the surface area analyses before and after MgO hydration and the amounts of magnesium hydroxide being formed. As expected, there was an increase in the citric acid reactivity test values with an increase in calcining time. As a result, the reactivity decreased with an increase in calcining time, resulting in a decrease in surface area with calcining time.

The surface area of MgO samples before hydration is smaller than that after hydration, confirming that the newly formed $Mg(OH)_2$ crystals arrange in such a way as to increase the surface area of the product. The amount of $Mg(OH)_2$ formed ranged from approximately 40 % for 1 hour calcined to about 15 % for MgO calcined for 6 hours. This indicates that a longer calcining time, results in a lower percentage of magnesium hydroxide being formed. This is also illustrated in Figure 5.1, where the influence of calcining time on the reactivity and the degree of hydration of MgO is shown.

Table 5.2 Effect of calcining time on MgO hydration

Calcining time (hours)	Citric acid reactivity (s)	Surface area before hydration ($m^2 g^{-1}$)	Surface area after hydration ($m^2 g^{-1}$)	% $Mg(OH)_2$ formed
1	648	4.41	17.68	40.1
2	937	2.88	7.31	19.1
4	1219	2.38	5.84	13.8
6	1156	2.37	6.82	14.6

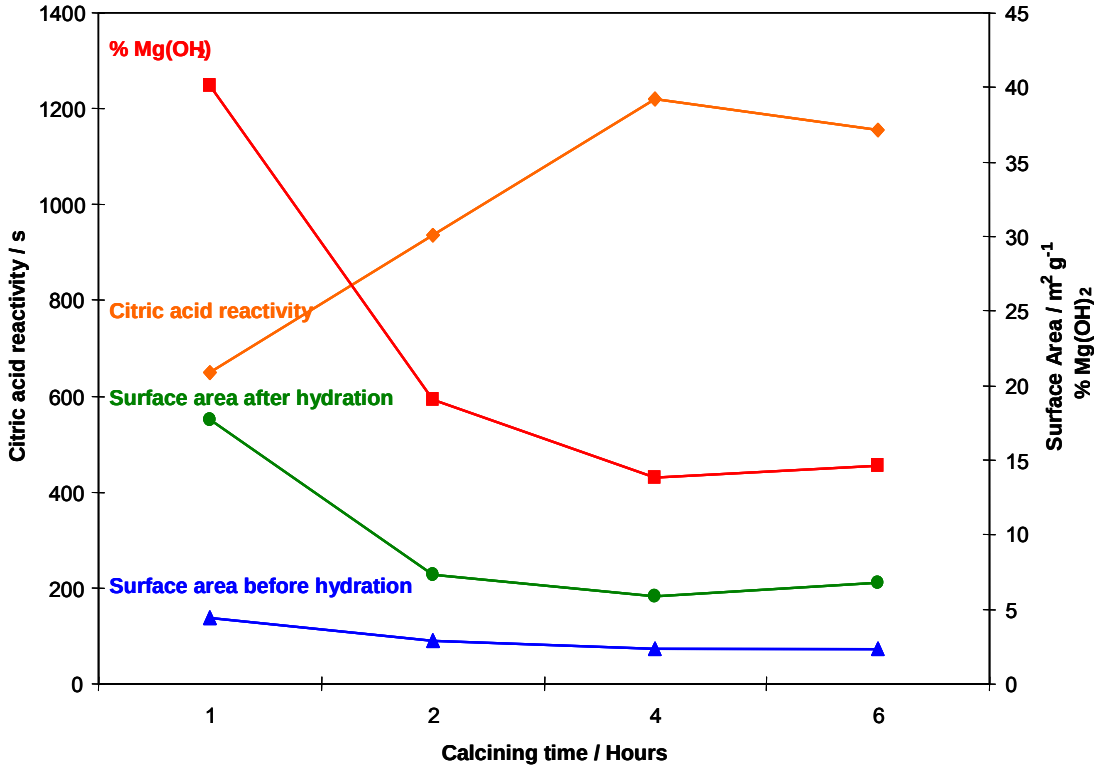

Figure 5.1 Effect of calcining time, surface area and reactivity of MgO on hydration

Figure 5.1 shows that the maximum influence of the calcining time is observed at about 4 hours of calcining, after which the citric acid reactivity and surface area of the products remained approximately the same. This was also confirmed by the results obtained from TG analysis, as shown in Figure 5.2. The products obtained after 4 and 6 hours of calcination were essentially the same.

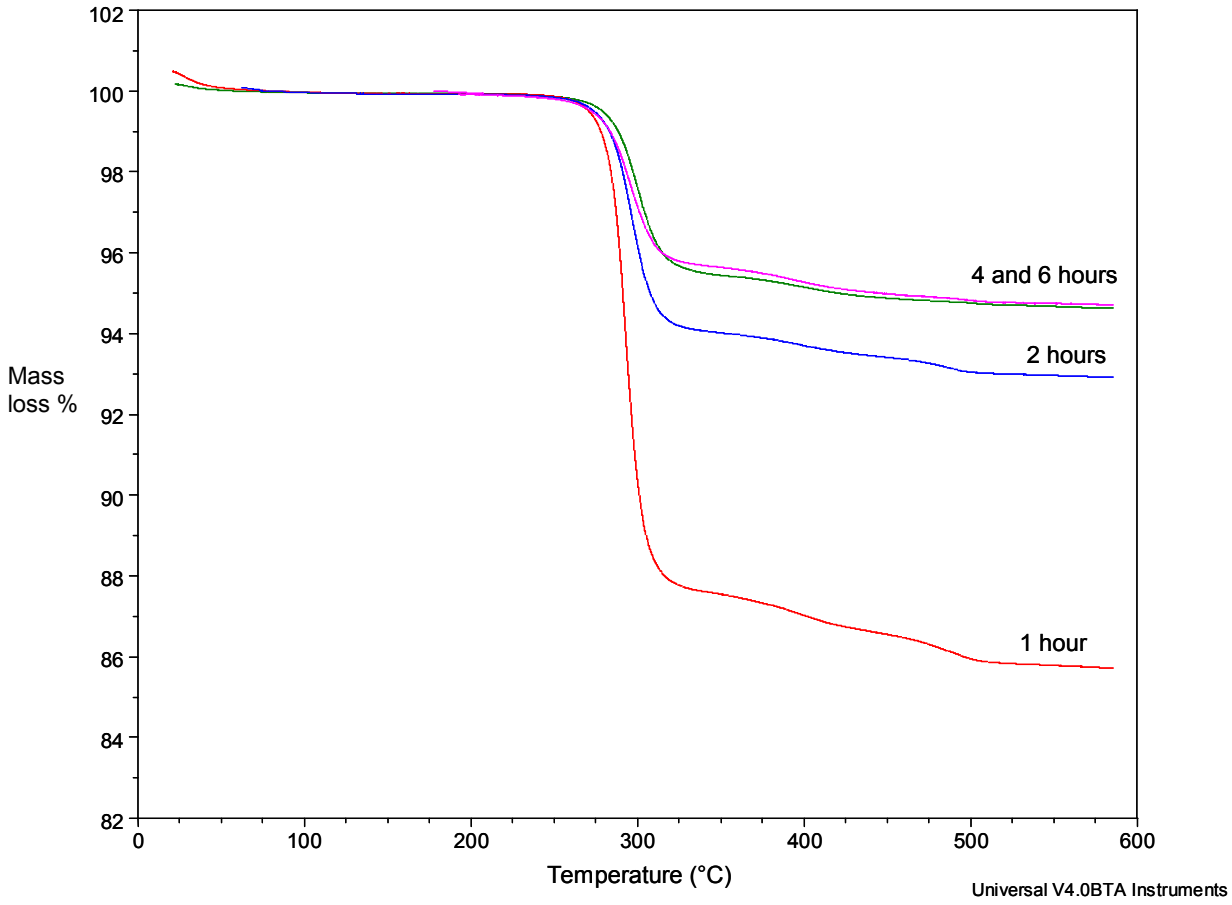

Figure 5.2 Effect of calcining time on MgO hydration

A possible reason for the change in MgO reactivity with a change in calcination temperature or time can be due to structural changes which are accompanied by changes in the calcination temperature. Sintering, which is a process in which a finely divided ore is heated until it collects to form larger particles, is taking place at higher temperatures. MgO is largely amorphous after calcining at 850^{o}C. At temperatures exceeding 1000^{o}C, crystallinity occurs because all the $MgCO_3$ crystals have decomposed. As the temperature increases, crystal size also increases and as a result surface area decreases, thus resulting in a decrease in MgO reactivity (Birchal et al, 2000; Girgis and Girgis, 1969; Rizwan et al., 1999).

5.5 Conclusion

The degree of hydration measured as percentage $Mg(OH)_2$ formed, decreased from about 40 % using a MgO sample calcined at 1200^oC for 1 hour, to about 14 % for a sample calcined for 6 hours at 1200^oC. This indicates that MgO calcined for longer times produces a very small amount of magnesium hydroxide, and is therefore very inactive towards the hydration to $Mg(OH)_2$. The surface areas after hydration are higher than the surface areas before hydration, indicating that the newly formed $Mg(OH)_2$ crystals arrange in such a way as to increase the surface area of the product. Birchall et al. (2000) have studied the effect of magnesite calcining conditions on magnesia hydration and found that the temperature is the main variable affecting the surface area and reactivity of MgO.

In order to obtain a hydration percentage of 40 % and more, it seems essential to keep the calcination time at one hour and increase the hydration time under these conditions. After analyzing the above results, it was found imperative to further investigate the effect of MgO hydration upon calcining MgO samples at different times and at different temperatures under similar experimental parameters, by using both pure water and magnesium acetate as hydrating agents.

CHAPTER 6

The effect of MgO reactivity on its hydration to $Mg(OH)_2$

6.1 Introduction

The results obtained in Chapter 5 indicated that the calcination time at a fixed temperature can be an important parameter affecting the MgO reactivity on hydration to $Mg(OH)_2$, however, one cannot conclude that the same is true if the experiments are performed at other temperatures.

Although Birchal et al. (2000) indicated that the calcination temperature is the main variable affecting the surface area of MgO sample, they did not vary the calcination time in their study. They studied the effect of magnesite calcination conditions of MgO hydration between 850 and 1000^{o}C only at fixed calcination times.

The main objective in the present study was to investigate which of the two variables, i.e., increase in calcination temperate or calcination time is the main variable affecting the reactivity of MgO samples on hydration to $Mg(OH)_2$. This can be achieved by fixing one variable (e.g., time), and varying the other (temperature), and vice-versa. The hydration parameters of hydration temperature (80^{o}C) and a 0.1 M concentration of magnesium acetate were chosen for same reasons given in Chapter 5. Water as a hydrating agent was chosen in this study for comparison of MgO hydration rate with magnesium acetate under these hydration conditions.

6.2 Experimental

6.2.1 Samples

Pure samples of magnesium acetate ($Mg(CH_3COO)_2 \cdot 4H_2O$) and citric acid, were obtained from Merck, South Africa. The medium reactive MgO was obtained from Chamotte Holdings, South Africa.

6.2.2 Sample preparation

A magnesia sample (MgO) was obtained by calcining of the natural magnesite ($MgCO_3$) from Chamotte Holdings, S.A. In order to study the effect of calcining time and temperature on the hydration of the MgO, the MgO samples were then calcined in the laboratory oven for 1 hour at 650, 800, 1000, 1200, and 1400^oC, and then for 2, 4 and 6 hours at the same temperatures, respectively (Table 6.1). The MgO samples were then milled by hand in a mortar and pestle and sieved to < 75 μm before they were used in the hydration studies. The reactivities of the resulting MgO samples were then tested by applying the citric acid reactivity test method and the BET surface area analysis method. A 0.1 M solution of magnesium acetate and distilled water were prepared to be used as hydrating agents.

Table 6.1 Preparation of different MgO samples

MgO sample number	Calcination time/ hours	Calcination temperatures/ ^oC
1	1	650, 800, 1000, 1200, and 1400^oC
2	2	650, 800, 1000, 1200, and 1400^oC
3	4	650, 800, 1000, 1200, and 1400^oC
4	6	650, 800, 1000, 1200, and 1400^oC

6.2.3 Experimental parameters and procedure

The experimental parameters for the hydration of MgO samples calcined at different temperatures and for different times are summarized in Table 6.2.

Table 6.2 Experimental parameters for the hydration of MgO samples calcined and sieved to a particle size of < 75 µm.

Hydration temperature	80°C
Hydrating agent	0.1 M magnesium acetate and distilled water
Solid to liquid ratio	10 g in 100 ml solution
Hydration time	30 minutes

The reaction took place in a 250 ml glass beaker immersed in a thermostated water bath at 80°C. A 10 g portion of the calcined and sieved MgO sample was poured into a 250 ml glass beaker having 100 ml magnesium acetate solution or water at 80°C, and the slurry was then continuously stirred at a constant rate of 250 rpm for 30 minutes. The reaction temperature was held constant at 80°C. The products were then filtered under vacuum, dried in an oven at 200°C for 2 hours and stored in a desiccator. The percentage $Mg(OH)_2$ was determined by TG analysis. BET surface area analysis was performed on the products.

6.2.4 Citric acid test

To determine the reactivity of all MgO samples calcined, the citric acid method of the determination of powder reactivity was used. This method was discussed in Chapter 2. The time taken by the MgO slurry to change from white to a pink colour was reported as the citric acid reactivity.

6.3 Instrumental analysis

6.3.1 TG analysis

A Q500 TGA (TA Instruments) was used to perform the thermogravimetric analysis on all the products. A heating rate of 10°C min^{-1} was used in a nitrogen atmosphere. Platinum pans were used, and the sample masses were weighed to approximately 10 mg. As in Chapter 4, the percentage $Mg(OH)_2$ in the products which were determined by TG analysis, were obtained from the curves of mass loss (%) and derivative mass (% $°C^{-1}$) versus temperature up to a temperature of 600°C.

6.3.2 BET surface area analysis

A NOVA 1000[e] Surface Area and Pore Size Analyzer from Quantachrome Instruments, using nitrogen gas as an adsorbent, was used to determine the surface areas of the products. The procedure as discussed in Chapter 4 was also applied in this study.

6.4 Results and Discussion

The results of the citric acid reactivity test for MgO samples calcined at different times and different temperatures, the surface area analyses before and after MgO hydration in both water and magnesium acetate solutions and the percentage of magnesium hydroxide formed are summarized in Tables 6.3 (a) to 6.3 (d).

Table 6.3a-d The Effect of calcining times/temperatures on MgO hydration

(a) 1 hour calcined

Calcining temp./ ^{o}C	**Citric acid reactivity (s)**	**Surface area before hydration ($m^2 g^{-1}$)**	**Surface area after hydration ($m^2 g^{-1}$), water**	**Surface area after hydration ($m^2 g^{-1}$), 0.1M MgAc**	**% $Mg(OH)_2$ (in water)**	**% $Mg(OH)_2$ (0.1M MgAc)**
650	239	19.16	10.83	37.05	34.8	68.2
800	300	14.26	8.95	35.91	34.2	63.4
1000	302	12.66	7.05	34.67	33.9	61.1
1200	949	2.51	3.40	6.45	3.3	16.9
1400	> 3000	0.65	0.88	2.10	0.61	2.2

(b) 2 Hours calcined

Calcining temp./ ^{o}C	Citric acid reactivity (s)	Surface area before hydration ($m^2 g^{-1}$)	Surface area after hydration ($m^2 g^{-1}$), water	Surface area after hydration ($m^2 g^{-1}$), 0.1M MgAc	% $Mg(OH)_2$ (in water)	% $Mg(OH)_2$ (0.1M MgAc)
650	225	19.61	13.46	40.62	35.79	65.33
800	253	13.75	12.37	38.98	31.42	64.71
1000	256	11.72	9.67	38.90	28.77	60.84
1200	761	2.89	4.27	11.56	5.05	23.98
1400	> 3000	0.61	1.18	1.46	0.45	1.00

(c) 4 Hours calcined

Calcining temp./ ^{o}C	Citric acid reactivity (s)	Surface area before hydration ($m^2 g^{-1}$)	Surface area after hydration ($m^2 g^{-1}$), water	Surface area after hydration ($m^2 g^{-1}$), 0.1M MgAc	% $Mg(OH)_2$ (in water)	% $Mg(OH)_2$ (0.1M MgAc)
650	245	18.27	9.71	41.79	34.43	67.48
800	246	14.32	8.80	40.20	31.65	63.24
1000	280	9.37	7.33	31.23	28.41	54.85
1200	1056	1.81	3.37	5.01	2.58	11.23
1400	> 3000	0.39	1.07	2.08	0.61	1.84

(d) 6 Hours calcined

Calcining temp./ ^{o}C	Citric acid reactivity (s)	Surface area before hydration ($m^2 g^{-1}$)	Surface area after hydration ($m^2 g^{-1}$), water	Surface area after hydration ($m^2 g^{-1}$), 0.1M MgAc	% $Mg(OH)_2$ (in water)	% $Mg(OH)_2$ (0.1M MgAc)
650	221	16.89	9.57	41.31	32.88	67.93
800	290	12.57	7.62	41.16	29.90	64.51
1000	278	10.85	7.36	38.32	26.93	62.33
1200	809	2.65	3.89	7.70	3.92	18.15
1400	> 3000	0.46	1.63	3.32	1.26	3.46

In general, as expected there was a decrease in the amounts of $Mg(OH)_2$ being formed with an increase in the calcination temperature of MgO from 650-1400^oC for 1, 2, 4 or 6 hour(s). These results are further confirmed by the citric acid reactivity results, surface area results and percentage $Mg(OH)_2$ being formed. The percentage $Mg(OH)_2$ formed from water as a hydrating agent are consistently less than those from magnesium acetate as a hydrating agent, indicating that magnesium acetate is a better hydrating agent than water under these conditions.

Figure 6.1 shows the TGA curves of the product obtained from hydration performed in water solutions. The products were obtained by hydration of MgO calcined between 650 and 1400^oC for 1 hour. The results show that by hydrating MgO calcined between 650 and 1000^oC, about the same percentage of $Mg(OH)_2$ was obtained, whereas at higher calcination temperatures (1200^oC or more) the percentage magnesium hydroxide decreases considerably. The same results were also observed for MgO calcined between 650 and 1400^oC for either 2, 4, or 6 hours in either water or magnesium acetate solutions.

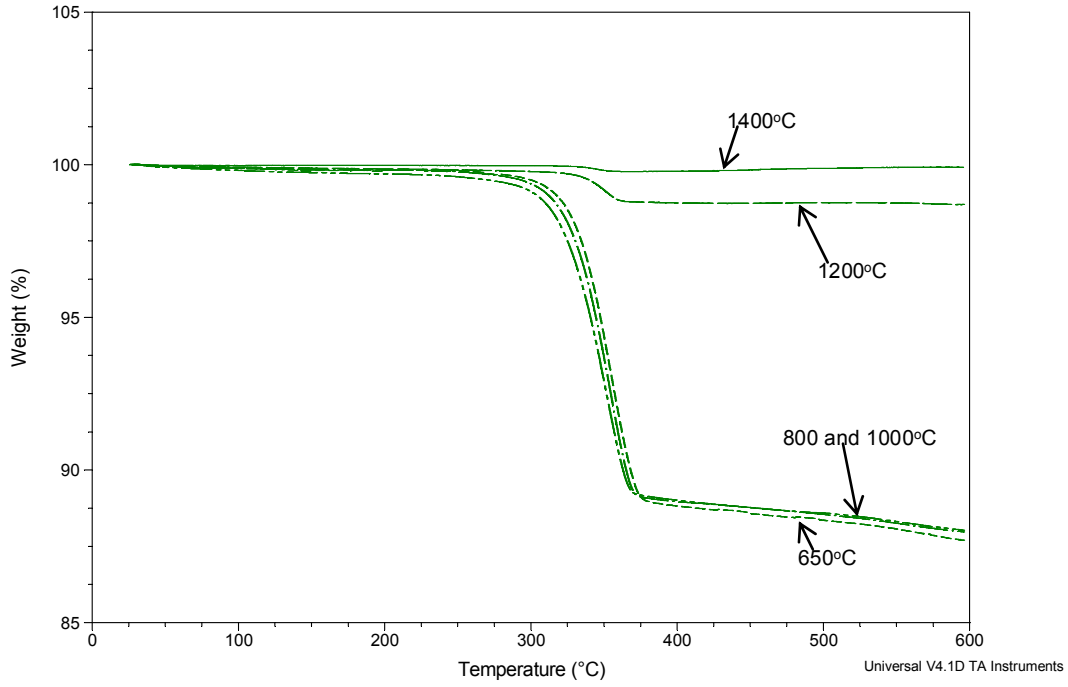

Figure 6.1 TGA curves of the $Mg(OH)_2$ produced in water solutions

Figure 6.2 shows the effect of calcination temperature on the surface areas of calcined MgO and the products obtained after hydration in magnesium acetate. The surface areas of the calcined MgO samples are less than those of the formed products, thus confirming that during hydration there was a decrease in the number of MgO particles and an increase in the number of $Mg(OH)_2$ particles. The surface areas of the MgO samples calcined at 1200°C or 1400°C are very low (0.39-2.89 $m^2 g^{-1}$), indicating an inactive MgO. As can be seen from the figure, the specific surface areas are nearly constant in the temperature range between 650-1000°C, and then decreases dramatically beyond approximately 1050°C. These results confirmed that the samples calcined between 650 and 1000°C were still in the region of a medium burnt MgO. Similar results were observed when water was used as a hydrating agent.

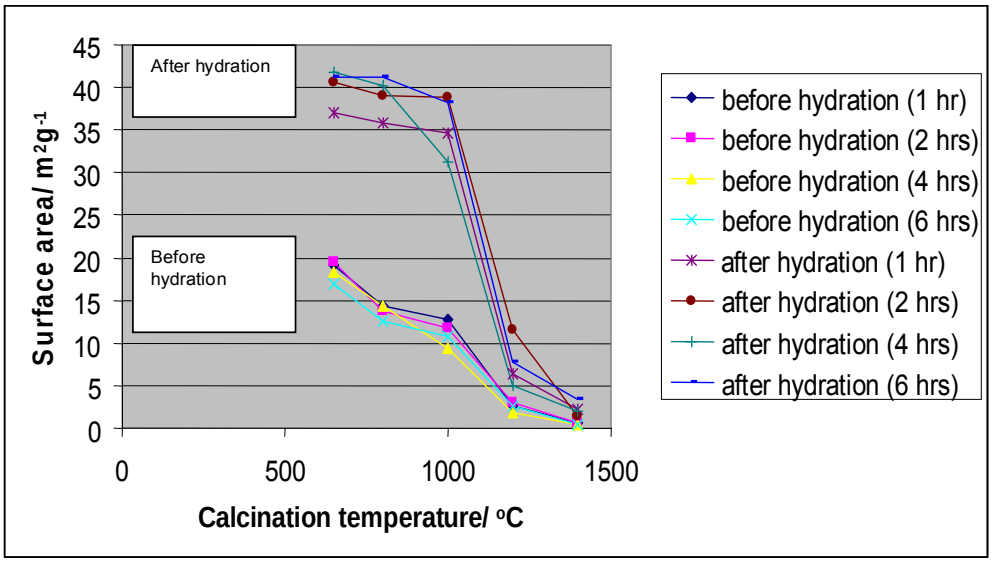

Figure 6.2 Effect of calcination temperature on MgO surface area

Figures 6.3 and 6.4 summarise the effect of calcination time and temperature on the percentage $Mg(OH)_2$ being formed. There was not a significant difference in the percentage $Mg(OH)_2$ being formed from MgO samples calcined between 650-1000°C for either 1, 2, 4 or 6 hours, where the results were between 27-35 % $Mg(OH)_2$ using water as hydrating agent and between 55-65 % $Mg(OH)_2$ in magnesium acetate. A considerable difference can be seen for MgO samples calcined at 1200°C and more. These results were confirmed by the surface area results, where the results were between 7 and 13 $m^2 g^{-1}$ using water and between 31-40 $m^2 g^{-1}$ when magnesium acetate was used as a hydrating agent.

This indicates that MgO samples calcined for either 1, 2, 4 or 6 hours between 650 and 1000°C are more reactive towards hydration to $Mg(OH)_2$, and it seems that calcining the MgO sample between 650-1000°C only removes the moisture and converts $Mg(OH)_2$ and $MgCO_3$ to MgO. Calcination of the MgO sample for 1, 2, 4 or 6 hours at 1200°C or more, result in the MgO sample being more inactive towards hydration as the amount of $Mg(OH)_2$ being formed is very low.

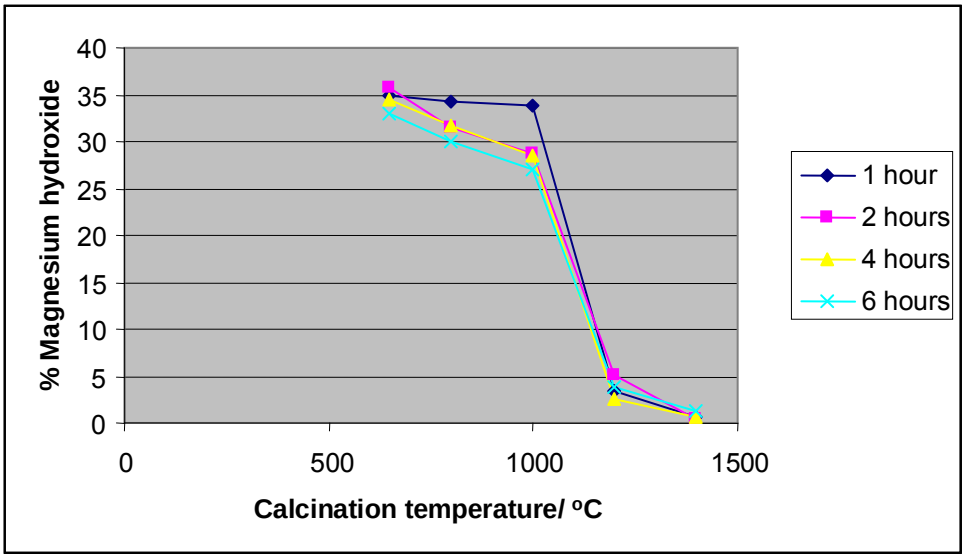

Figure 6.3 Effect of calcination temperature on the % $Mg(OH)_2$ obtained using water as a hydrating agent

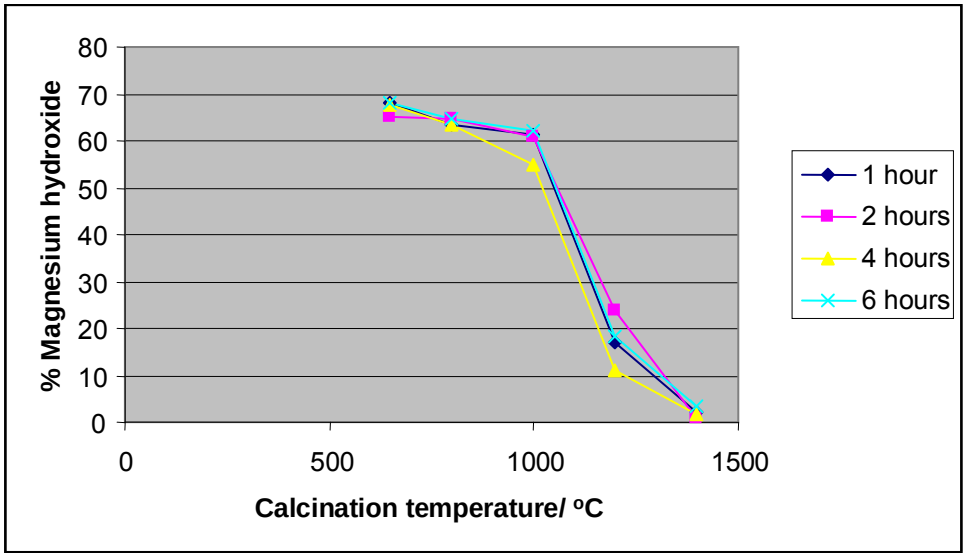

Figure 6.4 Effect of calcination temperature on the % $Mg(OH)_2$ obtained using magnesium acetate as a hydrating agent

Figures 6.5 and 6.6 show the effect of an increase in calcination time of MgO at different calcination temperatures on the percentage $Mg(OH)_2$ being formed in water and magnesium acetate solutions. It can clearly be seen that the calcination time is not a major variable affecting the reactivity of MgO samples. The percentage $Mg(OH)_2$ being formed from either water or magnesium acetate as hydrating agents, are nearly constant irrespective of the increase in calcination time.

These results thus confirm that the calcination temperature remains as the main variable affecting the surface properties and the reactivity of magnesium oxide towards hydration. It was observed from Figures 6.3 and 6.4 that there was a dramatic decrease in the amount of $Mg(OH)_2$ being formed with an increase in the temperature of calcination.

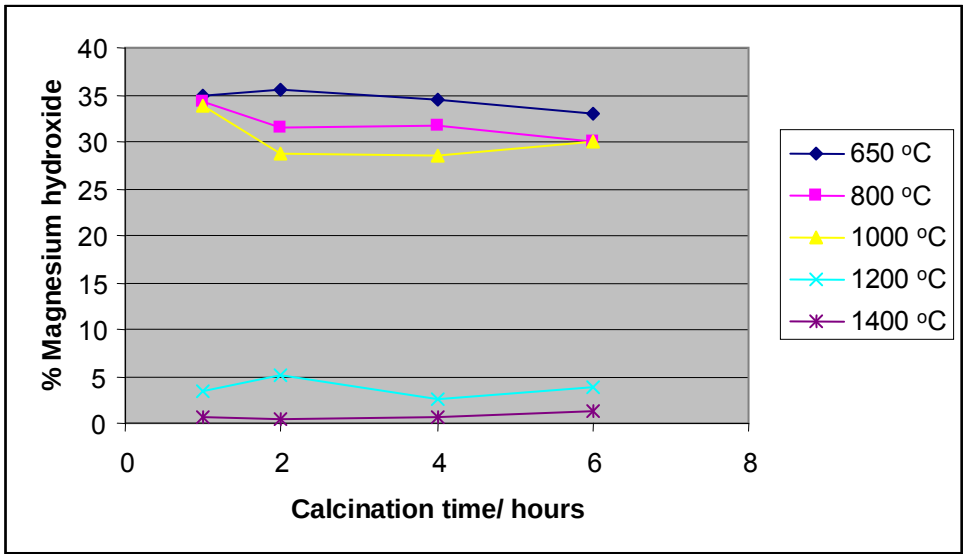

Figure 6.5 Effect of calcination time on the % $Mg(OH)_2$ formed using water as a hydrating agent

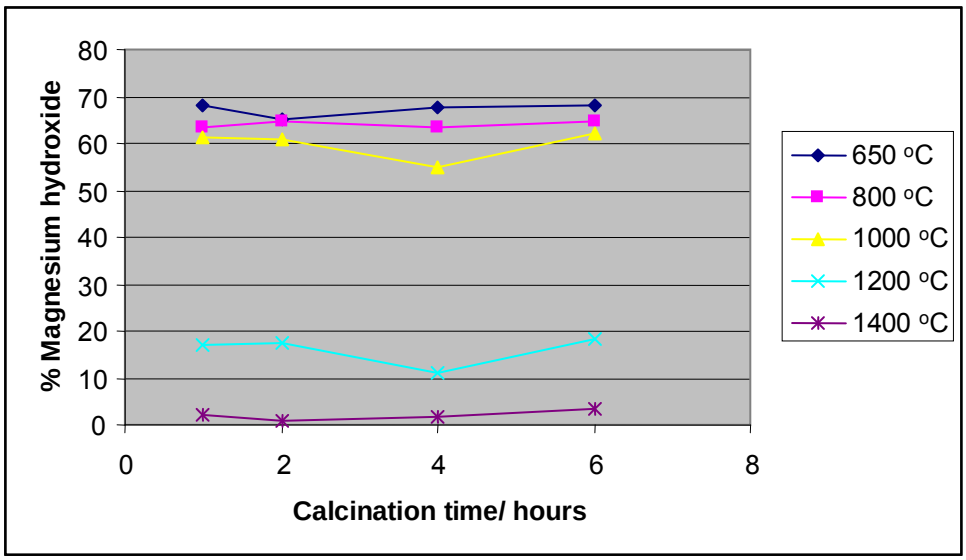

Figure 6.6 Effect of calcination time on the % $Mg(OH)_2$ formed using magnesium acetate as a hydrating agent

The effect of calcination temperature and calcination time on the citric acid reactivity values obtained are summarized in Figures 6.7 and 6.8, respectively. The citric acid reactivity values of the calcined magnesite increases with an increase in calcination temperature in Figure 6.7, but remains nearly constant when the calcination times are compared (Figure 6.8). In Figure 6.7, it can be seen that the citric acid reactivity values are nearly constant between 650 and 1000°C, which indicates a medium reactive MgO, where their citric acid reactivity values were between 225 and 300 s. The citric acid reactivity values rise dramatically beyond 1000°C. The lower citric acid values indicate the most reactive magnesia (higher MgO surface area), and correlates well with the higher percentage $Mg(OH)_2$ being formed. The higher citric acid reactivity values (lower MgO surface area) resulted in lower amounts of $Mg(OH)_2$ being formed.

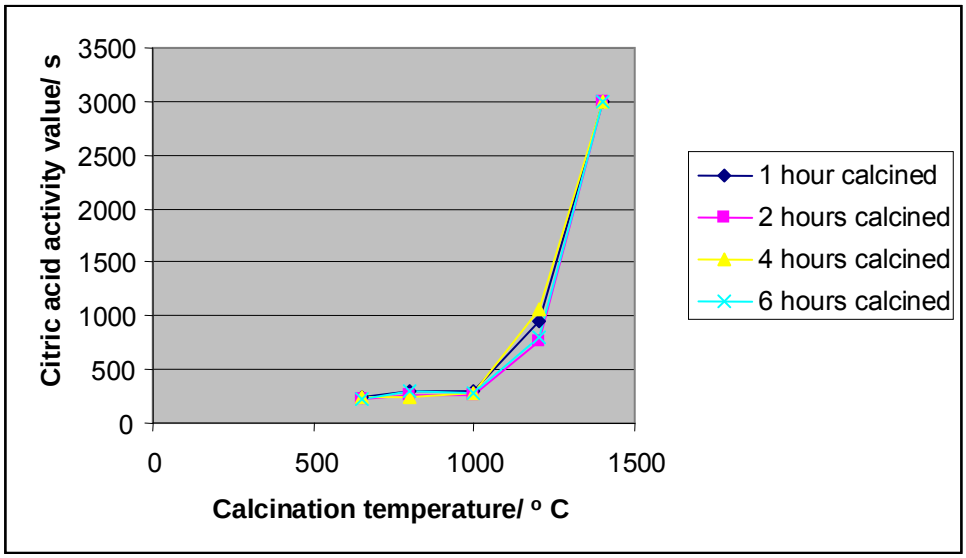

Figure 6.7 Effect of calcination temperature on citric acid reactivity value

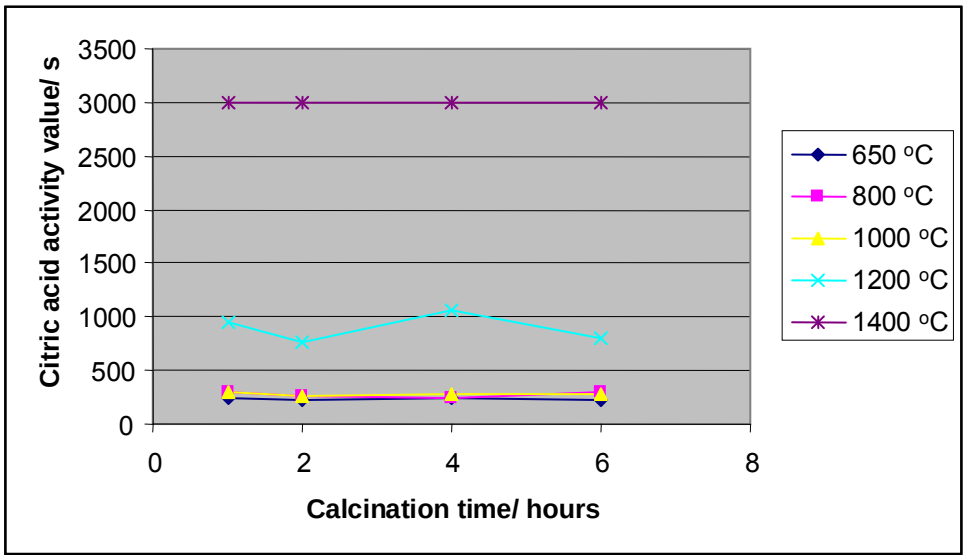

Figure 6.8 Effect of calcination time on citric acid reactivity value

Another interesting observation is that the surface areas of MgO samples calcined between 650-1000^{o}C for either 1, 2, 4 or 6 hours before hydration are still higher than those of $Mg(OH)_2$ formed from water as hydrating agent. This indicates that some MgO particles remained unreacted after 30 minutes of reaction, and only few reacted during hydration. This was not the case when magnesium acetate was used as a hydrating agent.

The results obtained in thus study agree well with the study performed by Sharma and Roy (1977) who studied the hydration characteristics of burnt magnesite in the range 550 to 950^{o}C and reported that the hydration behaviour of MgO calcined at any temperature between 550 and 750^{o}C is of the same order, but calcination at higher temperatures results in a decrease of hydration tendency, due to the formation of the more stable periclase.

Birchal et al. (2000) also reported that the temperature is the major variable affecting the reactivity of the calcined magnesite. They studied the effect of magnesite calcination conditions, and showed that the surface areas of MgO were nearly constant between 850 and 900^{o}C, and decreased with further increase in temperature.

Ranjitham and Khangaonkar (1989) reported that the calcination of magnesite at lower temperatures (650-850^{o}C) results in a higher degree of hydration due to the fact that the reactivity of magnesium oxide produced at a low temperature of calcination is influenced by lattice dilation and imperfect crystal structure. MgO calcined at lower temperatures, results in higher surface areas and higher reactivity of MgO.

Following the above observations, it seems that there is a possible transformation from amorphous MgO to a crystallite periclase during calcination of magnesite from 650 and higher temperatures. From the results obtained, it seems that crystallinity starts to occur at temperature above 1000^{o}C. After 1200^{o}C, the reactivity of MgO obtained on calcination is minimized as compared to the MgO obtained on calcining magnesite at 650 to 1000^{o}C. As mentioned in Chapter 5, a possible reason for the change in MgO reactivity with a change in calcination temperature can be due to structural changes accompanying change in calcination temperature.

Ekmekyapar et al. (1993) have reported that a decrease in MgO reactivity with increase in calcination temperature is due to sintering. During sintering, the cryptocrystalline material moves from the surface of wider pores to fill the smaller capillaries or pores, so that the average pore size increases whereas the surface area is decreased (Girgis and Girgis, 1969). As the temperature increases, crystal size also increases and as a result surface area decreases, thus resulting in a decrease in MgO reactivity.

6.5 Conclusion

In general, there was a decrease in the amounts of $Mg(OH)_2$ being formed with an increase in the calcination temperature from 650-1400^oC for either 1, 2, 4 or 6 hours. The specific surface areas of the MgO samples calcined between 650-1000^oC for 1, 2, 4 or 6 hour(s) are nearly constant, and so are the percentages of $Mg(OH)_2$ being formed. The surface area of MgO decreases dramatically as the calcination temperature increases. The degree of hydration reported as percentage $Mg(OH)_2$, decreased from approximately 33 % to 4 % (in water solutions) for MgO samples calcined between 650-1000^oC to MgO samples calcined between 1200-1400^oC. The degree of hydration also decreases from approximately 65 % to 10 % for MgO hydrated in a magnesium acetate solution.

The percentages of $Mg(OH)_2$ formed from water as a hydrating agent were consistently less than those from magnesium acetate as a hydrating agent, indicating that magnesium acetate is a better hydrating agent than water under these conditions. Hydration of MgO calcined between 650-1000^oC either 1, 2, 4 or 6 hours, resulted in nearly the same order of percentage $Mg(OH)_2$ being formed, whereas at higher temperatures (1200^oC and more), the percentage $Mg(OH)_2$ formed decreased. The surface areas of the calcined MgO are less than those of the formed products, indicating that during hydration, there was a decrease in the number of MgO particles and an increase in $Mg(OH)_2$ particles.

Calcination time did not significantly affect the specific area and the reactivity of MgO samples, and the results show that the temperature remains as the main variable affecting the surface area and reactivity of MgO.

The citric acid reactivity values of the calcined magnesite increase with an increase in calcination temperature, but remain nearly constant when the calcination times are compared. The most reactive samples (low reactivity value) showed the highest conversion level of hydration, and the least reactive MgO (high reactivity value) resulted in lower amounts of $Mg(OH)_2$ being formed.

Surface areas of the MgO samples calcined between 650 to 1000^oC for either 1, 2, 4 or 6 hours are higher than those of $Mg(OH)_2$ formed from water as a hydrating agent, indicating that some MgO particles remained unreacted after 30 minutes of hydration. Khangaonkar et al. (1990) mentioned that during hydration of MgO, the particle size of MgO decreases continuously as the hydration process progresses. This decrease in the particle size of MgO result in an increase in the number of particles of the product ($Mg(OH)_2$) and an increase in surface area of $Mg(OH)_2$ formed. The less surface area of $Mg(OH)_2$ formed from hydrating MgO in water after 30 minutes, implies that less Mg^{2+} ions are available to go into solution to react to form more $Mg(OH)_2$ which shows that water is not a better hydrating agent as compared to magnesium acetate during 30 minutes of hydration.

During calcination of MgO, there is a possible structural change with change in calcination temperature. A transformation from amorphous MgO to a crystalline MgO is a possible reason. There is a possible sintering on MgO calcination at 1000^oC and higher. Above 1200^oC, the reactivity of MgO obtained on calcination is minimized as compared to the MgO obtained on calcining magnesite between 650 and 1000^oC.

CHAPTER 7

Determination of maximum hydration time on the hydration of MgO using water and magnesium acetate as hydrating agents

7.1 Introduction

In Chapter 4, we have shown that by increasing the time of hydration, the amount of magnesium hydroxide produced using magnesium acetate as a hydrating agent is also increased. The studies were performed at a solution temperature of 25^{o}C and resulted in 54 % of $Mg(OH)_2$ being formed after 60 minutes. It will be of great interest to investigate the time of maximum MgO hydration using both water and magnesium acetate as hydrating agents.

The main aim in this chapter was to determine the time for maximum hydration of MgO to $Mg(OH)_2$. In the previous chapter, we have shown that magnesia calcined between 650 and 1000^{o}C produces a MgO that is reactive towards hydration, and as a result the time for maximum hydration experiments were performed using MgO calcined at 650 and 1000^{o}C. Although the MgO calcined at 1200^{o}C gives a small degree of hydration to magnesium hydroxide after 30 minutes of hydration, an attempt was also made to determine the time for maximum hydration time using MgO calcined at 1200^{o}C.

7.2 Experimental

7.2.1 Samples

Pure magnesium acetate ($Mg(CH_3COO)_2 \cdot 4H_2O$) was obtained from Merck, South Africa. The medium reactive MgO was obtained from Chamotte Holdings, South Africa.

7.2.2 Sample preparation

A magnesia sample (MgO) was obtained by calcining of the natural magnesite ($MgCO_3$) from Chamotte Holdings, S.A. Three magnesite samples were calcined in the laboratory at 650, 1000 and 1200^oC for 2 hours. The MgO samples were then milled by hand in a mortar and pestle and sieved to < 75 μm before they were used in the hydration studies. The surface area analyses were performed on the MgO samples before calcination (i.e., on the raw material), after calcination (i.e., before hydration studies), and after hydration (on the products obtained after hydration). TG analyses were also performed on all samples. XRD and XRF analyses were performed on the raw and calcined magnesite. A 0.1 M concentration of magnesium acetate and distilled water were prepared to be used as hydrating agents.

7.2.3 Experimental parameters and procedure

The experimental parameters for the hydration of MgO samples to determine the maximum time of its hydration to $Mg(OH)_2$ are summarized in Table 7.1.

Table 7.1 Experimental parameters for the hydration of MgO samples calcined and sieved to a particle size of < 75 μm.

Hydration temperature	80^oC
Hydrating agent	0.1 M magnesium acetate and distilled water
Solid to liquid ratio	10 g in 100 ml solution
Hydration time	30, 60, 90 minutes, etc

The reaction took place in a 250 ml glass beaker immersed in a thermostated water bath at 80^{o}C. A 10 g portion of the calcined and sieved MgO sample was poured into a 250 ml glass beaker having 100 ml magnesium acetate solution or water at 80^{o}C, and the slurry was then continuously stirred at a constant rate of 250 rpm for different times. The reaction temperature was held constant at 80^{o}C. The products were then filtered under vacuum, dried in an oven at 200^{o}C for 2 hours and stored in a desiccator. The percentage $Mg(OH)_2$ was determined by TG analysis. BET surface area analysis was performed on all products.

7.3 Instrumental analysis

7.3.1 TG analysis

A Q500 TGA (TA Instruments) was used to perform the thermogravimetric analysis on all the products. A heating rate of 10^{o}C min^{-1} was used in a nitrogen atmosphere. Platinum pans were used, and the sample masses were weighed to approximately 10 mg. As in Chapter 4, the percentage $Mg(OH)_2$ in the products which were determined by TG analysis, were obtained from the curves of mass loss (%) and derivative mass (% $^{o}C^{-1}$) versus temperature up to a temperature of 600^{o}C.

7.3.2 BET surface area analysis

A NOVA 1000^{e} Surface Area and Pore Size Analyzer from Quantachrome Instruments, using nitrogen gas as an adsorbent, was used to determine the surface areas of the products. The procedure as discussed in Chapter 4 was also applied in this study.

7.3.3 XRD analysis

X-ray powder diffraction analyses were performed on an automated Siemens D501 XRD spectrometer with a 40-position sample changer and monochromater CuK_{α} radiation. The results were analyzed with the use of the International Centre of Diffraction PDF database sets.

7.3.4 XRF analysis

For the X-ray Fluorescence analysis, the MgO sample was ground to < 75 μm in a Tungsten Carbide milling vessel and roasted at 1000°C to determine the Loss on ignition value (LOI). The milled MgO sample (1 g) was then mixed with 9 g $Li_2B_4O_7$ and fused into a glass bead. Major element analysis was executed on the fused bead using an ARL9400XP+ spectrometer. Another aliquot of the sample was pressed in a powder briquette for trace element analyses.

7.4 Results and Discussion

The magnesium oxide powder used in the hydration experiments was characterized with respect to its chemical composition by X-ray Fluorescence analysis, phase analysis by X-ray Diffraction, loss on ignition (LOI), particle size distribution by milling and sieving, surface area analysis by N_2 adsorption and by TG analysis. The same results for XRD, XRF and TG analysis of the raw and dried magnesite obtained in Chapter 4, were also obtained on the magnesite calcined between 650-1200^oC in this study.

Table 7.3 gives the physical properties of the MgO obtained before and after calcination at different temperatures. The surface area of the raw material (10.98 $m^2 g^{-1}$) increases to a value of 21.17 $m^2 g^{-1}$ after the removal of moisture, $MgCO_3$ and $Mg(OH)_2$. The value then decreases again with an increase in calcination temperature, probably due to sintering as discussed in Chapter 5 and 6. The loss on ignition value was reduced to zero after calcination. A particle size of < 75 μm was obtained by milling and sieving.

Table 7.3 The physical properties of MgO under different calcination conditions

Properties	**uncalcined**	**650^{o}C**	**1000^{o}C**	**1200^{o}C**
Loss on ignition	11.00 %	< 0.01 %	< 0.01 %	< 0.01 %
Surface area	10.98/ $m^2 g^{-1}$	21.17/ $m^2 g^{-1}$	11.72/ $m^2 g^{-1}$	4.32/ $m^2 g^{-1}$
particle size/ μm	> 75 μm	< 75 μm	< 75 μm	< 75 μm

Table 7.4 gives the results obtained for the surface area and the percentage of $Mg(OH)_2$ produced from MgO calcined at 650^oC, after hydration in magnesium acetate. It is clear that by increasing the time of hydration, the degree of hydration is increased. This can also be seen from Figure 7.1, which shows the effect of hydration time versus percentage $Mg(OH)_2$ formed. The graph levels off after 180 minutes and gives a maximum amount of $Mg(OH)_2$ of 84.4 % after 503 minutes. These values agree with the results obtained from surface area analysis, which also shows an increase with an increase in hydration time to give a maximum value of 50 $m^2 g^{-1}$.

Table 7.4 Surface area results and percentage $Mg(OH)_2$ formed from MgO calcined at 650^oC after hydration in magnesium acetate

Hydration time / minutes	Surface area after hydration/ $m^2 g^{-1}$	% Mass loss of $Mg(OH)_2$	% $Mg(OH)_2$
30	39.80	19.2	62.10
60	41.23	21.6	70.03
90	41.89	21.9	70.91
120	42.00	23.4	76.34
150	43.41	23.7	76.80
180	43.42	25.3	81.84
240	44.90	25.7	83.14
300	46.74	25.9	83.76
360	47.56	25.9	84.07
503	49.88	26.1	84.37

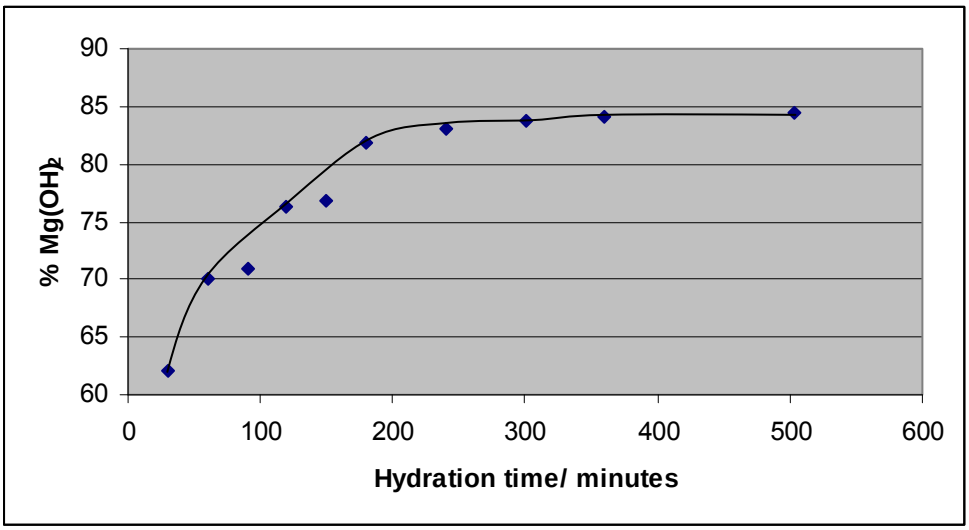

Figure 7.1 The effect of hydration time versus percentage $Mg(OH)_2$ formed from MgO calcined at 650°C after hydration in magnesium acetate

Similar results were obtained when the same experiments were performed using water as a hydrating reagent. Table 7.5 gives the results obtained for the surface area and percentage of $Mg(OH)_2$ produced from MgO calcined at 650°C, after hydration in water. After 960 minutes of hydration, a value of only 66 % was obtained by hydrating MgO calcined at 650°C in water. These results clearly demonstrate that magnesium acetate is a better hydrating agent when compared to water under these reaction conditions. Figure 7.2 shows the effect of hydration time on the amount of $Mg(OH)_2$ obtained in water. After 960 minutes, it seems that the degree of hydration is still increasing, and that the levelling effect observed upon hydration in magnesium acetate was not observed for water.

Table 7.5 Surface area results and percentage $Mg(OH)_2$ formed from MgO calcined at 650°C after hydration in water

Hydration time / minutes	Surface area after hydration/ $m^2 g^{-1}$	% Mass loss of $Mg(OH)_2$	% $Mg(OH)_2$
30	13.15	11.0	35.66
60	16.16	12.7	41.23
90	16.58	13.5	43.66
120	17.98	14.8	47.93
150	18.44	15.0	48.71
180	19.15	15.7	50.84
240	19.88	16.3	52.69
300	20.58	16.9	54.76
360	21.92	17.5	57.61
420	22.97	17.9	57.93
960	24.90	20.3	65.73

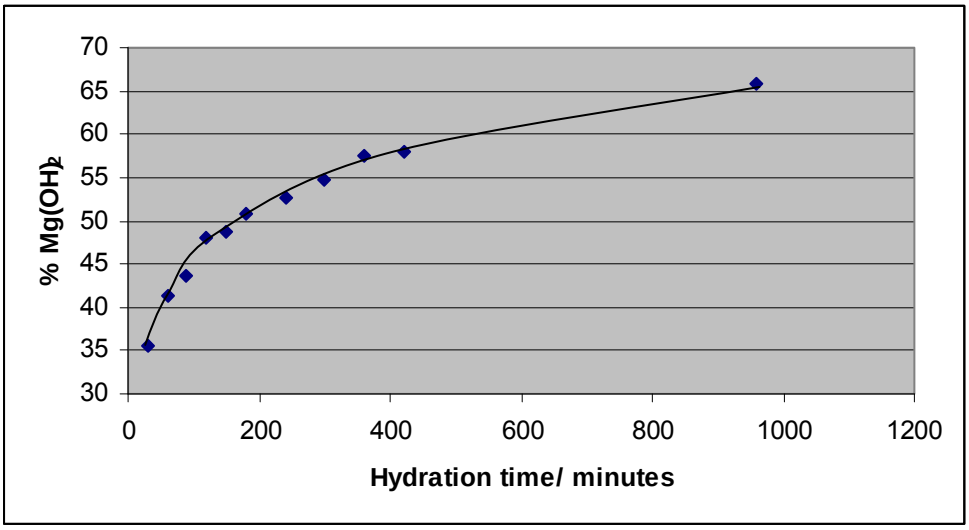

Figure 7.2 The effect of hydration time versus percentage $Mg(OH)_2$ formed from MgO calcined at 650°C after hydration in water

By performing the hydration experiments using MgO calcined at 1000°C, approximately the same results were obtained by using either water or magnesium acetate solutions as hydrating agents. Tables 7.6 and 7.7 gives the results obtained for the surface area and percentage of $Mg(OH)_2$ produced from MgO calcined at 1000°C, after hydration in magnesium acetate and water, respectively. Figures 7.3 and 7.4 also demonstrate the effect of increasing hydration time on the amount of magnesium hydroxide formed. The maximum time of hydration was obtained after 503 minutes in magnesium acetate as a hydrating agent, where 87 % of $Mg(OH)_2$ was obtained. As before, after 930 minutes, it seems that the degree of hydration is still increasing when MgO calcined at 1000°C is hydrated in water. After 930 minutes of hydration, an amount of only 63.3 % $Mg(OH)_2$ was obtained using water. These values also agree with the results obtained from surface area analysis, which also shows an increase with an increase in hydration time.

Table 7.6 Surface area results and percentage $Mg(OH)_2$ formed from MgO calcined at 1000°C after hydration in magnesium acetate

Hydration time / minutes	Surface area after hydration/ $m^2 g^{-1}$	% Mass loss of $Mg(OH)_2$	% $Mg(OH)_2$
30	38.98	18.8	60.84
60	41.78	21.8	70.68
90	42.21	23.7	76.67
120	42.36	24.0	77.73
300	44.37	25.6	82.98
360	45.10	26.3	85.24
420	45.22	26.6	86.15
503	47.33	26.8	86.86

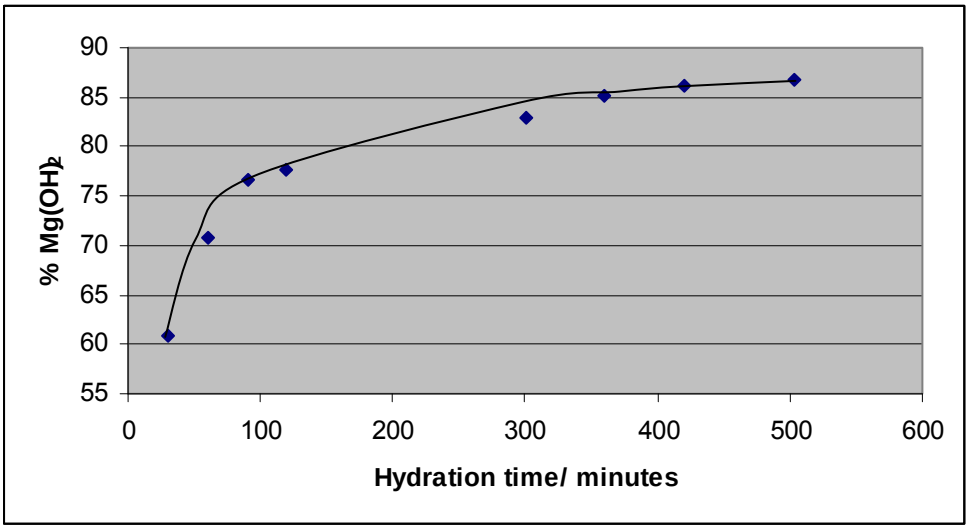

Figure 7.3 **The effect of hydration time versus percentage $Mg(OH)_2$ formed from MgO calcined at 1000°C after hydration in magnesium acetate**

Table 7.7 **Surface area results and percentage $Mg(OH)_2$ formed from MgO calcined at 1000°C after hydration in water**

Hydration time / minutes	Surface area after hydration/ $m^2 g^{-1}$	% Mass loss of $Mg(OH)_2$	% $Mg(OH)_2$
30	9.67	8.9	28.77
60	14.31	12.1	39.06
90	15.58	13.1	42.33
120	17.02	13.6	44.08
300	19.88	16.2	52.36
360	19.98	16.8	54.27
420	21.06	17.4	56.41
930	23.61	19.5	63.27

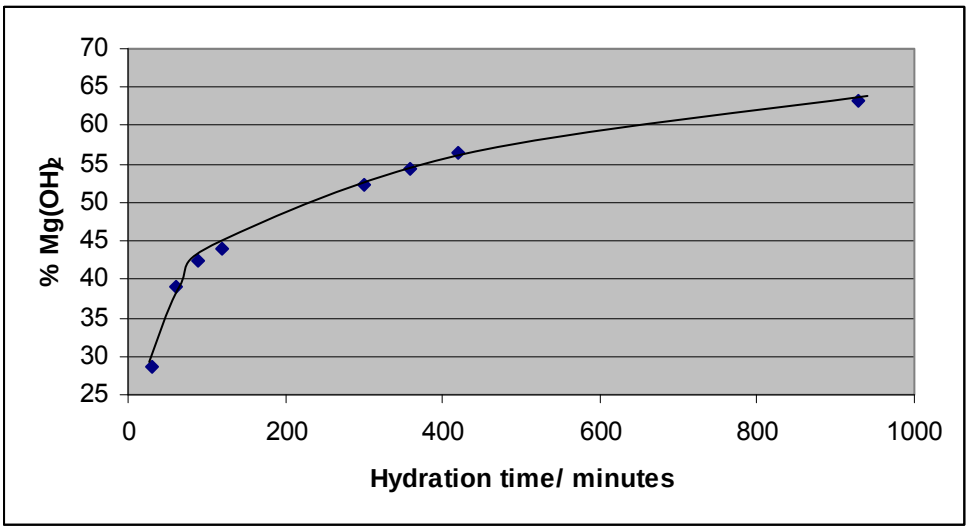

Figure 7.4 The effect of hydration time versus percentage $Mg(OH)_2$ formed from MgO calcined at 1000°C after hydration in water

Tables 7.8 and 7.9 give the results obtained for the surface area and percentage of $Mg(OH)_2$ produced from MgO calcined at 1200°C, after hydration in magnesium acetate and water, respectively. Figures 7.5 and 7.6 also demonstrate the effect of increasing hydration time of MgO calcined at 1200°C on the amount of magnesium hydroxide being formed. Although we have shown previously that after calcining the MgO sample at 1200°C a low degree of hydration is obtained, the results obtained here show that by increasing the hydration time, the amount of magnesium hydroxide is increased dramatically. By hydrating MgO calcined at 1200°C, only 9.4 % $Mg(OH)_2$ was obtained in water solutions and 32 % was obtained in magnesium acetate solutions after 30 minutes of hydration. However, the percentage $Mg(OH)_2$ increases dramatically with an increase in hydration time, and so are the surface areas. A maximum value of 87 % $Mg(OH)_2$ was obtained after 480 minutes in magnesium acetate, and 63 % after 1008 minutes in water solutions. As before, the levelling effect was observed when magnesium acetate was used as a hydrating agent, but not in water.

Table 7.8 Surface area results and percentage $Mg(OH)_2$ formed from MgO calcined at 1200°C after hydration in magnesium acetate

Hydration time / minutes	Surface area after hydration/ $m^2 g^{-1}$	% Mass loss of $Mg(OH)_2$	% $Mg(OH)_2$
30	16.13	10.0	32.35
60	30.30	19.6	63.40
90	36.93	23.9	77.28
120	38.29	24.3	78.71
210	41.55	25.8	83.43
270	43.91	26.2	84.72
360	44.72	26.7	86.28
480	45.01	26.9	87.09

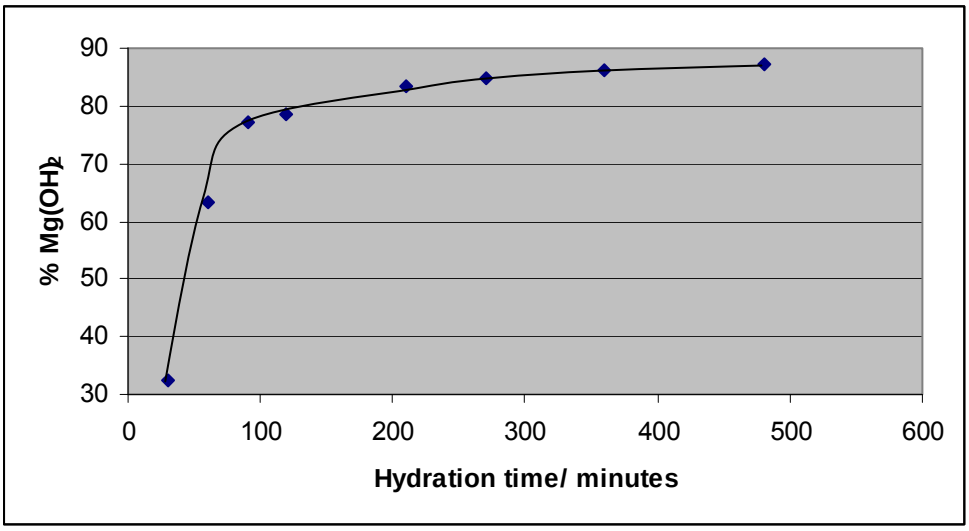

Figure 7.5 The effect of hydration time versus percentage $Mg(OH)_2$ formed from MgO calcined at 1200°C after hydration in magnesium acetate

Table 7.9 Surface area results and percentage $Mg(OH)_2$ formed from MgO calcined at 1200°C after hydration in water

Hydration time / minutes	Surface area after hydration/ $m^2 g^{-1}$	% Mass loss of $Mg(OH)_2$	% $Mg(OH)_2$
30	4.79	2.9	9.41
60	7.96	4.3	13.94
90	9.01	5.9	19.06
120	10.02	8.0	25.80
210	15.23	10.7	34.59
270	17.18	12.6	40.74
360	18.65	14.6	47.38
480	19.39	16.5	53.46
1008	22.93	19.5	63.20

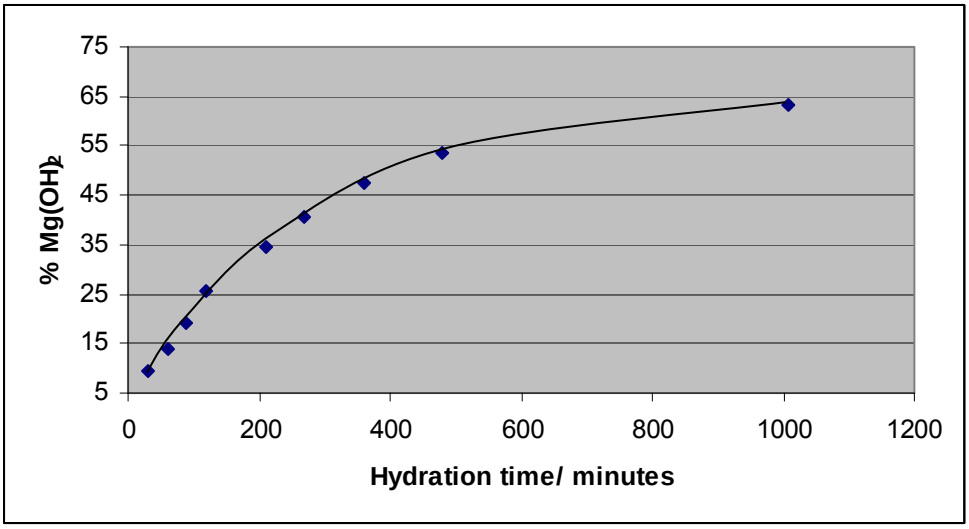

Figure 7.6 The effect of hydration time versus percentage $Mg(OH)_2$ formed from MgO calcined at 1200°C after hydration in water

Figure 7.7 presents the TGA curves showing the effect of increasing the hydration time on the percentage $Mg(OH)_2$ obtained from MgO calcined at 1200°C after hydration in magnesium acetate. It can clearly be seen that the amount of magnesium hydroxide levels off after 210 minutes. Similar TGA results were obtained for MgO calcined at 650 and 1000°C and hydrated in magnesium acetate, where the levelling effect was observed after different hydration times.

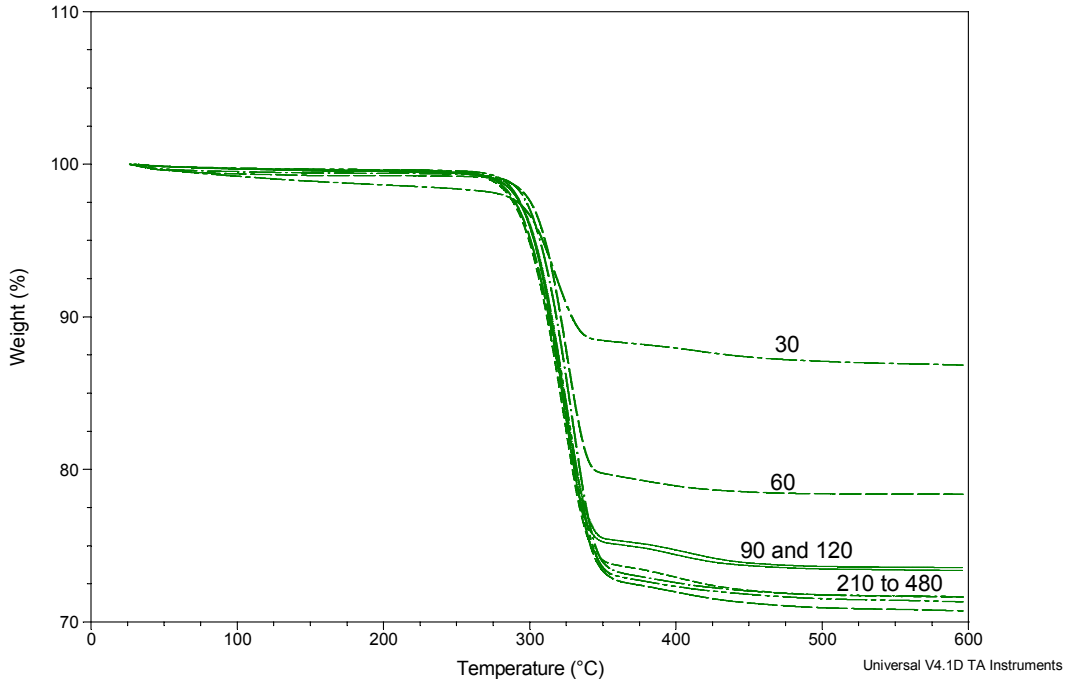

Figure 7.7 TGA curves showing the effect of increasing hydration time on percentage $Mg(OH)_2$ obtained in magnesium acetate after calcination at 1200°C

Figure 7.8 presents the TGA curves showing the effect of increasing the hydration time on the percentage $Mg(OH)_2$ obtained from MgO calcined at 1200^oC after hydration in water. From the figure, it is clear that the levelling effect observed in Figure 7.7, was not observed when water was used as a hydrating agent. After 1008 minutes, it seems that the degree of hydration is still increasing. Similar TGA results were obtained for MgO calcined at 650 and 1000^oC and hydrated in water.

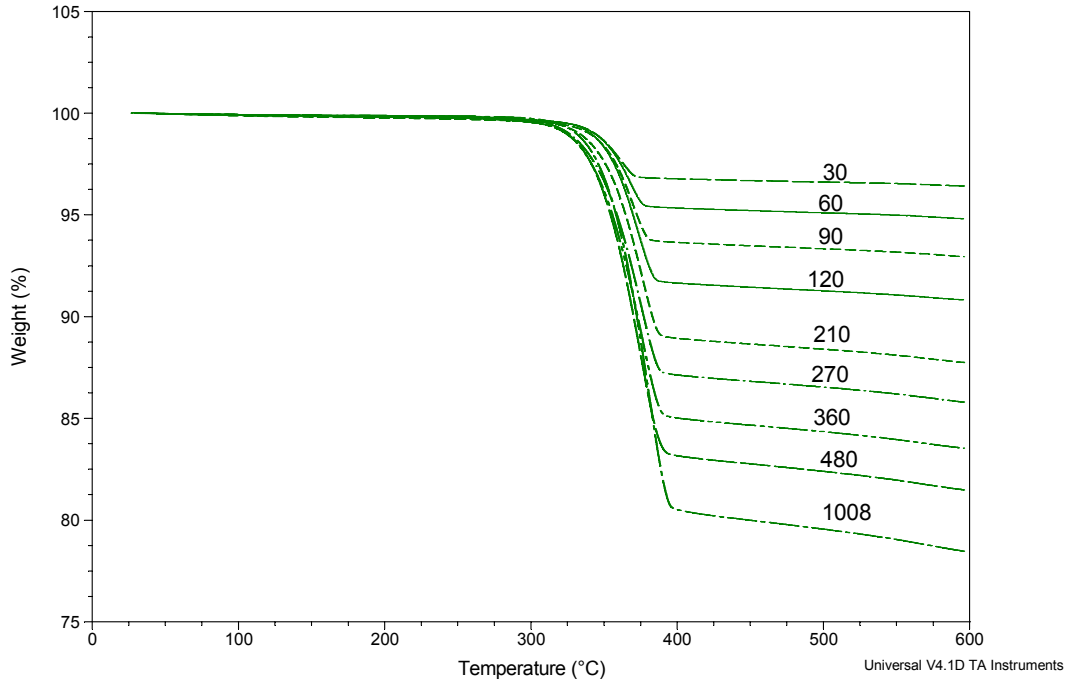

Figure 7.8 TGA curves showing the effect of increasing hydration time on percentage $Mg(OH)_2$ obtained in water after calcination at 1200^oC

Figure 7.9 shows the combined curves demonstrating the effect of increasing hydration time of MgO calcined at 650, 1000 and 1200°C on the percentage $Mg(OH)_2$ formed, obtained in both magnesium acetate and water. From the amounts of magnesium hydroxide obtained in magnesium acetate, it seems that the same maximum degree of hydration is obtained after different hydration times. The same levelling effect is obtained regardless of the calcination temperature of MgO. These results demonstrate that the influence of calcination temperature on the reactivity of MgO and on the rate of hydration is only relevant after short periods of hydration time. However, the same maximum amount of $Mg(OH)_2$ is obtained after longer times of hydration. The same is true when the hydration experiments were performed in water. We have shown previously that after short hydration times (30 minutes), the effect of calcination temperature on the rate of MgO seem to be a major effect on the percentage $Mg(OH)_2$ obtained. However, after longer hydration times, it seems that the calcination temperature is not such an important factor affecting the reactivity of MgO on hydration.

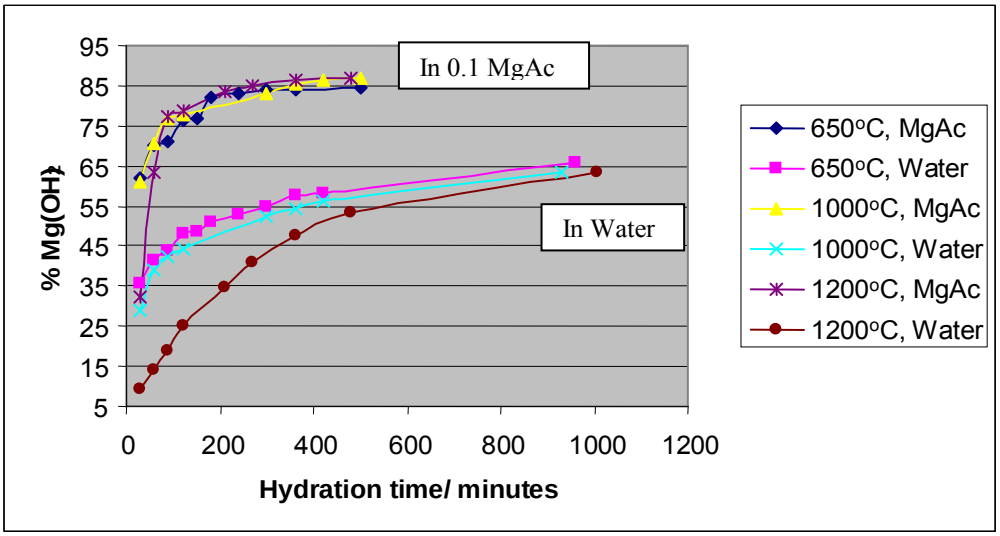

Figure 7.9 **The combined curves demonstrating the effect of increasing hydration time of MgO calcined at 650, 1000 and 1200°C on the percentage $Mg(OH)_2$ obtained in both magnesium acetate and water**

Considering the rate of MgO hydration to $Mg(OH)_2$, the hydration of MgO calcined at 1200°C is very slow within the first few minutes. Comparing the results obtained during the hydration of MgO calcined between 650 and 1000°C in magnesium acetate, an average percentage $Mg(OH)_2$ of 61% was obtained only after 30 minutes in comparison to 32 % $Mg(OH)_2$ obtained from MgO calcined at 1200°C after 30 minutes of hydration. The results obtained during the hydration of MgO calcined between 650 and 1000°C in water gave an average percentage $Mg(OH)_2$ of 46 % after 2 hours, and only 25 % $Mg(OH)_2$ was obtained from MgO calcined at 1200°C after the same time of hydration. Figure 7.10 shows the effect of percentage $Mg(OH)_2$ obtained from MgO hydrated in magnesium acetate on the surface area obtained. The surface area of the product rises exponentially as the percentage $Mg(OH)_2$ increases with longer hydration times. Similar results were also observed on the hydration of MgO in water.

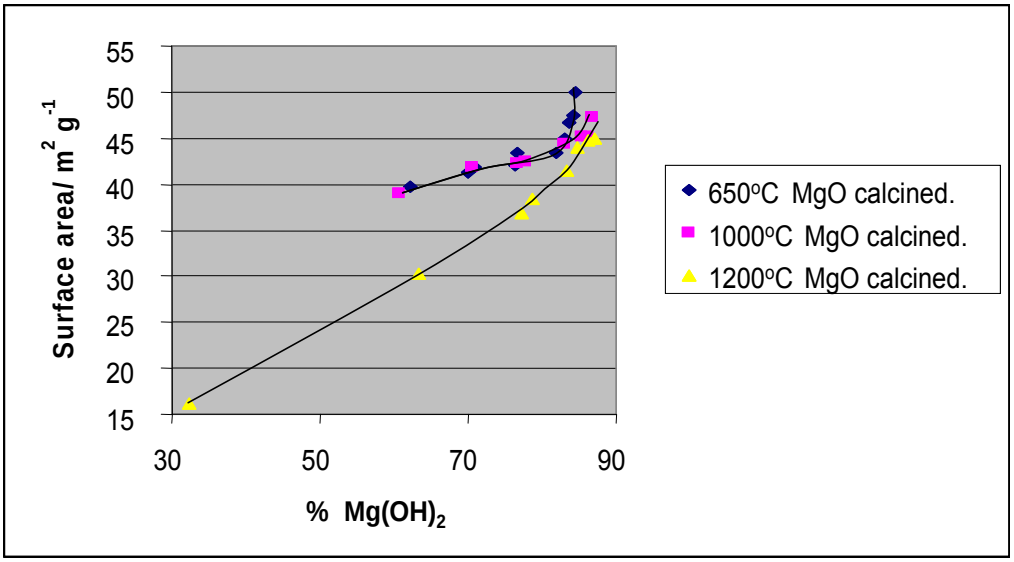

Figure 7.10 Effect of % $Mg(OH)_2$ obtained on the surface area of $Mg(OH)_2$ formed from hydration of MgO calcined at 650, 1000, and 1200°C

Khangaonkar et al. (1990) reported that the particle size of MgO during hydration decreases continuously in spite of the increase in the mass due to hydration and reduction in density, both involving an increase in volume. They reported that the process taking place is a breakage due to chemical reaction, with the product layer of magnesium hydroxide causing stress leading to breakage, instead of continued growth of the $Mg(OH)_2$ layer. This breakage then causes a fresh MgO surface to be made available for further rapid hydration and breakage. The repetitive cycle then leads to an exponential rise in the number of particles and surface area of $Mg(OH)_2$, particularly in the later stages of the hydration. In other words, as the hydration time increases, more breakage results and more MgO surface sites are available, leading to further hydration of MgO, and subsequently more $Mg(OH)_2$ is formed .

We have already mentioned in Chapters 5 and 6 that during calcination of MgO, the decrease in MgO reactivity with an increase in calcination temperature is due to structural changes. Maryska and Blaha (1997) have reported that the influence on the hydration rate of MgO is exhibited by the degree of crystallization and sintering of MgO, whose measure is its specific surface area. As the calcination temperature is raised, crystal sizes increase and as a result the surface area of MgO decreases, resulting in a decrease in the hydration rate of MgO. It seems that a smaller surface area implies less Mg^{2+} ions that go into solution to react to form $Mg(OH)_2$, however, as the hydration time is increased, the breakage causes more Mg^{2+} ions to be available to react in solution to form more $Mg(OH)_2$. At 1200^oC, there is more of the crystalline MgO (with a very low surface area) as compared to MgO calcined between 650-1000^oC, and therefore, hydrating MgO calcined at 1200^oC, will result in a smaller degree of hydration after short hydration times. However, for longer hydration times, the degree of hydration is enhanced, and reaches the same maximum hydration as obtained from the hydration of MgO calcined at 650 and 1000^oC. It seems that the diffusion of Mg^{2+} ions away from the surface is the rate determining step.

7.5 Conclusion

XRD analyses have shown that the phases present in the raw magnesite consisted mainly of periclase (MgO) with some $MgCO_3$ and $Mg(OH)_2$. TG analyses have shown that calcining the sample at 650, 1000 and 1200^oC for 2 hours, converts the $MgCO_3$ and $Mg(OH)_2$ to pure MgO. XRF analysis have also shown that after calcining of the raw magnesite, the MgO content increased from 85.00 % to 96.00 %, and the LOI value decreased from 11.00 % to < 0.01 %. As a result, the raw magnesite sample, as obtained from Chamotte need, to be dried prior to the hydration studies to remove $Mg(OH)_2$ and moisture.

By increasing the hydration time of MgO in water or in magnesium acetate solutions, the degree of hydration is increased dramatically. The surface areas of the $Mg(OH)_2$ obtained increases with an increase in hydration time in either water or magnesium acetate solutions. A levelling effect was observed on the percentage $Mg(OH)_2$ obtained from MgO calcined at 650^oC in magnesium acetate after 180 minutes, and a maximum amount of 84 % of $Mg(OH)_2$ was obtained after 503 minutes. However, the levelling effect observed in magnesium acetate was not observed when water was used as a hydrating agent. After 960 minutes, it seemed that the extent of hydration of MgO calcined at 650^oC was still increasing. The same results were obtained for the hydration of MgO calcined at 1000^oC in both water and in magnesium acetate solutions.

Despite the fact that the MgO calcined at 1200^oC resulted in a hard burnt and low reactivity sample, the degree of hydration also improved by increasing hydration time. Again, as in 650 or 1000^oC calcined MgO, a levelling effect was observed in magnesium acetate solutions, which was not the case in water. This levelling effect was observed after 210 minutes, and a maximum value of 87 % $Mg(OH)_2$ was obtained after 480 minutes using magnesium acetate. By increasing the time up to 1000 minutes, 63 % $Mg(OH)_2$ can be obtained in water as a hydrating agent. The surface areas of the $Mg(OH)_2$ obtained also increased with an increase in hydration time for both hydrating agents.

In averaging the above three results, it seemed that the same maximum degree of hydration was obtained after different hydration times. The same levelling effect is obtained regardless of different calcination temperatures of MgO. It seems that the influence of calcination temperature on the reactivity of MgO upon hydration is only relevant for shorter hydration times. The same degree of hydration can still be observed after longer hydration times. By increasing the calcination temperature, and therefore by lowering the reactivity of MgO, the rate of the hydration reaction is affected considerably.

CHAPTER 8

Conclusion

A Thermogravimetric analysis (TGA) method was successfully employed to quantitatively determine the amounts of $Mg(OH)_2$ and $Mg(CH_3COO)_2$ in a mixture thereof, by comparing the experimental mass losses of both components to their theoretical mass losses. Of the three methods developed for quantitative determination of magnesium hydroxide and magnesium acetate, only two methods provided accurate and reliable results. The other method failed due to the fact that the decomposition temperatures of both $Mg(OH)_2$ and $Mg(CH_3COO)_2$ changed as the composition of the mixtures changed. Although the third method gave reliable results, it can only be used where the mixture consists only of magnesium hydroxide and magnesium acetate. The minimum in the derivative mass versus temperature curve can be used to improve the resolution of stages of more complex TG curves.

For the purpose of hydration of MgO obtained from the calcination of magnesium carbonate, the raw magnesium carbonate has to be calcined prior to the hydration studies in order to remove moisture, and convert $Mg(OH)_2$ and $MgCO_3$ to MgO. XRD analyses have shown that the phases present in the raw magnesium carbonate, as obtained from Chamotte, consisted mainly of periclase (MgO) with some $Mg(OH)_2$ and $MgCO_3$. TG analyses have also shown that after calcination of the raw magnesite, the MgO obtained consisted no moisture, $Mg(OH)_2$ or $MgCO_3$. These three components were observed between 50 and 200^oC (moisture), between 200 and 450^oC ($Mg(OH)_2$) and between 450 and 600^oC ($MgCO_3$), respectively. Quantitative XRF analysis indicated that the raw material consisted of 85.00 % MgO and a LOI value of 11.00 % was obtained. After calcination, the LOI value was reduced to zero (< 0.01 %) and the percentage MgO was increased to 96.00 %.

Experimental parameters such as concentration of magnesium acetate, solution temperature, solid to liquid ratio and hydration time, are among the most important factors that can greatly influence the hydration rate of MgO to $Mg(OH)_2$.

Magnesium acetate seems to enhance the degree of hydration of MgO when compared to water. Filippou et al. (1999), who proposed a mechanism for MgO hydration in a magnesium acetate solution, have reported that an increase in the degree of MgO hydration in magnesium acetate is due to the complexation power of the complex formed by acetate ions and Mg^{2+}. The results obtained in this study have shown that the hydration in magnesium acetate solutions resulted in higher amount of $Mg(OH)_2$ being produced in comparison to hydration in pure water. A solid to liquid ratio of 10 g MgO per 100 ml of hydrating solution was proposed. An increase in the amount of MgO results in a decrease in the dissolution rate of MgO. Also, a solid to liquid ratio of more than 10 g MgO per 100 ml of hydrating solution, will result in about the same amount of magnesium hydroxide being formed. By increasing the hydration time, an increase in the percentage of magnesium hydroxide being formed was observed.

The effect of reactivity of MgO on its hydration to $Mg(OH)_2$ can be determined by (i) fixing calcination time and varying the calcination temperature and (ii) fixing the calcination temperature and varying calcination time. The results thereof will give an indication of which of the two variables (calcination time or temperature) is the main parameter affecting the surface area and the reactivity of MgO upon hydration to $Mg(OH)_2$. After performing the studies on calcination time and temperature of MgO, the results have shown that there was a decrease in the amount of $Mg(OH)_2$ being formed with an increase in the calcination temperature from 650 to 1400^{o}C for either 1, 2, 4 or 6 hours. The results were also confirmed by the surface areas obtained for the product, which showed a decrease with an increase in calcination temperature.

The specific surface areas of the MgO calcined between 650 and 1000^{o}C for either 1, 2, 4 and 6 hours were nearly constant, and so were the percentage $Mg(OH)_2$ being formed. Both the surface areas of MgO and the percentage $Mg(OH)_2$ decreased as the calcination temperature was increased further. Surface areas of the MgO samples calcined between 650 to 1000^{o}C for 1, 2, 4 or 6 hours were higher than those of the $Mg(OH)_2$ formed from water as a hydrating agent, indicating that some MgO particles remained unreacted after 30 minutes of hydration.

The results obtained have shown that the calcination time did not significantly affect the specific area and the reactivity of the MgO samples, and that the calcination temperature remains as the main variable affecting the surface area and reactivity of MgO.

The citric acid reactivity values of the calcined magnesite increases with an increase in calcination temperature, but remains nearly constant when the calcination times are compared. The most reactive samples (low citric acid reactivity value) showed the highest degree of hydration, and the least reactive MgO (high citric acid reactivity value) resulted in lower amounts of $Mg(OH)_2$ being formed.

The change in MgO reactivity with a change in calcination temperature or time can be due to structural changes with a change in calcination temperature. Sintering, which is a process in which a finely divided ore is heated until it collects to form larger particles, is taking place at higher temperatures. MgO is largely amorphous after calcining at 850^{o}C. At temperatures exceeding 1000^{o}C, crystallinity occurs because all the $MgCO_3$ crystals have decomposed. As the temperature increases, crystal size also increases and as a result surface area decreases, thus resulting in a decrease in MgO reactivity (Birchal et al., 2000; Girgis and Girgis, 1969; Rizwan et al., 1999).

The degree of hydration of MgO can be increased by increasing the hydration time. In the hydration studies performed using magnesium acetate as a hydrating agent, the same maximum degree of hydration was obtained regardless of different calcination temperatures of MgO. In order to obtain an optimum amount of $Mg(OH)_2$ of 87 % using 0.1 M magnesium acetate, it seems essential to increase the hydration time to 500 minutes. The same optimum amount is obtained regardless of different calcination temperatures of MgO. It seems that the influence of calcination temperature on the reactivity of MgO upon hydration is only relevant for shorter hydration times. It will be of great interest to further investigate the maximum degree of hydration of MgO in water solutions. MgO calcined at 1200^{o}C shows a small degree of hydration after 30 minutes of hydration. However, the degree of hydration is increased dramatically with an increase in hydration time.

The calcination of magnesite between 650 and 1000^{o}C resulted in MgO with a high reactivity and a higher degree of hydration. However, the MgO obtained from calcination of magnesite at 1200^{o}C resulted in a hard burnt MgO and lower reactivity. Filippou et al. (1999) reported that the hydration of hard burnt MgO proceeds in stages. In the initial stage, magnesium hydroxide forms and covers each MgO particle, causing slow MgO dissolution and low hydration rates due to product-layer diffusion control. It seems that this slow MgO dissolution is due to low a surface area which implies less surface active MgO points. However, as the degree of hydration increases, the hydroxide layer starts cracking and peeling off from the mother MgO particle. This is the second process stage that is surface-reaction controlled. The peeling off of the hydroxide results in fresh MgO particles and surface areas to be made available for further hydration to form more $Mg(OH)_2$. In the last process stage, all small MgO particles are totally converted to $Mg(OH)_2$, while the few relatively large MgO particles continue to hydrate very slowly.

In this study, we have demonstrated that the calcination temperature can affect the reactivity of MgO considerably, however, by increasing the hydration time, the degree of hydration of MgO to $Mg(OH)_2$ is increased as well.

APPENDIX

References

ANDERSON, P. J., HORLOCK, R. F. and OLIVER, J. F. (1965), *Transactions of the Faraday Society*, **61(12**), 2754-2762.

ARAL, H., HILL, B. D. and SPARROW, G. J. (2004), "Salts from saline waters and value added products from the salts", CSIRO minerals, Clayton, Victoria and Global Geoscience Services Inc., Adelaide, South Australia, pp 42-64.

ARAMENDIA, M. A., BORAU, V., JIMENEZ, C., MARINAS, J. M., RUIZ, J. R. and URBANO, F. J. (2003), *Applied Catalysis*, **244(2)**, 207-215.

BANERJEE, J. C., BANERJEE, S. P. and SIRCAR, N. R. (1967), *Transactions of the Indian Ceramic Society*, **26(6)**, 167-173.

BIRCHAL, V. S. S., ROCHA, S. D. F. and CIMINELLI, V. S. T. (2000), *Minerals Engineering*, **13(14-15)**, 1629-1633.

BIRCHAL, V. S., ROCHA, S. D. F., MANSUR, M. B. and CIMINELLI, V. S. T. (2001), *Canadian Journal of Chemical Engineering*, **79(4)**, 507-511.

BLAHA, J. (1995), *Ceramics-Silikaty*, **39(2)**, 45-51.

BOLDYREV, V. V. (1993), *Journal of Thermal Analysis*, **40(3)**, 1041-1062.

BOTHA, A. and STRYDOM, C. A. (2001), *Hydrometallurgy*, **62(3)**, 175-183.

BREWER, T. S. and HARVEY, P. K. (2005), *Spectroscopy Europe*, **17(3)**, 10-16.

BRIGGS, C. C. and LYTHE, T. W. (1971), "Magnesium hydroxide production from brines of seawater", *South African Patent*, ZA 7006943, p 24.

BROWN, M. E. (1998), "Introduction to Thermal Analysis: Techniques and Applications", Chapman and Hall, New York, pp 1-48.

CAMINO, G., MAFFEZZOLI, A., BRAGLIA, M., De LAZZARO, M. and ZAMMARANO, M. (2001), *Polymer Degradation and Stability*, **74(3)**, 457-464.

CANTERFORD, J. H. (1985), *Mineral Processing and Extractive Metallurgy Review*, **2(1-2)**, 57-104.

DANIELS, T. (1973), "Thermal analysis", Kogan Page Limited, London, pp 11-72.

EKMEKYAPAR, A., ERSAHAN, H. and DONMEZ, B. (1993), *Turk Muhendislik ve Cevre Bilimleri Dergisi*, **17(3)**, 197-204.

FILIPPOU, D., KATIFORIS, N., PAPASSIOPI, N. and ADAM, K. (1999), *Journal of Chemical Technology & Biotechnology*, **74(4)**, 322-328.

FOCKE, W. W., STRYDOM, C. A. and BARTIE, N. (1997), *South African Journal of Chemical Engineering*, **9(2)**, 41-51.

GIBERT, J. P., CUESTA, J. M. L., BERGERET, A. and CRESPY, A. (2000), *Polymer Degradation and Stability*, **67(3)**, 437-447.

GIRGIS, B. S. and GIRGIS, L. G. (1969), *Journal of Applied Chemistry*, **19(10)**, 292-297.

GREGG, S. J. and SING, K. S. (1967), "Adsorption Surface Area and Porosity", Academic Press Inc., London, pp 35-73.

GREXA, O., HORVATHOVA, E., BESINOVA, O. and LEHOCKY, P. (1999), *Polymer Degradation and Stability*, **64(3)**, 529-533.

HALIKIA, I., NEOU-SYNGOUNA, P. and KOLITSA, D. (1998), *Thermochimica Acta*, **320(1-2)**, 75-88.

HATAKEYAMA, T. and LIU, Z. (1998), "Handbook of Thermal Analysis", John Wiley and Sons, New York, pp 3-19.

HORNSBY, P. R. and MTHUPHA, A. (1994), *Journal of Materials Science*, **29(20)**, 5293-5301.

HORNSBY, P. R. and WATSON, C. L. (1990), *Polymer Degradation and Stability*, **30(1)**, 73-87.

HORNSBY, P. R., WANG, J., ROTHON, R., JACKSON, G., WILKINSON, G. and COSSICK, K. (1996), *Polymer Degradation and Stability*, **51(3)**, 235-249.

INNES, J. D. and COX, A. W. (1997), *Proceedings of the International Conference on Fire Safety*, **24**, 127-138, CAN 129:150786.

JENKINS, R. and SNYDER, R. (1996), "Introduction to X-Ray Powder Diffractometry", John Wiley and Sons, Inc., New York, pp 1-258.

JENKINS, R. (1999), "X-Ray Fluorescence Spectrometry", 2nd Edition, John Wiley and Sons, Inc., New York, pp 1-159.

JOHNSON, F. J., POMMER, A. G., VERNON, M. S., WINTER, R. M., CROSS, W. M. and KELLAR, J. J. (1999), *Minerals & Metallurgical Processing*, **16(1)**, 65-68.

JOST, H., BRAUN, M. and CARIUS, C. H. (1997), *Solid State Ionics*, **101-103(Pt. 1)**, 221-228.

KATO, Y., MASHITA, N., KOBAYASHI, K. and YOSHIZAWA, Y. (1996), *Applied Thermal Engineering*, **16(11)**, 853-862.

KHANGAONKAR, P. R., OTHMAN, R. and RANJITHAM, M. (1990), *Minerals Engineering*, **3(1-2)**, 227-235.

KIMYONGUR, N. and SCOTT, P. W. (1986), *Materials Science Forum*, **7**, 83-89.

KURODA, Y., YASUGI, E., AOI, H., MIURA, K. and MORIMOTO, T. (1988), *Journal of the Chemical Society, Faraday Transactions 1*, **84(7)**, 2421-2430.

LIU, X-H., ZHANG, X-G., WANG, X-Y. and LOU, N-Q. (1997), *International Journal of Mass Spectrometry and Ion Processes*, **171(1-3)**, L7-L11.

L'VOV, B. V., NOVICHIKHIN, A. V. and DYAKOV, A. Y O. (1998), *Thermochimica Acta*, **315(2)**, 135-143.

MARYSKA, M. and BLAHA, J. (1997), *Ceramics-Silikaty*, **41(4),** 121-123.

MELLOR, J. W. (1924), "A comprehensive Treatise on Inorganic and Theoretical Chemistry", Vol. IV, Longmans, London, pp 280-284.

MOLESKY, F. (1991), *Proceedings of the International Conference on Fire Safety*, **16**, 212-226, CAN 115:184525.

MULLER, R. H. and MEHNERT, W. (1997), "Particle and Surface Characterization Methods", Medpharm Scientific Publishers Stuttgart, Germany, pp 185-195.

NUFFIELD, E. W. (1966), "X-ray diffraction methods", John Wiley and Sons, Inc., New York, London, Sydney, pp 29-45.

RANJITHAM, A. M. and KHANGAONKAR, P. R. (1989), *Minerals Engineering*, **2(2)**, 263-270.

RASCHMAN, P. and FEDOROCKOVA, A. (2004), *Hydrometallurgy*, **71(3-4)**, 403-412.

RAZOUK, R. I. and MIKHAIL, R. S. H. (1958), *Journal of Physical Chemistry*, **62,** 920-925.

RAZOUK, R. I. and MIKHAIL, R. S. H. (1959), *Journal of Physical Chemistry*, **63**, 1050-1053.

RIZWAN, S., AGHA, H., ANSAR, S. A. and KHAN, A. A. (1999), *Proceedings of the International Symposium on Advanced Materials, 6th, Islamabad, Pakistan*, **Sept. 19-23**, 166-169.

ROCHA, S. D. F. and CIMINELLI, V. S. T. (2001), *Polimeros*: *Ciencia e Tecnologia,* **11(3)**, 116-120.

ROCHA, S. D. F., MANSUR, M. B. and CIMINELLI, V, S. T. (2004), *Journal of Chemical Technology and Biotechnology*, **79(8)**, 816-821.

ROTHON, R. N. and HORNSBY, P. R. (1996), *Polymer Degradation and Stability*, **54(2-3),** 383-385.

SHARMA, S. K. and ROY, H. (1977), *Fertilizer Technology*, **14(3)**, 247-250.

SKOOG, D. A., HOLLER, F. J. and NIEMAN, T. A. (1998), "Principles of instrumental analysis", 5th Edition, Harcourt Brace and Company, Florida, pp 272-296, 798-805.

SMITHSON, G. L. and BAKHSHI, N. N. (1969), *Canadian Journal of Chemical Engineering*, **47(5)**, 508-513.

TA instruments (2004), Thermogravimetric Analyzer operational manual, pp 13-24.

VAN DER MERWE, E. M., STRYDOM, C. A. and BOTHA, A. (2004), *Journal of Thermal Analysis and Calorimetry*, **77(1)**, 49-56.

VAN DER MERWE, E. M. and STRYDOM, C. A. (2006), *Journal of Thermal Analysis and Calorimetry*, **84(2)**, 149-156.

VERMILYEA, D. A. (1969), *Journal of the Electrochemical Society*, **16(9)**, 1179-1183.

WEST, A. R. (1996), "Basic Solid State Chemistry", 2nd Edition, John and Wiley, New York, pp 125-147, 203-210.

WHITSON, C. (1987) "X-ray Methods", John Wiley and Sons, London, pp 1-33.

WU, Y., ISAROV, A. V. and O'CONNELL, C. (1999), *Thermochimica Acta*, **340-341**, 205-220.

YOSHIDA, T., TANAKA, T., YOSHIDA, H., FUNABIKI, T., YOSHIDA, S. and MURATA, T. (1995), *Journal of Physical Chemistry*, **99(27)**, 10890-10896.

ZHANG, J., WANG, X., ZHANG, F. and HORROCKS, A. R. (2004), *Polymer Testing*, **23(2)**, 225-230.

URL-1 http://www.answers.com/topic/magnesium-oxide (Visited 15/10/2006).

URL-2 http://www.answers.com/topic/magnesium-hydroxide (Visited 15/10/2006).

URL-3 http://www.answers.com/topic/magnesium-carbonate (Visited 15/10/2006).

URL-4 http://www.chemistry.ohio-state.edu/~gallaghe/ta/calib_stand.htm (Visited 10/01/2007).

URL-5 http://www.osha.gov/SLTC/radiationionizing/introtoionizing/x-raytube.html (Visited 09/02/2007).